P-05-112

Forsmark site investigation

Rock mechanics characterisation of borehole KFM01A

Flavio Lanaro
Berg Bygg Konsult AB

August 2005

Svensk Kärnbränslehantering AB
Swedish Nuclear Fuel
and Waste Management Co
Box 5864
SE-102 40 Stockholm Sweden
Tel 08-459 84 00
+46 8 459 84 00
Fax 08-661 57 19
+46 8 661 57 19

ISSN 1651-4416
SKB P-05-112

Forsmark site investigation

Rock mechanics characterisation of borehole KFM01A

Flavio Lanaro
Berg Bygg Konsult AB

August 2005

Summary

This report contains the results of the rock mechanics “single-hole” interpretation of the geomechanical information from borehole KFM01A at Forsmark /Carlsten et al. 2004/. The geological data provided by borehole logging and sample testing (by May, 2004) are interpreted and integrated with data published from earlier projects at Forsmark to characterise the rock along the borehole. The empirical systems RMR (version 1989) and Q (version 2002) are used as tools for the estimation of the mechanical properties of the rock mass. In general, the rock quality assessed by means of RMR and Q is “very good rock” (RMR > 81, Q > 40) along most of the length of borehole KFM01A. “Good rock” (80 > RMR > 61; 40 > Q > 10) is expected down to 300 m depth. Sections of poorer rock can be observed at the depths 380–410, 480–490, 610–620, 650–685 and at about 850 m.

The deformation modulus of the rock mass determined based on the correlations with the two empirical systems is estimated. The obtained deformation modulus varies between 45 and 70 GPa and is characterised by a marked increase with depth. Since the effect of stress is not directly included in these results, the increase with depth should be completely be ascribed to lower fracture frequency and better fracture conditions. Also the uniaxial compressive strength, cohesion and friction angle are determined for the rock mass interpreted as a continuum medium. The rock mass quality and the derived mechanical properties exhibit scale dependency that emphasises the importance to know for what scale and what purpose the properties are used. The study covers also the issue of the uncertainty on the rock mass quality and mechanical properties. Some discussion about the methodology for rock mass characterisation and result storage in SKB’s SICADA database are also given.

Sammanfattning

Tillgänglig geomekanisk data är tolkad för att ta fram en bergmekanisk enhålstolkning av borrhål KFM01A i Forsmark. Geologisk data består av sprick- och bergartskartering av borrhålet, laboratorietester samt data från tidigare projekt i Forsmark (före maj 2004). De empiriska systemen RMR (version 1989) och Q (version 2002) användes för att uppskatta de mekaniska egenskaperna hos bergmassan längs borrhålet för karakterisering syfte. Systemen klassar bergmassan som ”mycket bra berg” (RMR > 81, Q > 40) i större delen av borrhål KFM01A. ”Bra berg” (80 < RMR < 61, 40 > Q > 10) bedöms t o m ett djup på 300 m. Sämre berg observeras vid 380–410, 480–490, 610–620, 650–685 och runt 850 m djup.

Bergmassans deformationsmodul är bestämd baserad på de empiriska sambanden med RMR- och Q-systemen och ges inte som en funktion av bergspänningen. Deformationsmodulen varierar mellan 45 och 70 GPa med en markerad ökning mot djupet som beror på minskad sprickfrekvens och bättre sprickegenskaper. Också den enaxiella tryckhållfastheten, kohesionen och friktionsvinkeln bestäms för bergmassan, tolkad som ett kontinuum medium. Bergmassans mekaniska kvalité och egenskaper visar sig vara skalberoende, vilket påvisar hur viktigt det är att använda rätt skala vid varje tillämpning av egenskaperna. Studien behandlar också temat om osäkerheter vid bestämning av bergmassans mekaniska kvalité och egenskaper. Den använda metodologin för bergmassans karakterisering samt lagringen av resultat i SKB:s SICADA databas också diskuteras.

Contents

1 Introduction

The site investigations carried out according to the program /SKB, 2001a/ produce a huge amount of geological/geothechnical information that can be used to evaluate the quality of the rock mass from a rock mechanics point of view. The objective of rock mechanics is then to infer the mechanical properties of the rock mass to be provided for the characterisation of the site and for the design of the underground excavations and their performance.

The results of this study on the empirical characterisation of the rock mass at Forsmark, and in particular along borehole KFM01A, will be part of the material on which next Site Descriptive Model versions (1.1 /SKB, 2004/ and 1.2) will be built on and developed starting from the version 0 /SKB, 2002/.

It is very likely that some of the assumptions and conclusions of this report will be improved or changed based on the future development of the Site Descriptive Model, thanks to its great potential for comparison, combination and integration of different disciplines and data sources (eg. surface features, other boreholes, laboratory tests, numerical models, etc).

1.1 Background

Borehole KFM01A is an almost vertical cored borehole with bearing direction of 318° and inclination of 85°. The total depth of the borehole is about 1,003 m. The first 100 m of the borehole were percussion drilled, thus there is no core available down to this depth. In Figure 1-1, the location of borehole KFM01A is given with respect to the candidate area of the Forsmark site /SKB, 2004/. The borehole is located on the western edge of the candidate area for the spent fuel deep repository in Forsmark, and it is just south of the nuclear power plants.

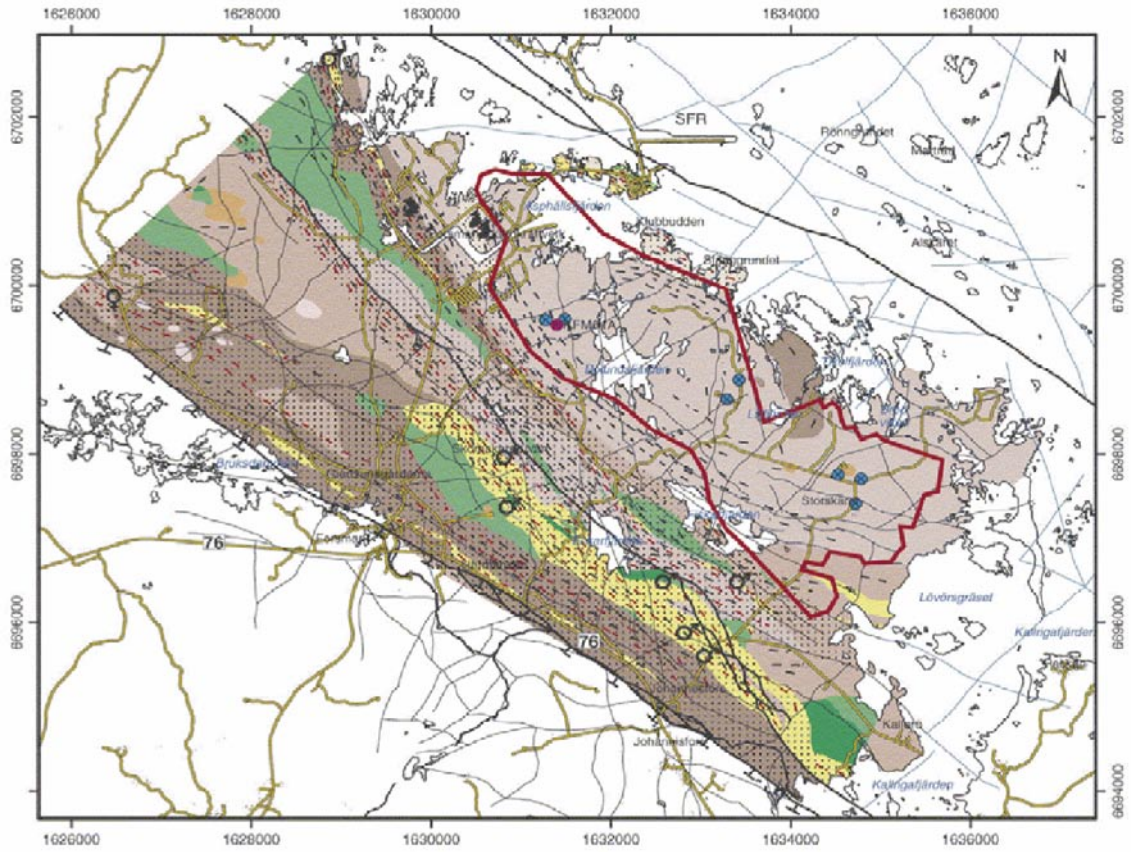

Figure 1-1. *Overview of the bedrock geology at the Forsmark site with indication of the candidate area and borehole KFM01A.*

1.2 Objectives

The objectives of this study are as follows:

- Evaluate the rock mass quality along borehole KFM01A by means of the empirical systems RMR and Q;
- Quantitatively characterise the rock mass by determining its deformation modulus, Poisson's ratio, uniaxial compressive strength, cohesion and friction angle;
- Identify pseudo-homogeneous rock domains and estimate their average mechanical properties;
- Discuss the issues of characterisation such as spatial variability, uncertainty, biases and scale effects;
- Comment on the collection of the input data and their processing for the purpose of characterisation.

1.3 Scope

The characterization of the rock mass along the borehole is performed mainly based on data that come directly from the borehole (geological "single-hole interpretation" /Carlsten et al. 2004/). This enables for a determination of the rock mass quality that applies locally and can highlight the spatial variation of the quality along borehole KFM01A. Exceptions are made every time the available data is inexistent or insufficient for the empirical rock quality evaluation.

This report is structured as follows:

- Summary of the BOREMAP data on rock types and fractures available by May, 2004. The fracture sets occurring along the borehole are illustrated together with their frequency and spacing;
- Summary of the mechanical properties of the common rock types at the site and of the rock fractures available by May, 2004. The statistics of the available mechanical properties are summarized;
- Application of the empirical systems RMR and Q for determination of the rock quality along borehole KFM01A. The determination of the input parameters is illustrated as well as spatial variation, scale effect and uncertainty are investigated;
- Determination of the continuum equivalent mechanical properties of the rock mass based on empirical relations to RMR and Q. The deformation modulus, Poisson's ratio, uniaxial compressive strength, cohesion and friction angle of the rock mass are determined and shown as a function of depth. In general, the deformation modulus is not given as a function of the rock stress. The uncertainties of the deformation modulus determination are also treated.
- Discussion of the results. In particular, the correlation RMR-Q is observed as well as the comparison between the histograms of the deformation modulus obtained by means of the two methods;
- Processing and storage of the results in to SICADA.

2 Boremap data

Borehole KFM01A was mapped by examining the core and the BIPS pictures taken on its wall /Petersson and Wängnerud , 2003/. The geological parameters obtained and stored in SKB's geological database SICADA were:

- Frequency of the fractures
- RQD evaluated on core lengths of 1 m
- Rock type, rock alteration and structural features.

In BOREMAP, each fracture observed along the borehole was classified among "open" or "closed" ("sealed"). The following geological features of the fractures were observed:

- Depth of occurrence
- Mineralization or infilling
- Roughness and surface features
- Alteration conditions
- Orientation (strike and dip)
- Width and aperture.

A direct estimation of the Q-parameter Joint Alteration Number (J_a) was performed by the geologists during the site investigations. The information listed above is contained in the geological and rock mechanics digital database SICADA by SKB.

For the rock mass characterisation by means of empirical methods, only the "open fractures" were considered in terms of fracture orientation, frequency, size and strength. The rock mechanics evaluation of the geological information made use of some more parameters:

- Bias correction of the orientation and spacing by Terzaghi's weighting
- Assignation of each fracture to fracture sets or to a group of random fractures.

The recognition of the main fracture sets occurring in the rock mass along the borehole was based, not only of the BOREMAP information directly available, but also on the indications of earlier studies for the construction of the Unit 3 of the Nuclear Power Plant and for the SFR repository for low and intermediate active nuclear waste (Figure 2-1) /Carlsson and Olsson, 1982; Carlsson and Christiansson, 1987/. For this purpose, also the newly collected data at the drilling stations for borehole KFM02A–B and KFM03A–B were considered to reduce the bias due to the borehole linear sampling of fractures /Hermanson et al. 2003/. The fractures in borehole KFM01A were assigned to the five main fracture sets predicted for the site according to windows similar to those shown on the pole plot in Figure 2-2. Table 2-1 show a summary of the fracture set orientations with some of the Fisher's constant that quantify the dispersion /SKB, 2004/. Some of the fractures at different depth were not assigned to any fracture set (random fractures).

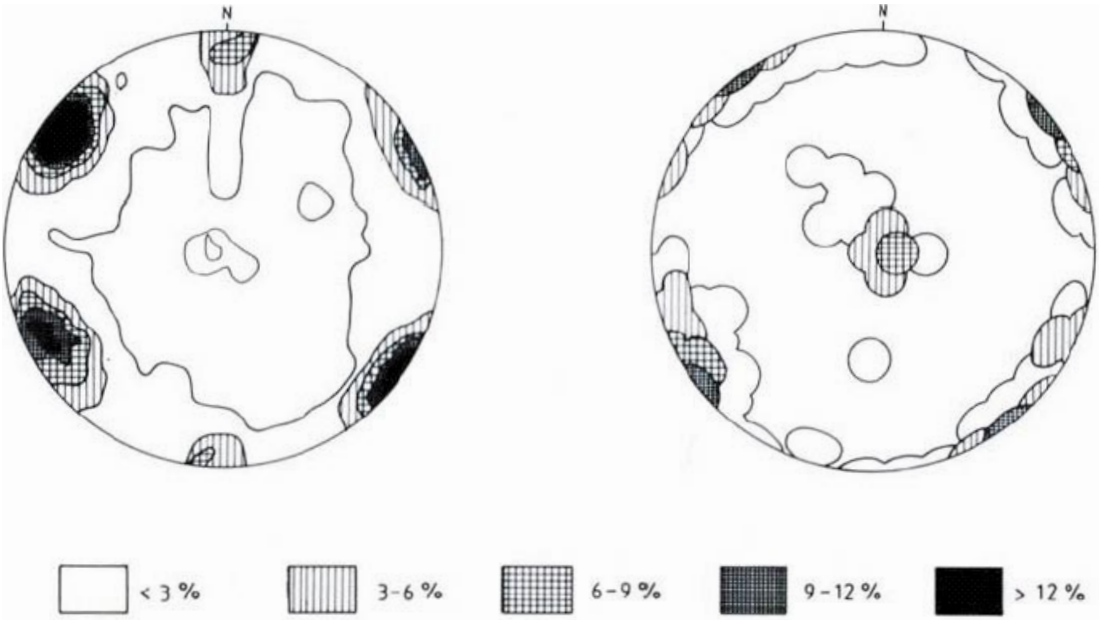

Figure 2-1. *Equiangle pole plots of the fractures mapped at the SRF repository (left) and at the Unit 3 of the Power Plant (right) /Carlsson and Christiansson, 1987/.*

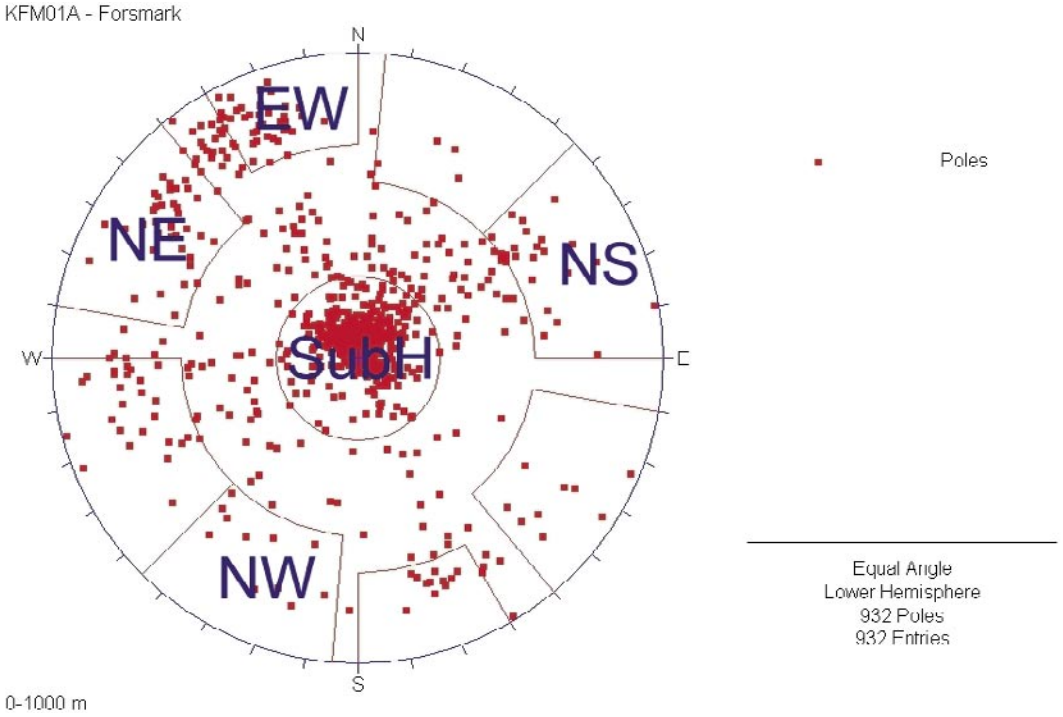

Figure 2-2. *Equiangle pole plots of the fractures logged along borehole KFM01A and indication of the main fracture sets. The borehole orientation is 318/18.*

Table 2-1. Summary of the fracture set analysis of the BOREMAP data for borehole KFM01A (see also /SKB, 2004/).

Fracture set	Weighted mean strike/dip angle (right hand rule)	Number of fractures	Fisher's K constant
EW	094/86	34	10.7
NW	139/87	89	10.1
NE	053/84	592	17.4
NS	354/82	191	19.3
SubH	060/11	609	11.8

Figure 2-3 show the total fracture frequency, the frequency of the sub-horizontal fracture set, the RQD and the number of fracture sets contemporarily occurring at the same depth for the open fractures. As it can be observed, the total fracture frequency is moderate (i.e. 3–5 fractures/m) up to a depth of 300 m. This observation is also supported by SRF's data that give a fracture frequency of about 5 fractures/m /Hagkonsult, 1982a/. For larger depth, the frequency along the borehole drops significantly down to less than 2 fractures/m, with the exceptions of two locations at about 400 and 660 m, respectively. The background frequency below 300 m is less than 1 fracture/m. A similar pattern can be seen on the frequency distribution of the sub-horizontal fractures. While the high frequency in the upper 300 m of the core is mainly due to frequency of the sub-horizontal fractures, this does not seem to contribute to the peaks of the total frequency at 300, 400 and 660 m. This can be explained by the fact that the two frequency peaks are primarily due to sub-vertical fractures. This observation is confirmed by the plot of the number of fracture sets observed at each depth. This diagram shows how many of the five recognised fracture sets occur at different depths. It can be observed that the five fracture sets never appear at the same time for a certain depth. Three or four fracture sets are observed frequently above 400 m depth and at the depth of 400, 660 and 840 m. Along the rest of the borehole, only one or two fracture sets are generally observed. Due orientation of the borehole, the bias due to the preferential sampling of the sub-horizontal fractures by the vertical borehole cannot be completely avoided. Figure 2-3 also shows the main rock type groups occurring at the site.

Similarly to the total fracture frequency, RQD is slightly lower in the upper 400 m of the borehole than in the deeper part. A very localised minimum can be observed for a depth of 400 m. For larger depths, RQD is generally, with a few exceptions, equal to 100.

The spacing of each fracture set was evaluated taking into account the Terzaghi's correction for the fracture orientation with respect to the borehole axis. In Figure 2-4, the variation of spacing with depth for all the fracture sets is given. It can be observed that the fracture spacing of all fracture sets is larger than 10 m for most of the borehole deeper that about 550 m.

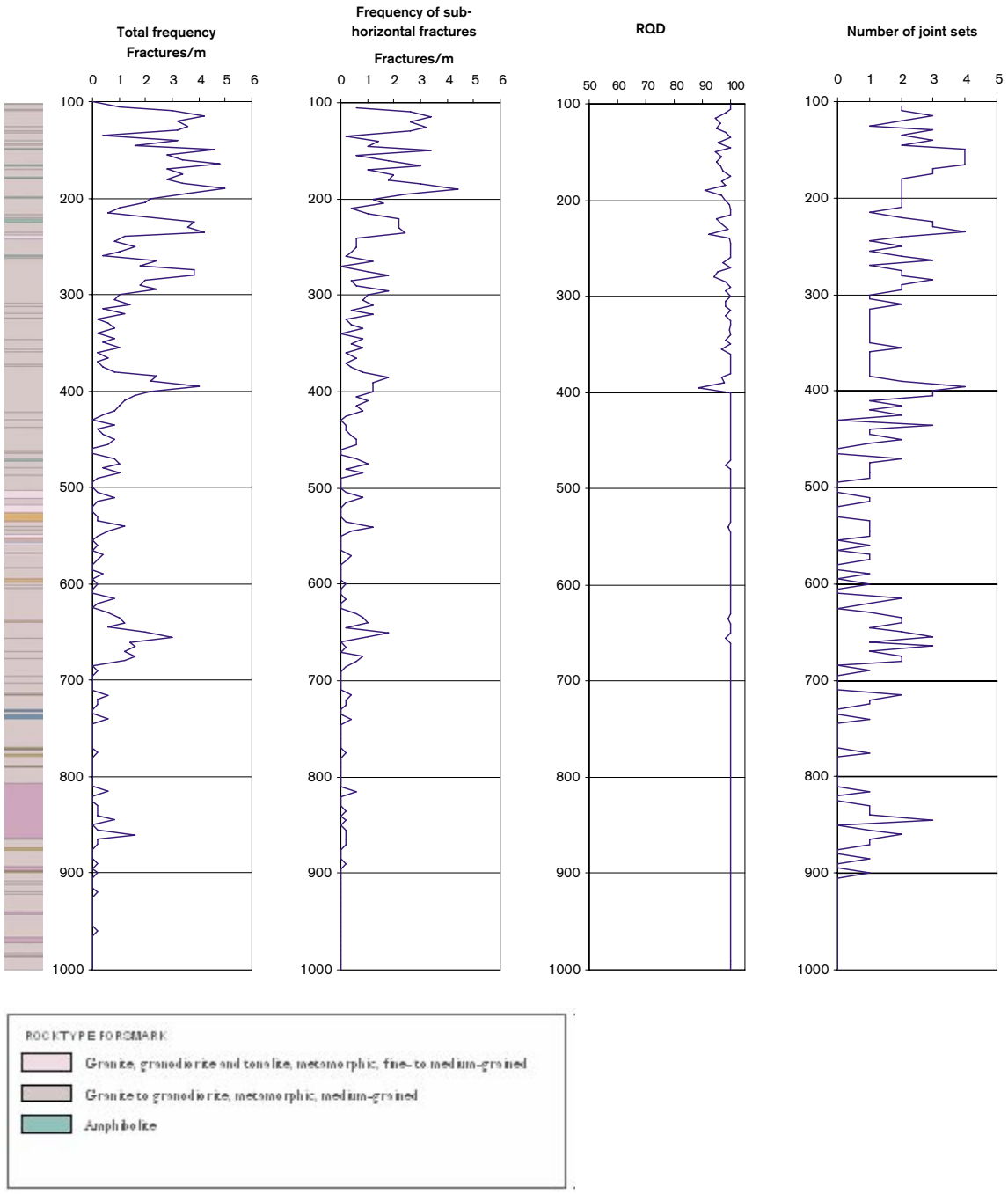

Figure 2-3. *Variation of the total fracture frequency, frequency of the sub-horizontal fractures, RQD and number of "joint" (fracture) sets with depth for borehole KFM01A. The values are averaged for each 5 m length of borehole.*

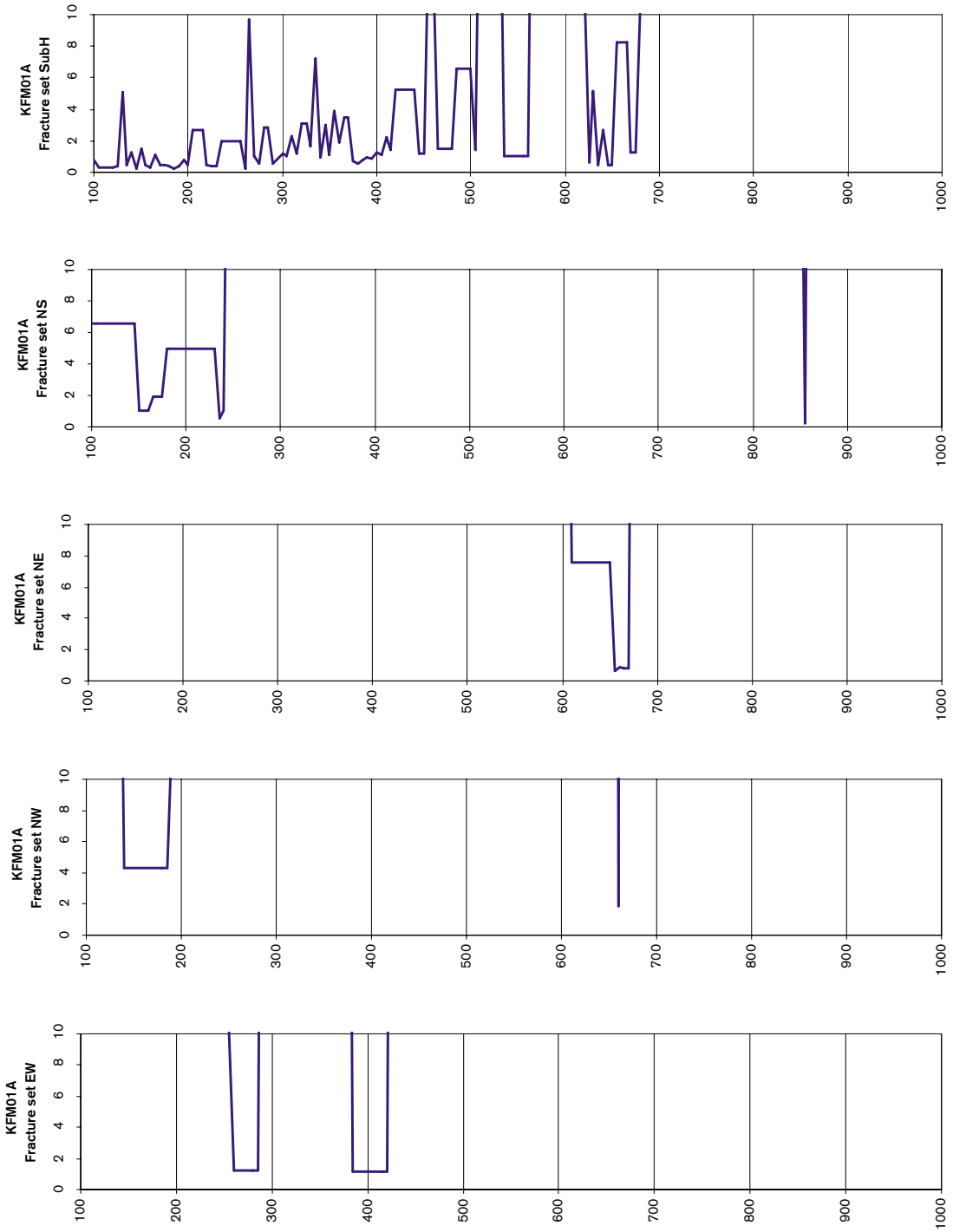

Figure 2-4. *Fracture spacing with depth for the five observed fracture sets in borehole KFM01A. The values are averaged for each 5 m length of borehole.*

3 Mechanical tests

Most of the available results of mechanical tests were collected for the design of the SRF repository for low and medium active waste. Samples were collected from boreholes KFR19, KFR20, KFR21, KFR22, KFR23, KFR24, KFR25 and KFR27 between the ground surface and a depth of about 250 m. The following tests were carried out between 1981 and 1985 on intact rock samples and rock fractures /Hagkonsult, 1982a,b; Delin, 1983; Stille et al. 1985/:

- 88 uniaxial compressive tests
- 40 determination of the Young's modulus and Poisson's ratio
- 162 point load tests at the site and 88 in laboratory
- 17 determination of the intact rock density
- 11 shear tests on natural rock joints.

Additionally, 41 tilt tests on rock joints were performed after the drilling of borehole KFM01A according to ISRM recommendations /Chryssanthakis, 2003/. The tests were conducted on the different rock types observed at the site, which means gneiss, metavolcanic rock, pegmatite, gneissic granite and mylonite. The geological investigations at SFR show that about 70% of the rock consists of gneissic granite, followed by 20% of pegmatite, and about 10% of metavolcanic rock (amphybolite). To mirror this distribution at SFR, about 63% of the samples were taken in gneissic granite and gneiss, 18% in metavolcanic rock and 21% in pegmatite. However, the rock type mapping of borehole KFM01A shows a rather different rock type distribution: 82% granodiorite, 7% amphybolite, 5% tonalite, 3% granite and 2% pegmatite.

3.1 Intact rock properties

In this section, a summary of the mechanical properties of the intact rock is given for laboratory tests and point load test (see also Appendix A). The test results show that the mechanical properties recorded are typical for Swedish host rock (Table 3-1) /Delin, 1983; Stille et al. 1985/. The uniaxial compressive strength of the rock is derived from the size-corrected Point Load Index $I_s(50)$ (Table 3-2, Table 3-3). During the investigations for the SFR, it was observed that the values of the uniaxial compressive strength correlated well with the $I_s(50)$ when this was multiplied by 20 (instead of 24, as suggested in the literature) /Hagkonsult, 1982a,b/. The point load tests in laboratory were mainly carried out on dry samples. Saturated samples showed a 14% lower uniaxial compressive strength than the dry samples.

Table 3-1. Summary of the mechanical properties from uniaxial compressive tests on intact rock samples /Hagkonsult, 1982b; Delin, 1983; Stille et al. 1985/.

Rock type	Mechanical property	Minimum	Average	Median	Maximum	Standard deviation
Gneiss	UCS (MPa)	119	248	262	322	52
	E (GPa)	60	78	77	93	7
	ν (–)	0.20	0.23	0.22	0.29	0.03
	Density (g/cm^3)	2.64	2.65	2.64	2.67	0.01
Metavolcanic rock	UCS (MPa)	31	118	127	212	57
	E (GPa)	55	80	81	101	23
	ν (–)	0.33	0.37	0.36	0.43	0.04
	Density (g/cm^3)	2.86	2.89	2.89	2.91	0.02
Pegmatite	UCS (MPa)	80	148	151	198	28
	E (GPa)	41	70	75	83	13
	ν (–)	0.11	0.24	0.26	0.32	0.06
	Density (g/cm^3)	2.63	2.63	2.63	2.64	0.01
Gneissic granite	UCS (MPa)	87	234	234	330	69
	E (GPa)	62	72	73	84	6
	ν (–)	0.17	0.21	0.22	0.23	0.02
	Density (g/cm^3)	–	–	–	–	–
All rock types	UCS (MPa)	31	203	203	330	69
	E (GPa)	41	75	76	101	6
	ν (–)	0.11	0.24	0.23	0.43	0.02
	Density (g/cm^3)	2.63	2.70	2.64	2.91	0.11

Table 3-2. Summary of the uniaxial compressive strength UCS from point load tests performed in-situ on intact rock samples /Hagkonsult, 1982b/. (The values in brackets are the absolute minima.)

Rock type	Minimum UCS (MPa)*	Average UCS (MPa)*	Median UCS (MPa)*	Maximum UCS (MPa)*	Standard deviation UCS (MPa)*
Gneiss	14	248	271	381	82
Metavolcanic rock	(4) 8	99	117	250	78
Pegmatite	13	163	180	283	89
Gneissic granite	13	276	298	360	66
Mylonite	7	179	209	344	119
All rock types	(4) 8	212	241	381	106

* The values are obtained through an empirical relation from the Size-corrected Point Load Index $I_S(50)$ with proportionality constant equal to 20.

Table 3-3. Summary of the mechanical properties from point load tests performed in laboratory on intact rock samples /Hagkonsult, 1982b; Delin, 1983; Stille et al. 1985/.

Rock type	Mechanical property	Minimum	Average	Median	Maximum	Standard deviation
Gneiss	UCS* (MPa)	106	243	239	350	53
	IS50 (MPa)	5.3	12.2	11.9	17.5	2.6
Metavolcanic rock	UCS* (MPa)	50	143	134	256	62
	IS50 (MPa)	(0.2) 2.5	7.1	6.7	12.8	3.1
Pegmatite	UCS* (MPa)	66	179	184	274	60
	IS50 (MPa)	3.3	8.9	9.2	13.7	3.0
Gneissic granite	UCS* (MPa)	126	207	208	272	33
	IS50 (MPa)	6.3	10.3	10.4	13.6	1.7
All rock types	UCS* (MPa)	(4) 50	202	210	350	65
	IS50 (MPa)	2.5	10.2	10.5	17.5	3.3

* The values are obtained through an empirical relation from the Size-corrected Point Load Index $I_S(50)$ with proportionality constant equal to 20.

3.2 Rock fracture properties

In this section, a summary of all available results by May, 2004, on shear and tilt tests on rock fractures is presented /Stille et al. 1985; Chryssanthakis, 2003/. The frictional parameters and the normal and shear stiffness of 11 samples of rock fracture were determined in laboratory for assigned stress levels. The data are presented in Table 3-4 by assigning the samples to the five identified fracture sets described in Section 2 (Table 2-1).

Table 3-5 summarizes the results of tilt tests performed on rock fractures sampled from the core of borehole KFM01A. Each fracture set is provided with a range of variation of the basic friction angle, Joint Roughness Coefficient (JRC), Joint wall Compressive Strength (JCS) up-scaled to 100 cm and the residual friction angle /Chryssanthakis, 2003/.

From the data summarised in Table 3-5 and Appendix B, it is possible to make some comments about the parameter variation with depth and their correlation with each other. The basic friction angle appears rather constant with depth without much difference between the fracture sets. JRC is lowest for fracture set SubH and slightly diminishes with depth for all fracture sets. Fracture set EW appears at the surface and exhibits the largest JRC among all samples. JCS spans between 50 and 150, with lowest values for fracture set SubH and highest for NE, respectively. The residual friction angle shows a positive correlation with JCS.

Table 3-4. Summary of the results of shear tests performed on rock fractures /Stille et al. 1985/.

Fracture set	Normal stiffness (MPa/mm)	Shear stiffness (MPa/mm)	Friction angle 1 (°)	Friction angle 2 (°)	Apparent cohesion (MPa)
Stress range (MPa)	0.04–0.9	1.6	0–0.5	0.5–1.5	0.5–1.5
EW	37	4.8	48	35	0.2
NW	29	4.4	51	37	0.4
NE	31	2.8	48	29	0.4
NS	24	2.7	48	30	0.3
SubH	24	8.3	55	32	0.4
Random	25	10.4	54	38	0.5
All joints	32	5.4	51	35	0.4

Table 3-5. Summary of the results of tilt tests performed on rock fractures /Chryssanthakis, 2003/.

Fracture set	Number of samples	Basic friction angle (°)	JRC (100)	JCS (100)	Residual friction angle (°)
EW	4	25–31	5–9	61–141	21–25
NW	1	29	7	105	24
NE	6	28–32	4–7	106–156	25–31
NS	4	24–31	4–8	93–126	20–29
SubH	15	27–31	2–9	62–134	22–29
Random	10	24–31	4–9	65–136	20–30
All joints	40	29	6	102	25

4 Characterisation of the rock mass along the borehole

According to the methodology for rock mass characterisation /Andersson et al. 2002; Röshoff et al. 2002/, two empirical classification systems have been chosen for the purpose of determination of the mechanical property of the rock mass: the Rock Mass Rating (RMR) /Bieniawski, 1989/ and the Rock Quality Index (Q) /Barton, 2002/. These classification systems are used here for the "characterisation" of the rock mass, in contraposition to their general use for "design" of underground excavations. Thus, considerations about the shape and orientation of the excavation are neglected as well as technical considerations about stability and stress related problems. Moreover, some of the ratings and indexes are assumed in agreement to the suggestions expressly provided for characterisation of the rock mass by the Authors.

The RMR and Q systems are applied to borehole sections of 5 m and 20 m. This means that, for every borehole section, the range of possible variation of the indexes and ratings was identified based on the raw data. A range of physically possible values of Q and RMR are obtained and, based on them, a range of possible mechanical properties of the rock mass.

This technique can be applied to the mean values of the indexes and ratings so that a range of variation of the mean rock quality can be identified. This will mirror the spatial variability of the parameter better than the degree of confidence in the choice of each particular index or rating. The range of variation of the mean value can be used to quantify the natural variability of a certain derived rock parameter or mechanical property. The differences between the ranges of the possible maximum and minimum value of a rock property, on one side, and the range of variation of the mean value, on the other side, would give a measure of the "confidence" on the rock mass property.

4.1 Equations for RMR and Q

The very well known relations for RMR /Bieniawski, 1989/ and Q /Barton, 2002/ are reported here for convenience of the reader:

$$RMR = RMR_{strength} + RMR_{RQD} + RMR_{spacing} + RMR_{conditions} + \\ + RMR_{water} + RMR_{orientation} \quad (1)$$

where the subscripts strength, RQD, spacing, conditions, water, orientation refer to the strength of the intact rock, the Rock Quality Designation (RQD), the conditions and spacing of the fractures, the groundwater conditions and the orientation of the fracture sets with respect to the hypothetical tunnel orientation, respectively. In the references, each rating is provided with a description and a table.

For Q, the equation is:

$$Q = \frac{RQD}{J_n} \times \frac{J_r}{J_a} \times \frac{J_w}{SRF} \quad (2)$$

where, besides RQD, J_n depends on the number of fracture joint sets, J_r and J_a on the roughness and alteration of the fractures, J_w on the groundwater conditions and the Stress Reduction Factor (SRF) takes into account the effect of the stresses and fracture zones on the strength and deformability of the rock mass. Also these parameters are described and tabulated in the references.

4.2 Input parameters for RMR and Q

RQD is a parameter used by both the empirical systems. RQD was provided by the geological investigations for each metre of core length. For coherence with the assumed characterisation length, the values are averaged for each 5 and 20 m, respectively. Minimum, average, most frequent and maximum values are also determined. For the Q system, the values of RQD are inputted directly, while the correspondent RMR ratings are determined by means of Chart B /Bieniawski, 1989/.

The orientations of the fractures mapped along borehole KFM01A are plotted on a lower hemispherical equiangle projection in Figure 2-2. Based on the results of the fracture set analysis in Section 3.2, the fractures are assigned to five fracture sets. Some of the fractures do not appear to belong to any of the sets, thus are assigned to a group of fractures called "random".

Based on the distance between the fractures, the fracture spacing can be evaluated. Along the borehole, sections of rather constant total frequency are isolated. For each of the sections, the minimum, average, most frequent and maximum spacing are determined for each fracture set separately as shown in Section 3.2. Terzaghi's weighting is applied for reducing the bias due to the orientation of the borehole with respect to the fracture orientation. Fracture spacing is used for determining the rating for RMR according to Chart C in /Bieniawski, 1989/. In this case, the minimum, average and most frequent and maximum spacing are chosen from all values for all the fracture sets.

Among the fractures occurring inside each 5 or 20 m core length, the fracture sets determined in Section 3.2 are recognised. In most of the cases, only some of the fracture sets are represented by at least one fracture. The number of fracture sets for the Q system is counted based on the represented fracture set in the core section. If more than 10% of the total number of fractures can not be assigned to the fracture sets, then the group "random fractures" is considered. According to Figure 2-3, the number of fracture sets occurring at the same time for each core section varies between zero and four. This method implies that the core sections of 20 m length exhibit more fracture sets because the longer the section, the higher the probability that fractures with different orientations are sampled. The Q value determined on longer core section is then expected to be smaller than that for short sections.

The fracture length, that gives a measure of the persistence and continuity of the fractures, is largely unknown. Based on earlier experiences at the SFR Repository, the fracture length is estimated on average about 3 m. This value happens to be one of the thresholds suggested by /Bieniawski, 1989/ for the classes in Chart E. For this reason, a rating of 3 (fracture length of about 3 m) is assumed here for the average and most frequent value, while 4 and 2 are assumed for the maximum and minimum expected values (fracture length of 1 m and 10 m), respectively.

The uniaxial compressive strength of the intact rock is used in RMR, and indirectly in Q for determining Q_c. There are not yet available results from compression tests on rock samples taken from borehole KFM01A. Thus, the data in Section 3.1 are used for estimating the strength of the intact rock. The range of values for the uniaxial compressive strength and RMR strength ratings used in this report are listed in Table 4-1. These values also seem to summarize well the results from in-situ point load and laboratory tests (Table 3-4).

For the parameters quantifying the roughness of the fractures, the descriptions provided by the geological core mapping in terms of roughness and surface properties are used. Table A3 in /Barton, 2002/ and Chart E in /Bieniawski, 1989/ are applied. For Q, fracture roughness, aperture and infilling information are combined to obtain the Joint Roughness Number J_r and the Alteration Number J_a. In the data from SICADA used in the present characterisation, all open fracture with aperture smaller than 1 mm are given a width of 1 mm and an aperture of 0 mm because the applied aperture determination technique is not able to measure it more accurately. This does not have a remarkable influence on Q parameters, but it does on RMR aperture classes. For this reason RMR rating for aperture can never be the highest (6), which applies to clean and open fractures with aperture smaller than 0.1 mm. This drawback was later removed, but the fracture mapping had to be repeated again. The new results were not available by the time the characterisation in this report was carried out. Q is not sensitive to this bias.

The weathering rating for RMR (Chart E in /Bieniawski, 1989/) and J_a for Q (Table A4 in /Barton, 2002/) are deducted from the description of the fracture alteration and from the information about the thickness of the fracture infilling. Particular attention has been devoted to the records of gauge and clay fillings in the fractures.

Borehole KFM01A is observed to be almost dry for its whole length. The groundwater rating for RMR is therefore put to 15. For the Q-system, the Joint Water Reduction Factor (J_w) is assumed equal to 1.0, which applies to dry excavation and conditions of minor inflows. This case constitutes an exception to values suggested by /Barton, 2002/ because the hydraulic connectivity of the fractures is very low along most of the borehole (RQD/J_n varies between 5 and 200, with an average of 28).

The Stress Reduction Factor SRF for characterisation with Q is suggested by /Barton, 2002/ as 5, 2.5, 1 and 0.5 for depth increases from 0–5, 5–25, 25–250 to > 250 m, respectively.

RMR requires a rating that takes into account the orientation of the excavation with respect to the orientation of the fractures. For characterisation, this rating is chosen equal to zero as suggested by /Andersson et al. 2002/.

The RMR ratings and Q numbers are also presented in detail in Appendix C.

Table 4-1. Estimated uniaxial compressive strength of the intact rock and RMR strength rating for borehole KFM01A.

	Minimum	Average	Median	Maximum
Uniaxial compressive strength (MPa)	100	200	210	300
RMR strength rating	9.5	14	14.3	15

4.3 Characterisation by RMR

RMR and its ratings calculated for 5 m long core sections are shown in Figure 4-1 as a function of depth. The local variations of RMR are rather contained. A slight increase of the RMR is observed with depth. For depth smaller than 300 m, RMR classes the rock mass on average as "good rock" (61 < RMR < 80). RMR seems to stabilise for depths larger than 400 m, and its values correspond in average to "very good rock" (RMR > 81).

The difference between the minimum and mean RMR value (about 10 points) seems to be quite constant with depth. This is due to the assigned classes of the RMR-ratings. On the other hand, the difference between the mean and maximum RMR diminishes with depth down to 400 m (between 10 and 2 points), and then becomes almost constant.

If core sections of 20 m are considered (Figure 4-2), a general phenomenon of smoothing is observed for RMR and its ratings. The minimum RMR values envelope the graphs obtained for core sections of 5 m in a way that only the lowest minima are touched. The same phenomenon occurs for the maximum RMR values that are always smaller or equal to the results for 5 m core sections. In other words, most of the peaks with very high RMR values disappear from the charts. For what concerns the mean and frequent RMR values, they seem to average the results observed for 5 m core sections. Some depth delay can sometimes be observed for the peaks and troughs due to the way the 20 m core sections are isolated along the borehole.

4.4 Characterisation by Q

The input Q-numbers and Q values are shown in Figure 4-3 as a function of depth. Here, Q is plotted in a logarithmic scale due to its wide range of variation. For the first 200 m, Q seems to continuously diminish with depth. The rock is here classified as "good". Between 300 and 400 m the values are scattered around a Q value of 100 ("very good rock"). For depths larger than 400 m, the difference between the minimum, maximum and mean Q value becomes negligible, with the exception of some more fractured zones at about 400, 480, 620, 660 and 860 m. While the other fractured zones were already clearly visible from the plot of RQD and of the total fracture frequency, the zone at about 480 m seems to be caused by the heaver alteration conditions and smoother surface of the fractures. Like RMR, also Q suffers somewhat of the stepped way the numbers are tabulated. On average, the rock below 400 m is classified as "extremely good rock" by the Q-system (Q > 100).

Also for Q, the characterisation was performed for core length of 20 m for the purpose of comparison with RMR (Figure 4-4). In this case, the minimum, average, most frequent and maximum Q values follow the troughs of the correspondent diagrams for a core length of 5 m. This implies that in general the mean Q value diminishes when passing from a core section length of 5 m to one of 20 m. Thus, the averaging effect observed for RMR does not occur for Q. For Q, almost all the peaks with values of about 1,000 disappear when enlarging the scale of analysis, except for two very well defined peaks at about 755 and 800 m.

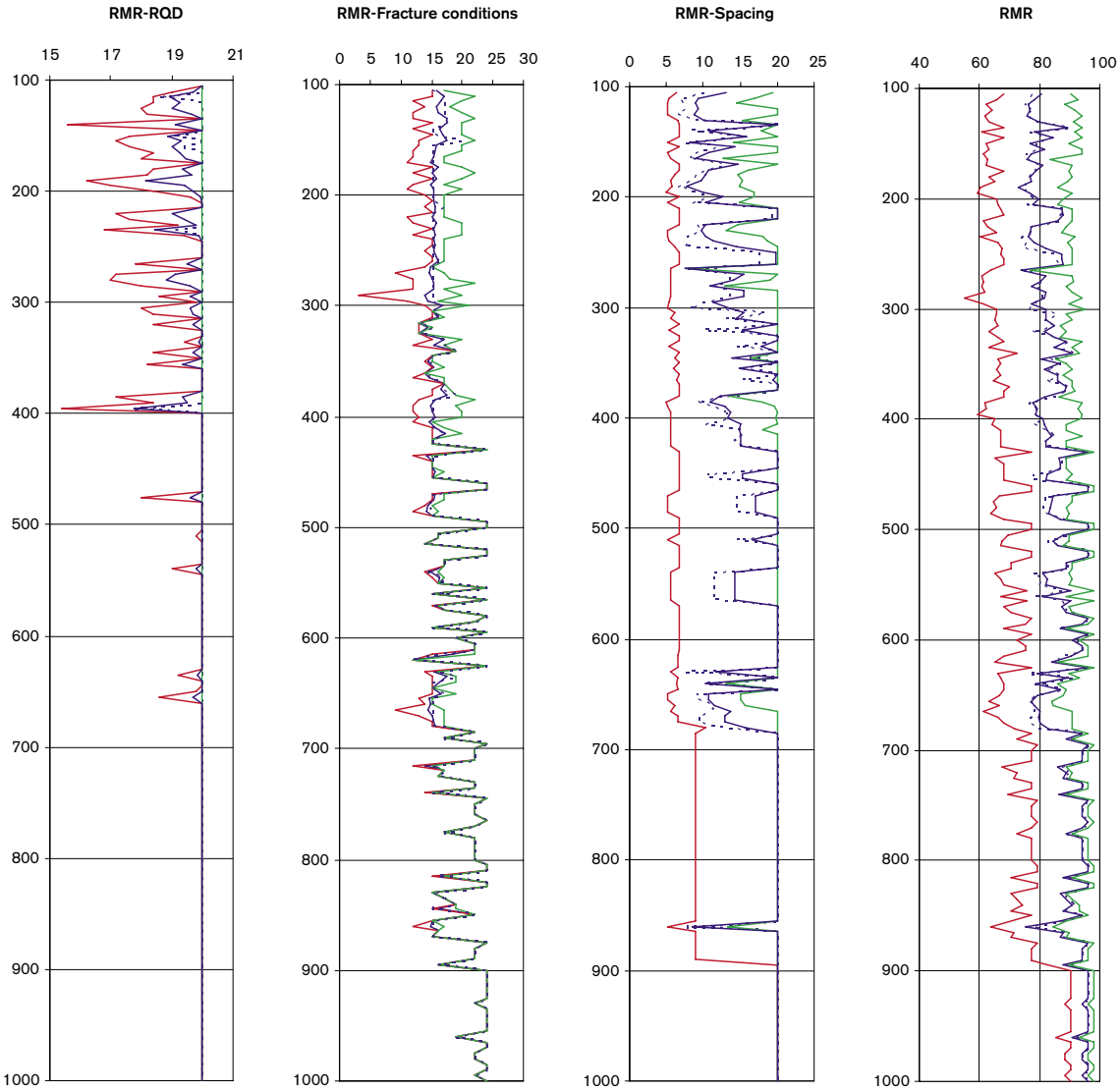

Figure 4-1. *RMR-ratings and RMR as a function of depth for borehole KFM01A. Minimum, average, most frequent and maximum values are plotted in red, blue, dashed blue and green, respectively. Core lengths of 5 m are considered.*

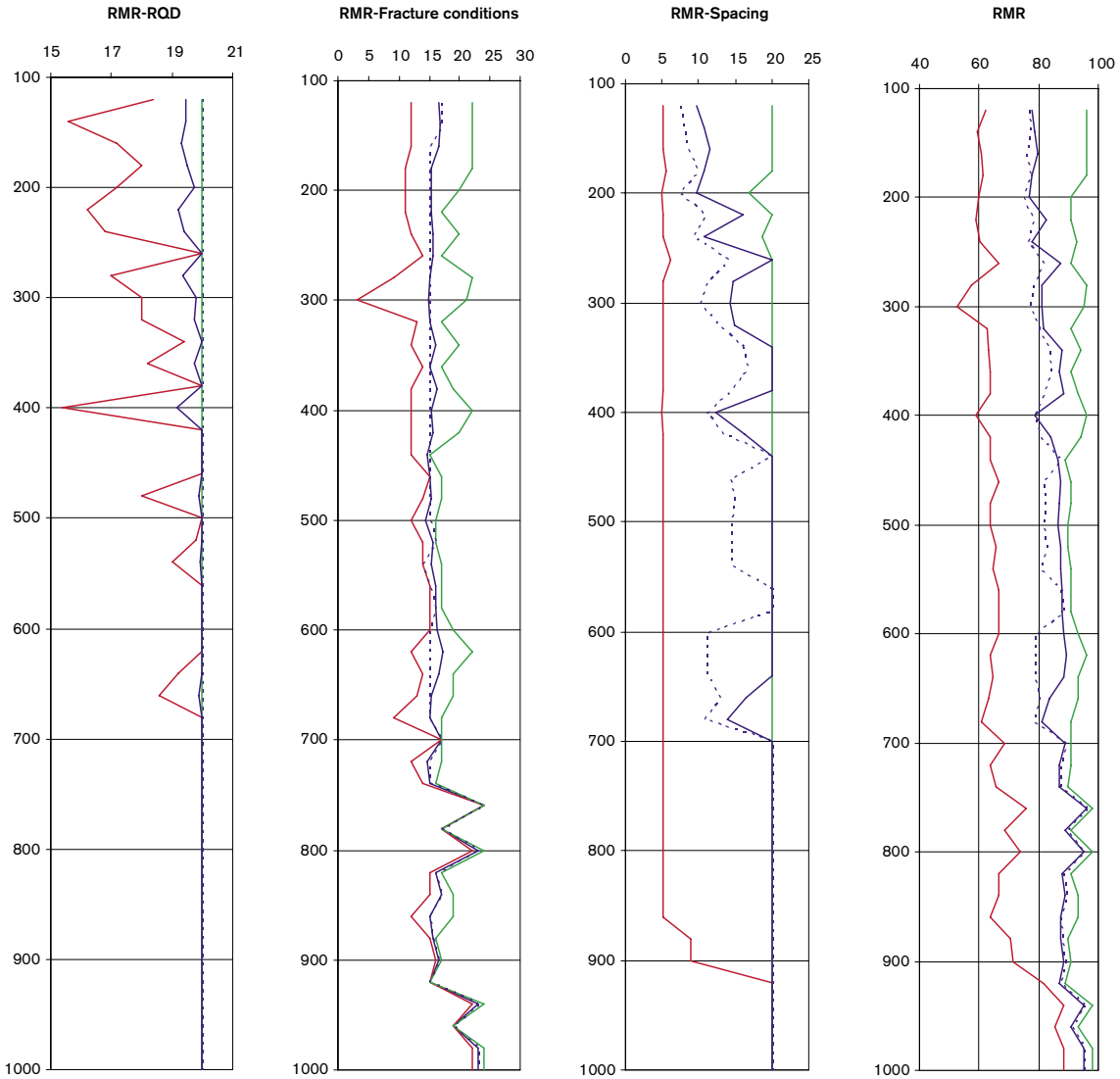

Figure 4-2. *RMR and RMR ratings as a function of depth for borehole KFM01A. Minimum, average, most frequent and maximum values are plotted in red, blue, dashed blue and green, respectively. Core sections of 20 m are considered.*

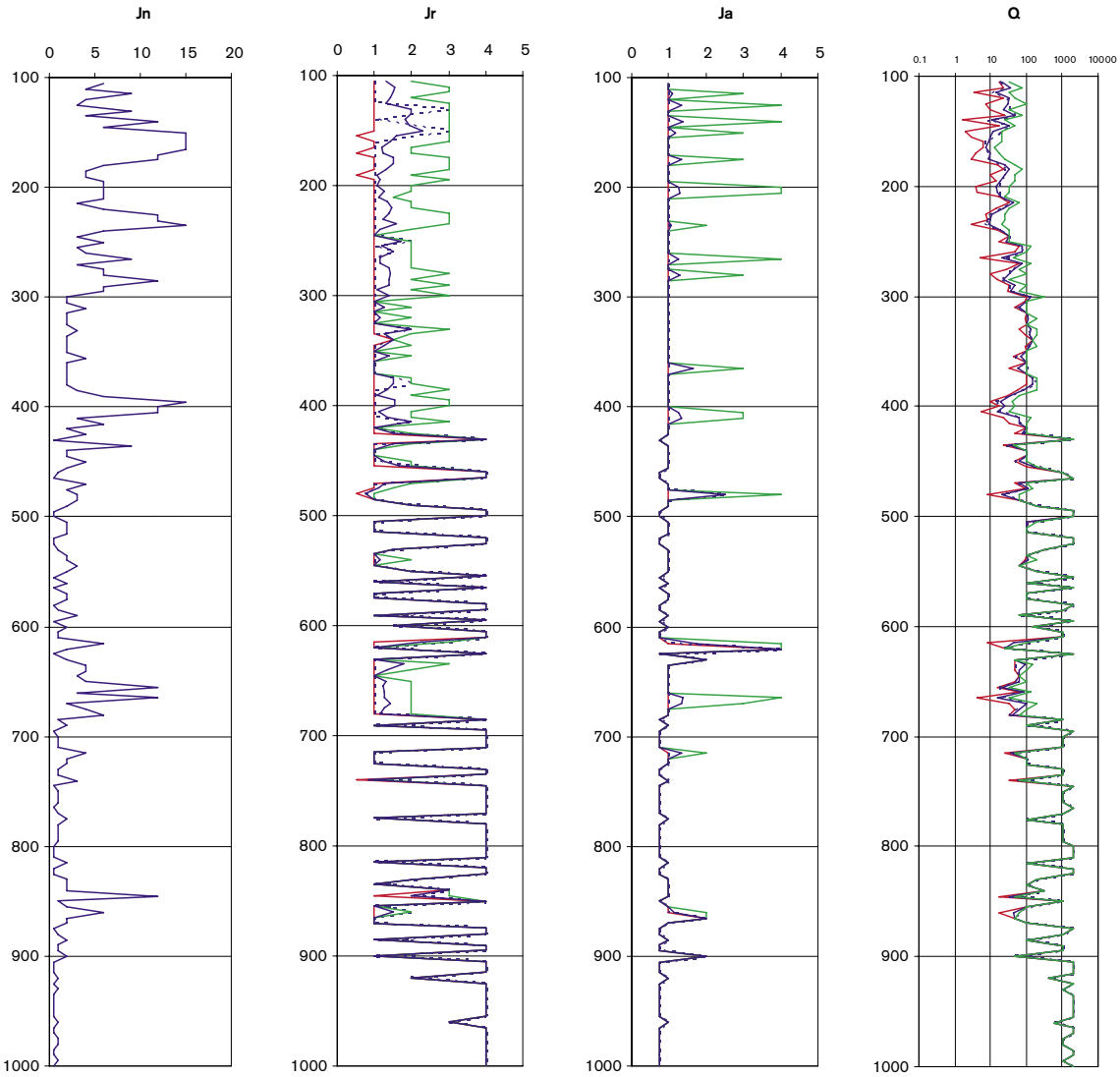

Figure 4-3. *Q and Q numbers as a function of depth for borehole KFM01A. Minimum, average, most frequent and maximum values are plotted in red, blue, dashed blue and green, respectively. Core lengths of 5 m are considered.*

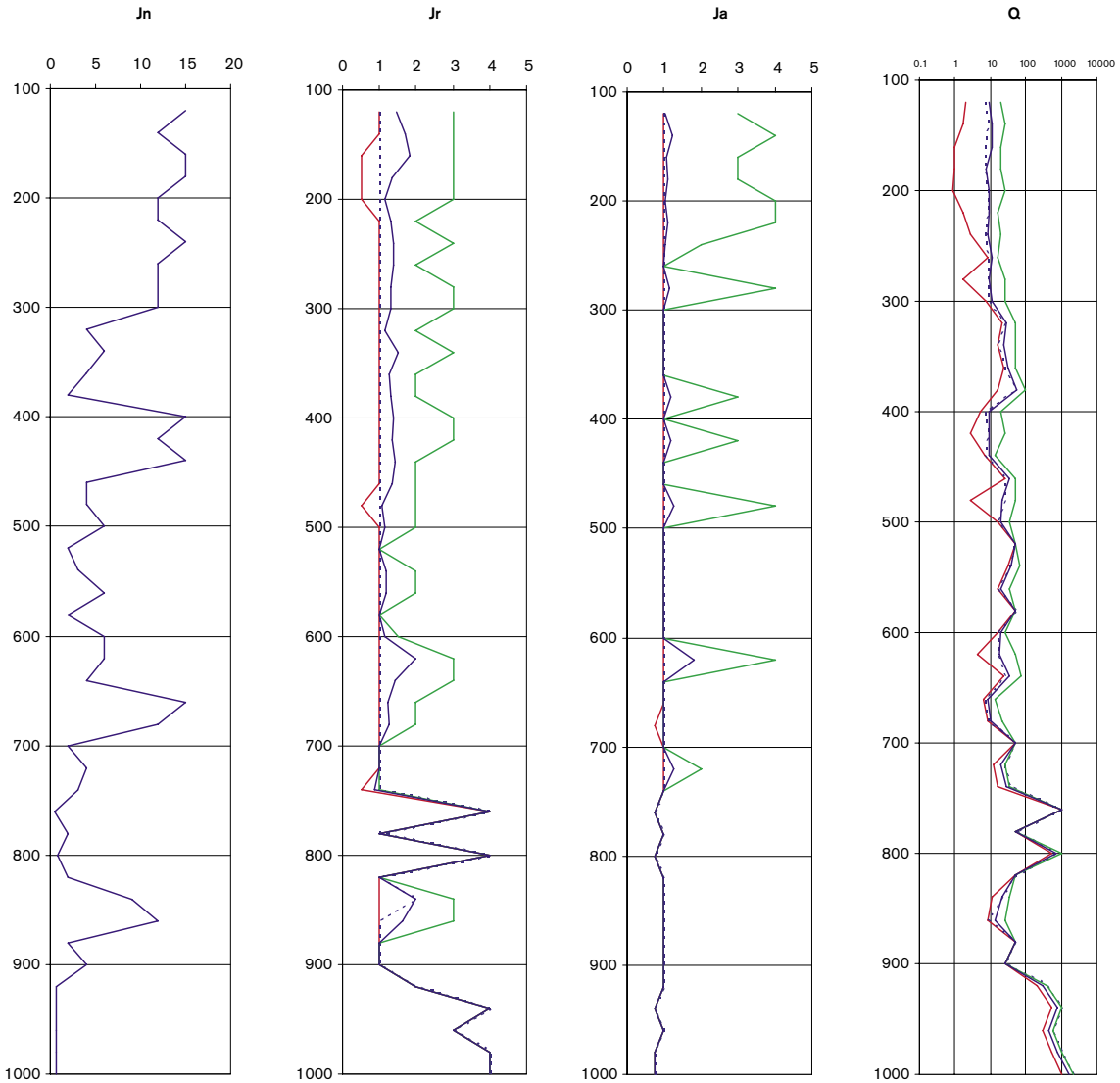

Figure 4-4. *Q and Q numbers as a function of depth for borehole KFM01A. Minimum, average, most frequent and maximum values are plotted in red, blue, dashed blue and green, respectively. core lengths of 20 m are considered.*

4.5 Partitioning the borehole into rock units

The borehole was partitioned into a number of pseudo-homogeneous “rock units”. These units do not necessarily coincide with the rock domains defined by the Site Descriptive Model for Forsmark version 0 /SKB, 2002/. However, the partitioning should not differ much from that that will be used for the identification of the site rock domains when information from surface surveying and other boreholes are gathered together in next site model (versions 1.1 and 1.2). At the time of the characterisation of borehole KFM01A reported here, the geological “single-hole” interpretation /Carlsten et al. 2004/ was not available.

Borehole KFM01A was divided into 9 rock units. This partitioning was chosen based on the analysis of RQD information, fracture spacing, number of occurring fracture sets and fracture properties reported in Figure 4-1 and Figure 4-3. Due to the lithological homogeneity of the rock along the borehole, rock types were not considered. The same partitioning was also adopted by /Barton, 2003/ for an independent characterisation of the borehole by Q-logging only.

Each rock unit contains a certain number of core sections of 5 or 20 m. Thus, a certain number of the minimum, average, most frequent and maximum values of the rock mass quality concern the same rock unit. If only the mean RMR and Q values are considered, then the variation from rock unit to rock unit would represent the spatial variability of the rock quality and show the value spans of the mean RMR and Q for the rock units in borehole KFM01A (Figure 4-5 and Figure 4-6).

When the data for the 20 m borehole interval contained in Figure 4-2 and Figure 4-4 are treated the same way as for the 5 m interval, the results are slightly different. In fact, each rock domain contains less core sections of 20 m compared to those of length of 5 m. A larger degree of averaging of the geotechnical parameters applies when longer core sections are considered. This results into much narrower variation spans for the mean RMR and Q. In other words, almost all local variability is hidden by the averaging process. Q shows more sensibility to the length of the core sections chosen for characterisation. In general, the mean value reduces to about 1/2 and sometimes to 1/10. This can be explained by the fact that longer core sections can contain fractures from several fracture sets. In consequence, J_n increases because more fracture sets are observed, and Q diminishes.

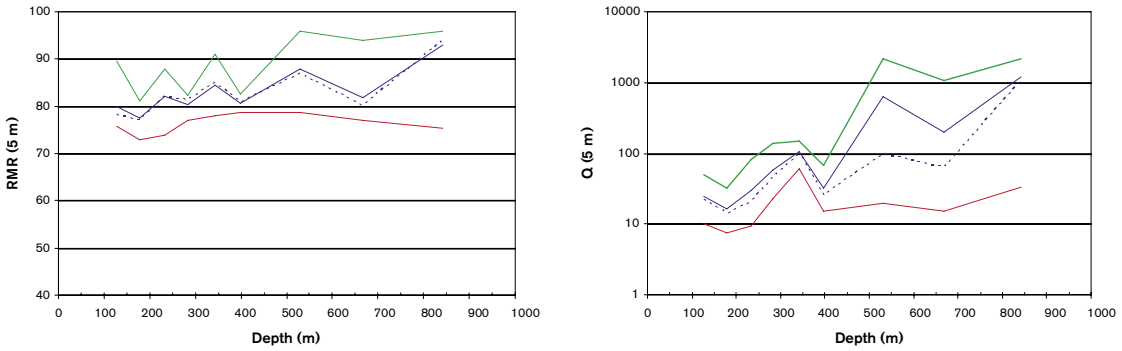

Figure 4-5. *Variation of RMR and Q for the rock units. Minimum, average, most frequent and maximum values are plotted in red, blue, dashed blue and green, respectively. Core lengths of 5 m are considered.*

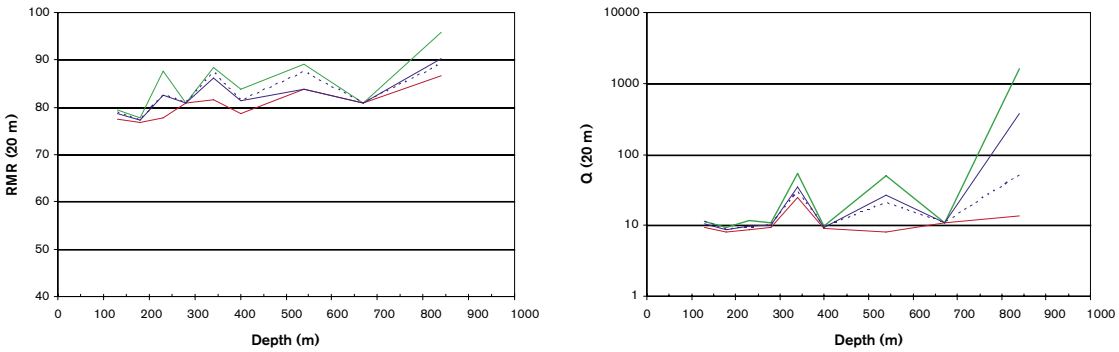

Figure 4-6. *Variation of RMR and Q for the rock units. Minimum, average, most frequent and maximum values are plotted in red, blue, dashed blue and green, respectively. Core lengths of 20 m are considered.*

4.6 Evaluation of uncertainties

When applying the empirical classification systems for characterisation of the rock mass, the uncertainties on the geological and rock mechanical data mirrors into the uncertainties of the indexes and ratings. Also the intrinsic uncertainties of the empirical characterisation methods as such have to be considered. These uncertainties derive from the way the empirical methods are built up, to the size of the database of case-histories and the generality of the cases on which they are based on, and to the lack of strict theoretical and constitutive equations supporting the structure of the empirical methods. The combination of the different indexes and ratings to obtain Q and RMR values is affected by all these kind of uncertainties.

The uncertainty on a single parameter can widely vary depending on the acquisition technique, subjective interpretation or size of the sample population. But uncertainty can also derive from the way the values of the indexes and ratings are combined with each other. The value of Q or RMR for a certain section of borehole may result from the combination of the possible ratings ranging from the minimum or maximum value occurring in a certain borehole interval or rock mass volume. For these reasons, it was decided here to correlate the uncertainty on Q and RMR to the range of their possible values derived from the width of the interval between the minimum and maximum occurring value of each index or rating in each core section. The range of the possible minimum and maximum values of RMR and Q is obtained by combining the ratings and indices in the most unfavourable and favourable way, respectively. This range of possible values is believed to estimate all uncertainties concerning the empirical methods. Finally, the smaller the span of variation of RMR and Q, the higher the accuracy of the determination and the homogeneity of the rock domain.

Furthermore, to consider the fact that the spatial variability of the geological parameters interfere with the evaluation of the uncertainties, the uncertainty on the mean value of the rating is given. This is achieved by determining the average number of values on which the mean is calculated for each rock unit. For borehole sections of 5 m, the number of sections in a rock unit in competent rock is evaluated to be about 28 values of RMR and Q, while for the number of sections in a rock unit in fractured rock is evaluated to be about 7 values. Based on these sample sizes, the concept of confidence interval of a population mean is used. According to the “Central Limit Theorem” /Peebles, 1993/, the 95% confidence interval $\Delta_{conf\,mean}$ of the mean is obtained as:

$$\Delta_{conf\ mean} = \pm \frac{1.96\,\sigma}{\sqrt{n}} \tag{3}$$

where σ is the standard deviation of the population of confidence intervals ΔP and n is the number of values of the sample. In practice, two confidence intervals are determined by the proposed technique, one related to the maximum value of RMR and Q, and the other related to the minimum value:

$$\Delta P_{+conf\ mean} = \frac{P_{MAX} - P_{MEAN}}{\sqrt{n}}$$
$$\Delta P_{-conf\ mean} = \frac{P_{MEAN} - P_{MIN}}{\sqrt{n}} \tag{4}$$

where P is the rating, either RMR or Q, with its maximum, minimum and mean values respectively. This technique also applies to the rock mechanical parameters derived from the empirical systems such as: deformation modulus, Poisson's ratio, uniaxial compressive strength, friction angle and cohesion of the rock mass.

For the mean values of RMR and Q, the confidence interval are very close and rather small for that concerning rock of better quality ("competent rock") (Table 4-2). For more fractured rock, however, the confidence span becomes wider compared to the confidence span for competent rock. Furthermore, the confidence span for Q is much larger than that for RMR, due to the possibility of variation of Q on a logarithmic scale.

For borehole sections of 20 m, the confidence intervals change mainly due to two facts: i) the characterisation results are somewhat scale-dependent; ii) the amount of values composing the characterisation results for a certain rock unit are in general reduced to one fourth. This implies that new confidence levels are larger according to Table 4-3.

It can be observed that the scale of RMR determination does only marginally affect the confidence of the characterisation results. Differences could only be observed for the deepest rock domains. The confidence span of Q, on the other hand, seems to be very sensitive to the scale of the determination. Besides the effect of scale on the mean values, the uncertainty spans are significantly increasing when passing from core section lengths of 5 m to lengths of 20 m. This can be explained with the fact that Q contains parameters that regard the borehole section as a whole (J_n), thus are more sensitive to scaling. Differently, the ratings of RMR are determined based on singular minimum features observed along the borehole section that do not change when the length of borehole section is increased. Among these, the ratings that were estimated based on expert judgement because of lack of data are also included.

Table 4-2. Confidence on the mean values of RMR and Q for borehole KFM01A and borehole sections of 5 m.

	Competent rock		Fractured rock	
	Lower confidence on the mean	Upper confidence on the mean	Lower confidence on the mean	Upper confidence on the mean
RMR	–3%	+1%	–7%	+4%
Q	–3%	+6%	–13%	+28%

Table 4-3. Confidence on the mean values of RMR and Q for borehole KFM01A and borehole sections of 20 m.

	Competent rock		Fractured rock	
	Lower confidence on the mean	Upper confidence on the mean	Lower confidence on the mean	Upper confidence on the mean
RMR	–9%	+3%	–18%	+11%
Q	–15%	+26%	–21%	+69%

5 Mechanical properties of the rock mass

An estimation of the mechanical properties of the rock mass can be made by using the empirical relations available in the literature. Among the large amount of relations provided with RMR and Q, the relations most commonly used in practice and tested against many case histories were chosen to determine the deformation modulus, uniaxial compressive strength, cohesion and friction angle of the rock mass /Andersson et al. 2002; Röshoff et al. 2002/. Appendix D presents some more detailed results of the determination of the rock mass property.

5.1 Deformation modulus of the rock mass

The deformation modulus is calculated, from RMR, according to the relation provided by /Serafim and Pereira, 1983/:

$$E_m = 10^{\frac{RMR-10}{40}} \text{ (GPa)} \tag{5}$$

For Q, the deformation modulus is calculated through Q_c /Barton, 1995/:

$$Q_c = \frac{RQD}{J_n} \times \frac{J_r}{J_a} \times \frac{J_w}{SRF} \times \frac{\sigma_c}{100} = Q \times \frac{\sigma_c}{100} \tag{6}$$

and according to /Barton, 2002/:

$$E_m \approx 10\, Q_c^{1/3} \text{ (GPa)} \tag{7}$$

Since, the relations in Equations (5) and (7) sometimes exceed the limit of values of the deformation modulus that are physically possible, the values in Table 3-4 are assumed as upper boundary of the empirical results. These values are the minimum, average, most frequent and maximum value of the Young's modulus measured for the intact rock (Table 5-1).

In Figure 5-1, the values of the deformation modulus of the rock mass obtained from the values of RMR and Q_c are plotted against depth and compared with each other. The E_m obtained from RMR does not experience the same sharp variations as E_m from Q_c does. Moreover, it can be observed that both methods tend to give values larger than the Young's modulus of the intact rock. This justifies the levelling of E_m for larger depths. The mean E_m from RMR varies between 45 and 75 GPa, while the mean E_m from Q_c extends from 25 to 75 GPa. However, even if independently obtained, the values from the two methods seem to agree quite well as shown in the comparison in Figure 5-1, especially for the sections of lower rock quality.

Table 5-1. Upper boundary of the physically possible values of the deformation modulus of the rock mass based on the available intact rock testing reported in Section 3.1.

	Minimum	Average	Median	Maximum
Maximum possible deformation modulus of the rock mass (GPa)	40	75	75	90

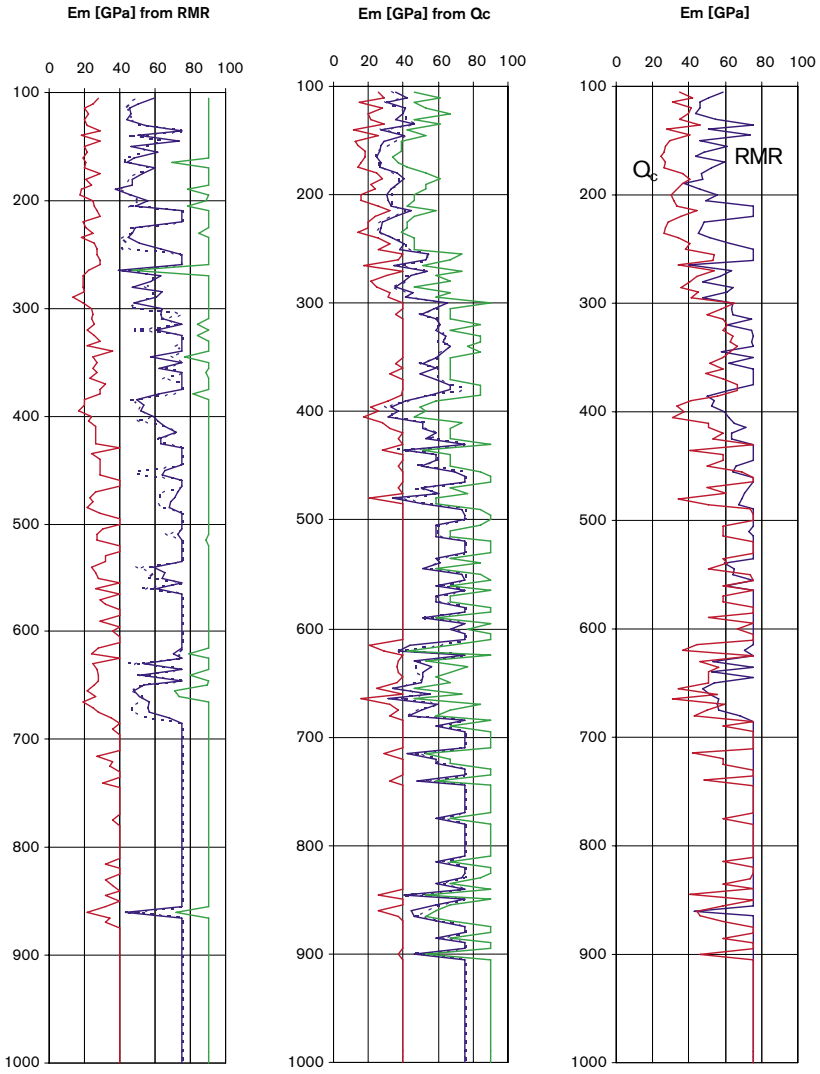

Figure 5-1. *Variation of the deformation modulus of the rock mass obtained from RMR and Q with depth. The values are given every 5 m.*

5.1.1 Spatial variability

The ranges of variation of the deformation modulus obtained from the mean value of Q_c and RMR for each rock unit are shown in Figure 5-2. There, it can be noticed that the mean value of the deformation modulus increases with depth independently of the method used for its calculation. In the same way, the deformation modulus increases for the sections of borehole with lower fracture frequency and higher RQD. The values obtained through Q_c are in general lower than those obtained from RMR, which also experiences smaller variation between the section with better and poorer rock. The figures also show that the range of variation of the deformation modulus is wider for the values calculated from RMR.

5.1.2 Uncertainty

The confidence intervals for the mean deformation modulus calculated from Q_c are smaller than those calculated from RMR. The upper confidence is almost the same because both methods tend to give the maximum deformation modulus physically possible for this rock mass (90 GPa). Even if the deformation modulus from RMR is in general larger than that from Q_c, the minimum possible deformation modulus obtained from RMR is approximately

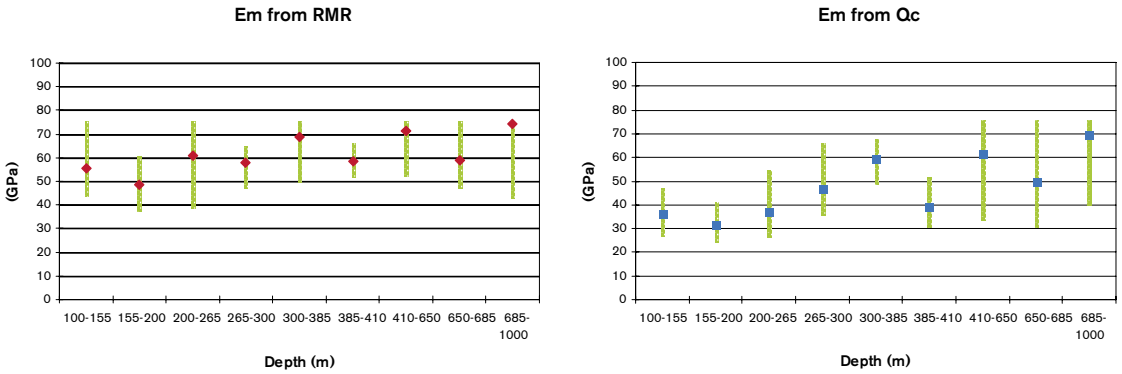

Figure 5-2. *Range of variation of the mean deformation modulus obtained from RMR and Q_c for the rock units. The average of all calculated values for each rock unit is marked by a label and refers to 5 m core sections.*

Table 5-2. Confidence on the mean values of the deformation modulus E_m from RMR and Q_c for borehole KFM01A and borehole sections of 5 m.

	Competent rock		Fractured rock	
	Lower confidence on the mean	Upper confidence on the mean	Lower confidence on the mean	Upper confidence on the mean
E_m (RMR)	–11%	+6%	–22%	+19%
E_m (Q_c)	–7%	+5%	–13%	+16%

as large as that obtained from Q_c. This explains why the lower confidence interval on the mean deformation modulus from RMR is larger than that from Q_c. This also means that RMR is more sensitive to effects of the uncertainty on the indexes and ratings than Q_c.

As mentioned in Section 4.1, some biases on the values of Q and RMR are introduced due to the way in which the data collection is performed. This is particularly the case for fracture aperture. The fact that the fracture width is seldom 0 mm for open fractures makes it impossible to assign certain values to J_a and to RMR-aperture. It can be estimated that due to this bias, Q could generally increase about 30%. This implies an increase of the deformation modulus of about 10% (for the range of Q values occurring in KFM01A). For what concerns RMR, RMR-aperture could very rarely be equal to 6 but often took the value of 4. Moreover, the infilling parameter would often be 4 (infilling < 5 mm) but never 6 because all open fractures are reported to have width of at least 1 mm (according to the BOREMAP data by May, 2004). In general, the bias on RMR would be of 4 points (5%). On average, such difference could cause an underestimation of the deformation modulus of about 25%. Considering that RMR and Q sometimes concern infilled fractures that actually exhibit a width of 1 mm and an aperture of 0 mm, it can be estimated that the deformation modulus obtained from Q can be 5% larger and that from RMR 10% larger than the values reported here, respectively for a certain rock unit.

5.2 Poisson's ratio of the rock mass

The Poisson's ratio of the rock mass has been related to the Poisson's ratio of the intact rock by means of the ratio between the deformation modulus of the rock mass and that of the intact rock in the borehole. Thus, the calculated values strongly depend on the quality of the obtained deformation modulus of the rock mass. The Poisson's ratio of the rock mass ν_m is given in symbols as:

$$\nu_m = \nu \times \frac{E_m}{E} \quad (8)$$

A rough estimation of the variation of the Poisson's ratio of the rock mass can be given (Table 5-3) based on the results of the Young's modulus and Poisson's ratio of the intact rock summarised in Section 3.1 together with the values of the rock mass deformation modulus in Section 5.1. The uncertainties on the deformation modulus E_m in Section 5.1.2 will directly mirror on the uncertainty of the Poisson's ratio due to their direct relation (Equation (8)).

Table 5-3. Estimation of the minimum and maximum Poisson's ratio of the rock mass at different depths.

ν_m (–)	Minimum	Maximum
100–200 m	0.10	0.18
200–400 m	0.12	0.22
400–1,000 m	0.16	0.24

5.3 Uniaxial compressive strength of the rock mass

The uniaxial compressive strength of the rock mass σ_{cm}, or also UCS_m, can be calculated from the values of RMR by means of Geological Strength Index (GSI) and the /Hoek and Brown, 1997/'s criterion as:

$$\sigma_{cm} = \sigma_c (s)^a \quad (9)$$

where s and a are parameters dependent upon the characteristics of the rock mass, and σ_c is the uniaxial compressive strength of the intact rock material. The value of s can be obtained as a function of RMR according to /Hoek and Brown, 1997/ or, with minor adjustment, /Hoek et al. 2002/ for undisturbed rock masses.

For comparison with the values obtained from RMR, also Q_c could be assimilated to a compressive strength parameter. However, in this case some physical limits have to be applied to Q_c when it becomes larger than the values of uniaxial compressive strength of the intact rock in Table 5-1.

According to the definition of confidence interval of the mean in Section 4.6, the confidence interval of the mean compressive strength UCS_m according to Hoek and Brown's criterion can be summarised as in Table 5-4. The confidence interval is rather wide for both the competent and fractured rock along the borehole indicating the uncertainties in the determination.

The results in Figure 5-3 show the uniaxial compressive strength obtained from RMR by means of Equation (9) with the exponent a equal to 0.5. However, according to the current opinion, the rock mass at Forsmark should have a higher uniaxial compressive strength. This could also be the conclusion when comparing the RMR determination with Q_c in the same figure. Another attempt to determine the uniaxial compressive strength of the rock mass could be carried out by using the following Hoek and Brown's exponent a, which should strictly only apply for RMR smaller than 30:

$$a = 0.65 - \frac{RMR - 105}{200} \quad (10)$$

In consequence of this change, the uniaxial compressive strength of the rock mass almost doubles, as it is shown in Figure 5-4.

Table 5-4. Confidence on the mean values of the uniaxial compressive strength UCS_m from RMR for borehole KFM01A and borehole sections of 5 m.

	Competent rock		Fractured rock	
	Lower confidence on the mean	Upper confidence on the mean	Lower confidence on the mean	Upper confidence on the mean
UCS_m (RMR)	–15%	+20%	–30%	+56%

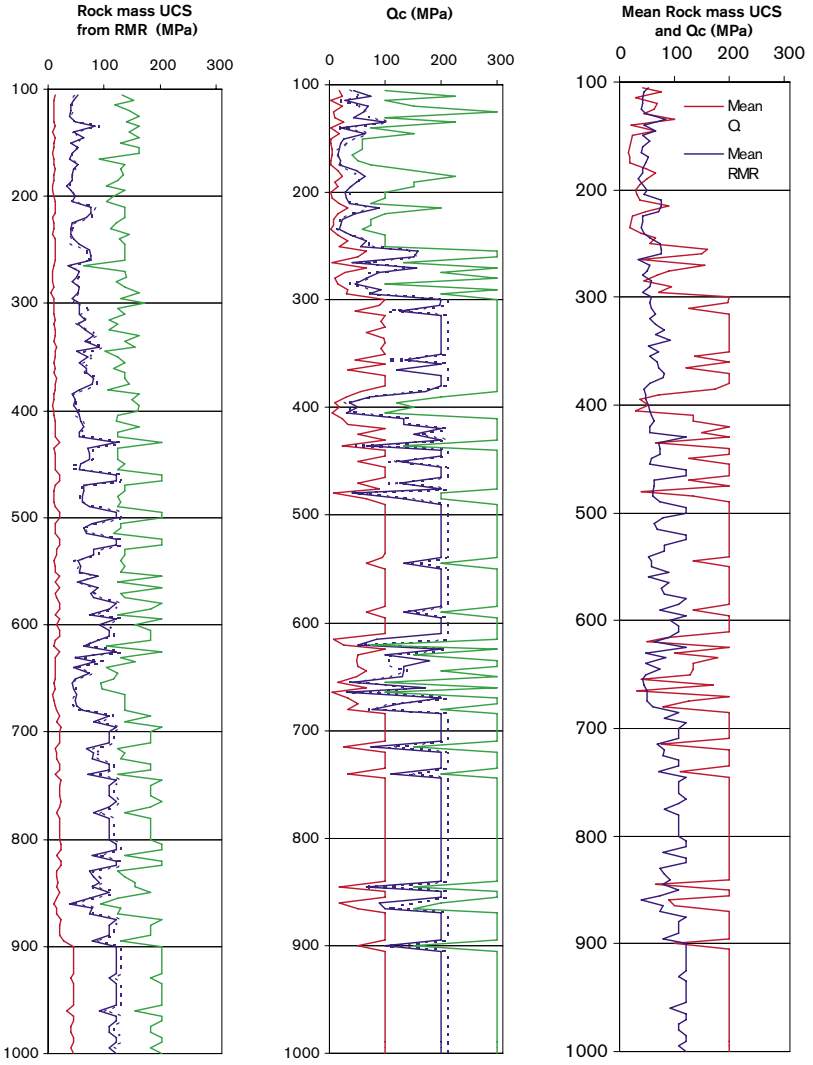

Figure 5-3. *Variation of the rock mass compressive strength from RMR and Q for borehole KFM01A (Hoek and Brown's exponent a = 0.5).*

5.4 Cohesion and friction angle of the rock mass

The strength of the rock mass can be quantified in terms of equivalent cohesion and friction angle for a certain level of stress confinement. By linear approximation of /Hoek and Brown, 1997/'s criterion (only minor differences respect to /Hoek et al. 2002/), the strength of the rock mass can be described by the equation:

$$\sigma_1 = \sigma_{cm(M-C)} + k\sigma_3 \qquad (11)$$

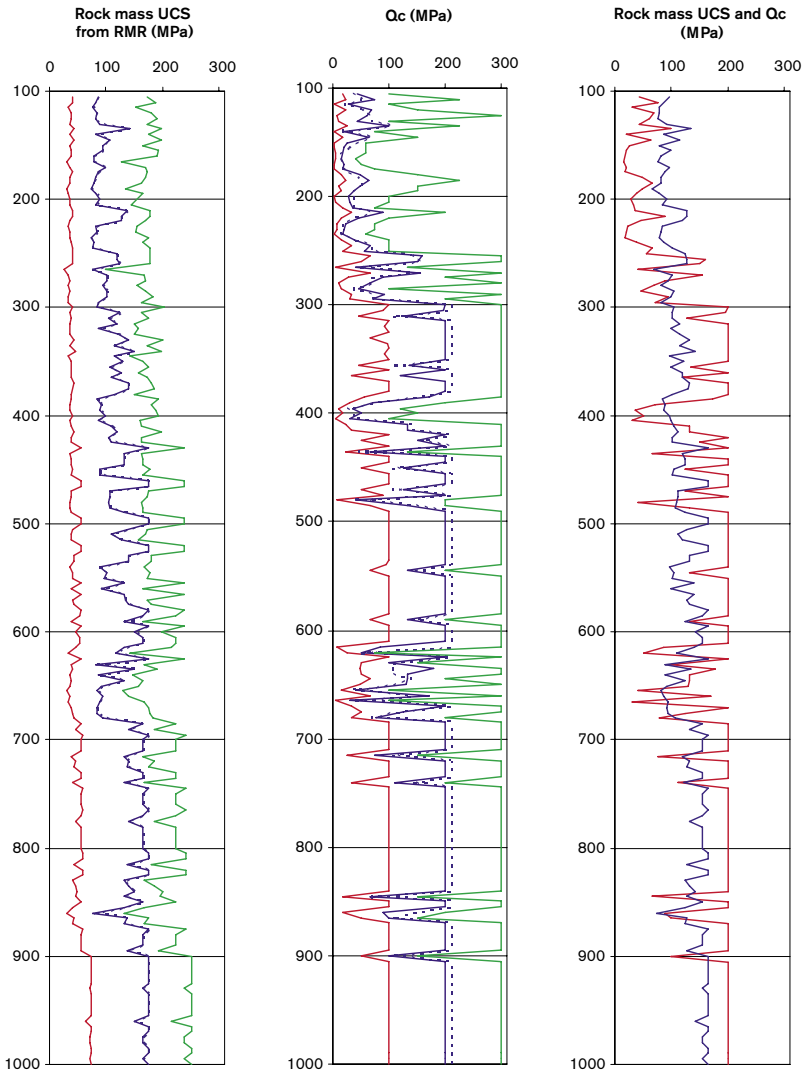

Figure 5-4. *Variation of the rock mass compressive strength from RMR and Q for borehole KFM01A (Hoek and Brown's exponent a according to Equation (10)).*

where σ_1 and σ_3 are the major and confinement pressure, respectively, $\sigma_{cm(M-C)}$ is the apparent uniaxial compressive strength of the rock mass. From the slope k in Equation (11), the friction angle φ' and cohesion c' of the rock mass can be determined as:

$$\phi' = \sin^{-1}\frac{k-1}{k+1} \tag{12}$$

$$c' = \frac{\sigma_{cm(M-C)}}{2\sqrt{k}} \tag{13}$$

A set of equations is also provided together with Q for evaluating the "frictional and cohesive components" FC and CC of the rock mass /Barton, 2002/. In symbols:

$$FC = \tan^{-1}\left(\frac{J_r}{J_a}\times J_w\right) \tag{14}$$

$$CC = \frac{RQD}{J_n}\times\frac{1}{SRF}\times\frac{\sigma_c}{100}\ (\text{MPa}) \tag{15}$$

Concerning the cohesion and friction angle determined by using /Hoek et al. 2002/, the same considerations in Section 5.3 apply here. Figure 5-5 shows the results obtained for a Hoek and Brown's exponent a of 0.5 and a confinement pressure between 0 and 5 MPa. These results are compared with FC and CC obtained from Q. Also this comparison seems to indicate that the values obtained by the two methods are not completely compatible. The frictional component from Q applying for low stress confinement spans between 45° to 70° with very sudden variations. The cohesive component from Q is almost constant with depth and is about 27 MPa. When Equation (10) is used, the results from the two independent RMR and Q methods produce results closer to each other. It is worth to report that the cohesion and friction angle of the intact rock would be on average 52° and 34 MPa, respectively.

The values of the rock mass friction angle and cohesion from RMR in Figure 5-6 are obtained for confining pressure between 10 and 30 MPa. The average friction angle slightly increases with depth from about 47° to 51°. The rock mass cohesion increases on average with depth from about 21 MPa to up to 30 MPa due to the effect of the increasing rock quality.

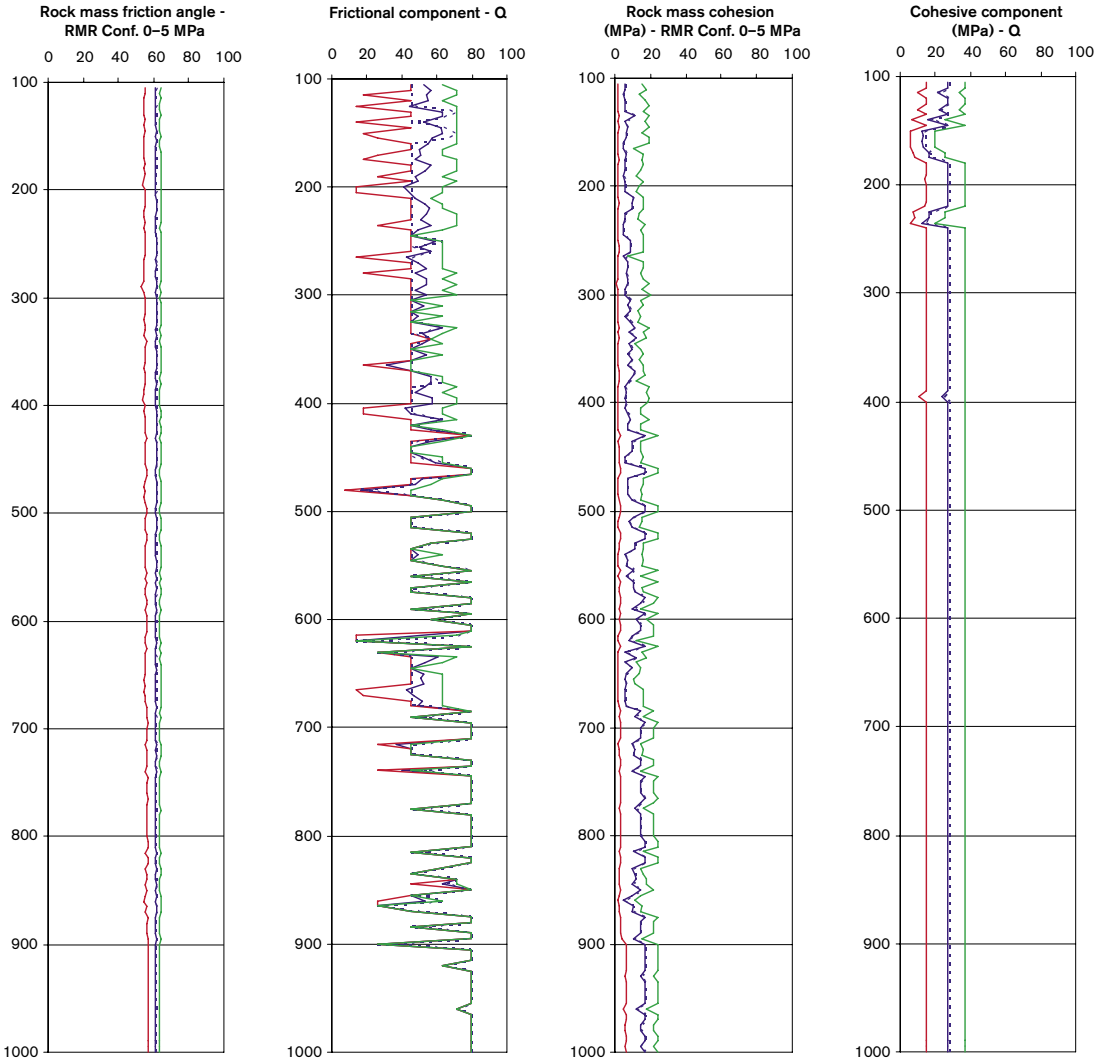

Figure 5-5. *Variation of the rock mass friction angle and cohesion from RMR and Q for borehole KFM01A under stress confinement between 0 and 5 MPa (Hoek and Brown's exponent a = 0.5).*

From Equation (11) it derives that the cohesion and friction angle depend on the stress level on which the linear approximation of the convex Hoek and Brown's Criterion is performed. For the characterisation of the rock mass, a range of confinement stresses between 10 and 30 MPa is assumed. In Figure 5-6, the cohesion and friction angle for this interval of confining pressure are shown.

The confidence intervals for the mean values of the cohesion and friction angle obtained by means of RMR and Equations (12) and (13) can be calculated as in Table 5-5 for a range of confinement stress between 10 and 30 MPa.

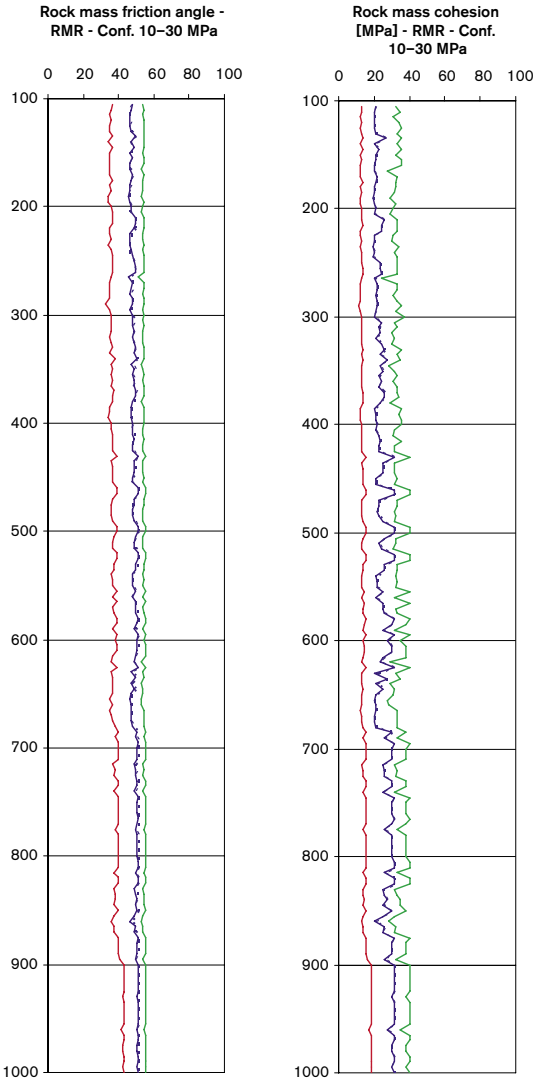

Figure 5-6. *Variation of the rock mass friction angle and cohesion from RMR under stress confinement between 10 and 30 MPa (Hoek and Brown's exponent a = 0.5).*

Table 5-5. Confidence on the mean values of the cohesion c' and friction angle ϕ' from RMR for borehole KFM01A and borehole sections of 5 m (confinement stress between 10 and 30 MPa).

	Competent rock		Fractured rock	
	Lower confidence on the mean	Upper confidence on the mean	Lower confidence on the mean	Upper confidence on the mean
c'	–8%	+7%	–15%	+18%
ϕ'	–4%	+2%	–9%	+5%

6 P-wave velocity along the borehole

/Tunbridge and Chryssanthakis, 2003/ report about the P-wave velocity measurements performed along the core of borehole KFM01A. The measurements were carried out on core sections of about 0.2–0.5 m spaced about 50 m along the entire core axis. The maximum velocity was found to reach a top at approximately 500 m depth (about 5,700 m/s) and then tended to reduce for deeper measurements (to about 5,000 m/s). This could be explained by some micro-cracking occurring on the core because of the release of very high stresses. The orientation of the maximum P-wave velocity was also found to agree well with the orientation of the foliation planes, especially when the velocity exhibited anisotropic values. This was mainly true for core sections deeper than 500 m. A summary of the results by /Tunbridge and Chryssanthakis, 2003/ is given in Figure 6-1 where the orientation of the foliation is also reported. On average, the orientation of the maximum P-wave velocity is 166° with respect to the North.

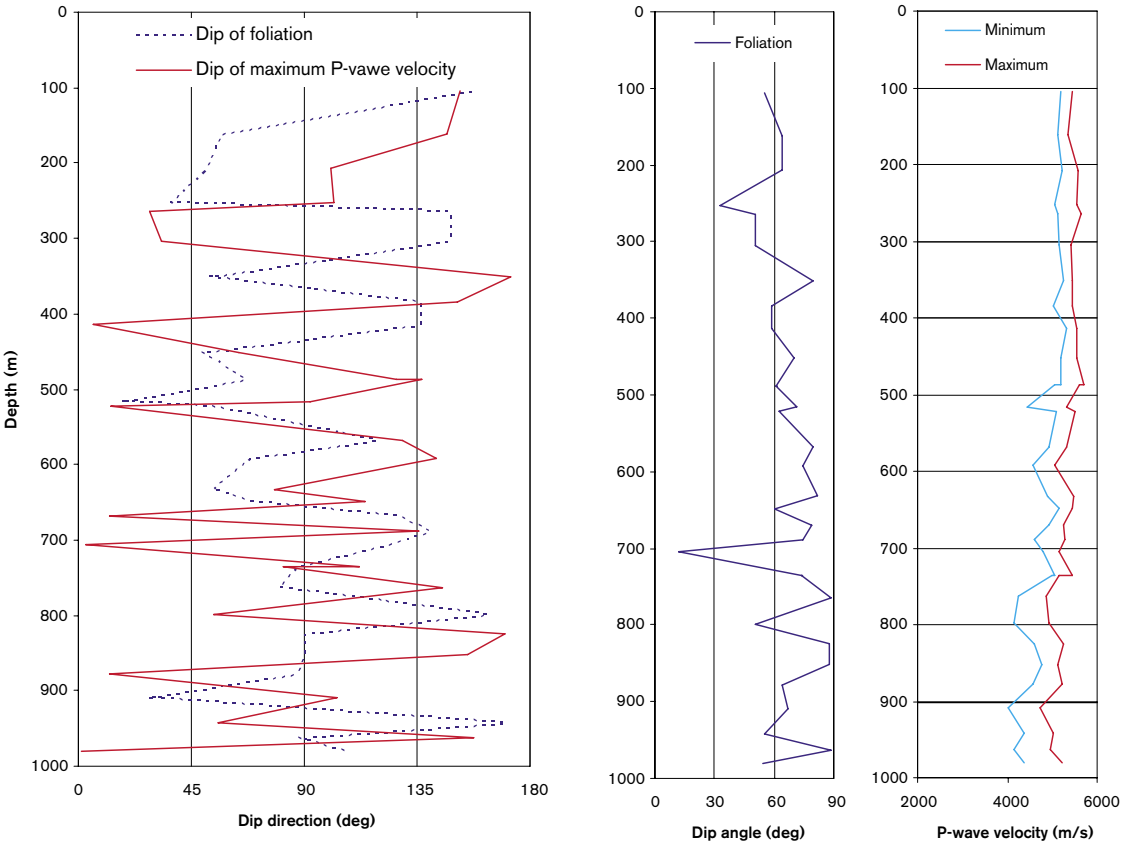

Figure 6-1. *Orientation and magnitude of the P-wave measured perpendicular to the core axis of borehole KFM01A. The orientation of the foliation is also shown as it is reported in SICADA.*

7 Discussion

In this report, the two independent systems for rock mass quality determination RMR and Q are applied for characterisation of the rock mass along borehole KFM01A. Their values cannot be quantitatively compared since RMR and Q have different ranges of variation. However, the values of RMR and Q for each analysed borehole section of 5 or 20 m can be set into a diagram that makes it possible to assess the consistency between the rock mass quality systems and the results previously published in the literature. In Figure 7-1, the characterisation results for KFM01A are compared with several other empirical relations between RMR and Q obtained for the purpose of tunnel design. The diagram shows a slight overestimation of RMR as a function of Q. This is due to the difference between the approach for characterisation of the rock mass and that for design of underground structures considered in the literature. It is worth noting that the version of the Q-system adopted here for characterisation uses more favourable SRF factors compared to their use for design (original Q-system). This produces higher values of Q than the original Q-system. Considering that the empirical relations apply on average, however, the characterisation results can be considered satisfactory. The linear regression of the data shown in Figure 7-1 and Figure 7-2 can be expressed in mathematical terms as:

$$RMR_{(5\,m)} = 3.36 \cdot \ln(Q) + 70.04 \ (R^2 = 0.7717) \quad (16)$$

$$RMR_{(20\,m)} = 2.75 \cdot \ln(Q) + 76.58 \ (R^2 = 0.6622) \quad (17)$$

These relations imply that small values of Q (e.g. 0.1) are associated to moderately high values of RMR (e.g. 62–70).

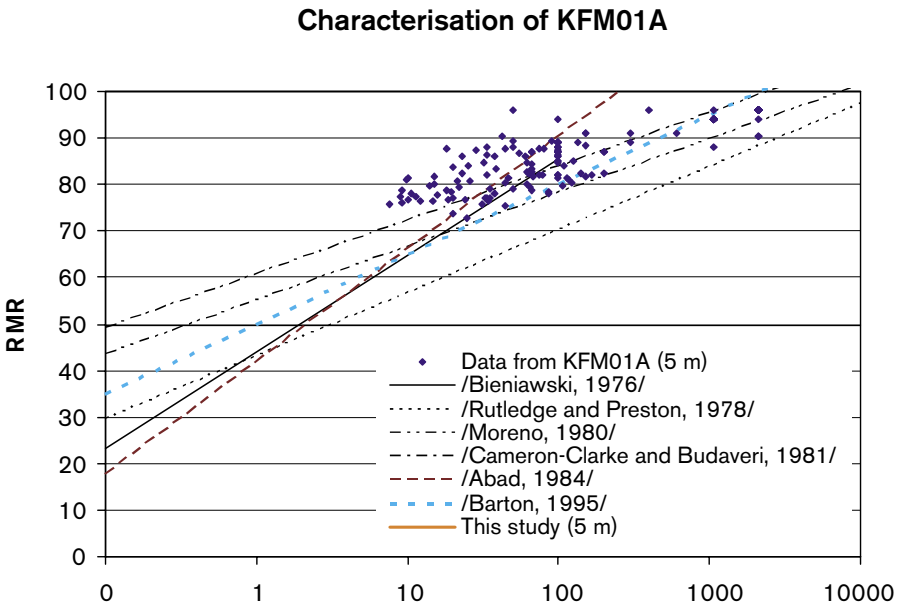

Figure 7-1. *Correlation between RMR and Q for the characterisation of the rock mass along borehole KFM01A (core sections of 5 m). The characterisation results are compared with some design relations from the literature.*

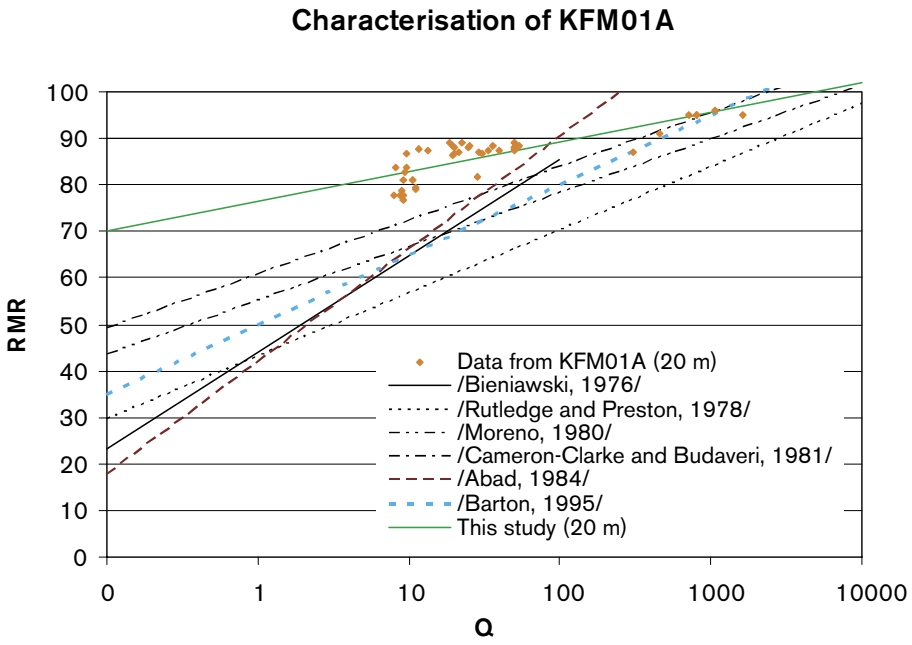

Figure 7-2. *Correlation between RMR and Q for the characterisation of the rock mass along borehole KFM01A (core sections of 20 m). The characterisation results are compared with some design relations from the literature.*

As demonstrated in Section 5.1, the scale of evaluation, or the length of the core sections (5 and 20 m), affects the result of the characterisation (Figure 7-3). The analysis of longer core sections applies an averaging process that smoothen all the extreme values of most of the geological input parameters. This averaging process affects RMR and Q in different ways. Figure 7-2 shows that for core sections of 20 m, the interval of RMR values stays the same (75–95), while that of Q tend to move toward lower Q values (10–100). As mentioned in Section 5, this probably depends, for example, on the Joint Set Number J_n that tends to diminish when longer core sections are considered. Also the fact that the SRF factor of 2.5 is applied to the fractured zones contributes to this drop. In fact, this factor is sometimes applied to a whole core section of 20 m although not all the rock in the section consists of very fractured rock.

RMR and Q cannot directly be compared, but the other rock mass mechanical parameters obtained from them can. This is the case for the deformation modulus, cohesion and friction angle. As presented in Section 5, the properties obtained by means of different methods do not necessarily coincide. The range of values of a certain property could be assumed as a measure of the uncertainty on the property. The uncertainty results from the sum of the measurement errors, interpretation unconformities and defects in the adopted models.

For longer core sections, the range of variation becomes narrower if the same characterisation system and the same rock unit are concerned. For example, the deformation modulus obtained from Q seems to be affected by a reduction that does not appear for that obtained from RMR (Figure 7-3). The deformation modulus also shows that the spatial variability of the geological parameters inside each core section does have different implications on Q and RMR. In conclusion, the scale of analysis should be carefully studied and maybe not assigned a-priori (i.e. 30 m) as recommended in /SKB, 2002/.

The histograms of the deformation modulus obtained by mean of RMR and Q for each rock units can be compared. This comparison shows agreements between the two frequency distributions (Figure 7-4). However, the agreement is better for rock mass of very good quality, probably because of the cut-off of the empirical values applied by the Young's modulus of the intact rock. In general, Q produces deformation moduli lower than RMR.

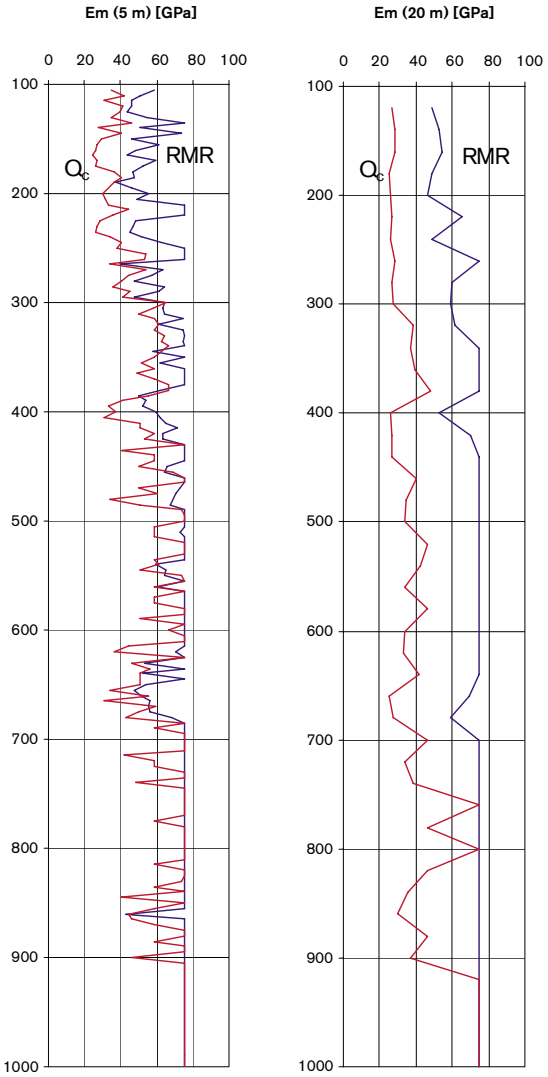

Figure 7-3. *Scale effect on the deformation modulus of the rock mass obtained from RMR and Q.*

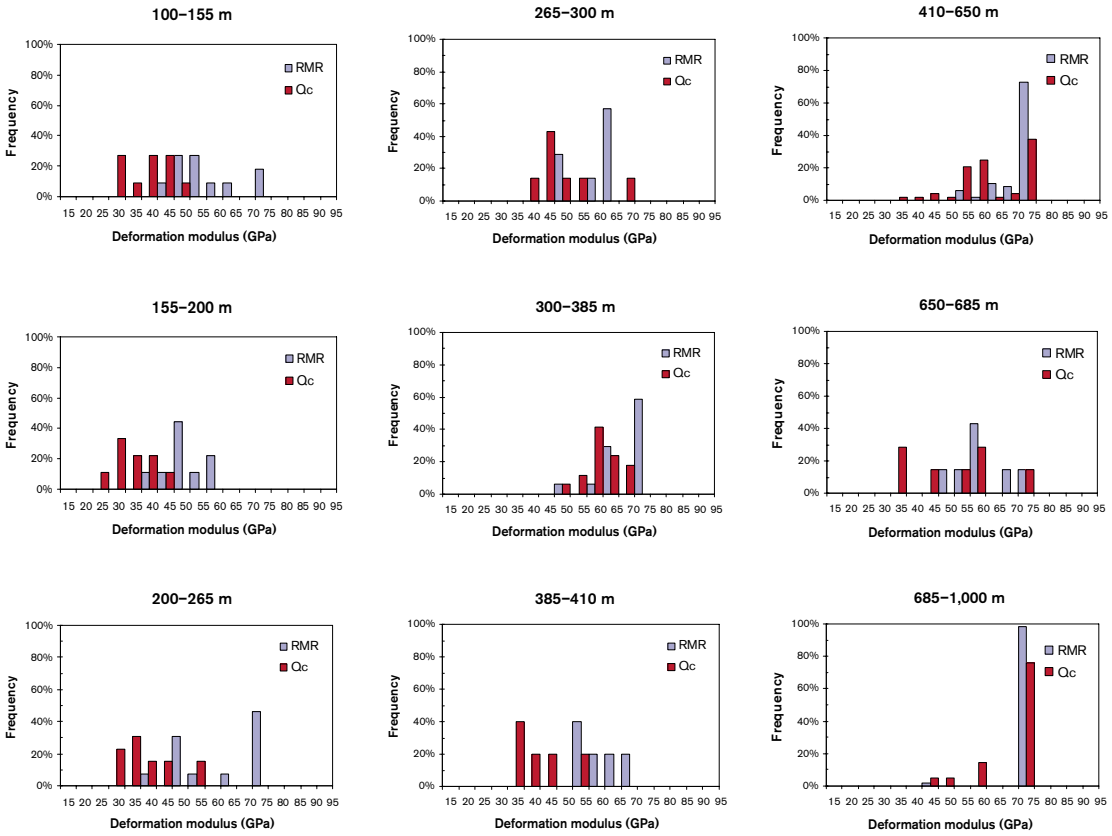

Figure 7-4. *Histograms of the deformation modulus obtained from RMR and Q for each rock unit (core sections of 5 m).*

8 Conclusions

This report concerns the application of the empirical systems RMR and Q for the characterisation of the rock mass along borehole KFM01A. The input data is mainly provided by historical records from the construction of the nuclear power plants and of the SFR Repository in Forsmark, and by the data collected along the borehole core and walls (BIPS images) and stored in SICADA (by May, 2004).

The application of RMR and Q to borehole data requires the partition of the borehole into homogenous sections on which the values of the input parameters can be selected as representative. The partitioning of the borehole can be carried out in different ways. In this study, RQD, the fracture frequency, rock type and rock alteration were used for identify homogenous sections according to /Andersson et al. 2002; Röshoff et al. 2002/.

In general, the rock quality assessed by means of RMR is "very good rock" (RMR > 81) along most of the length of borehole KFM01A. Zones of "good rock" (80 < RMR < 65) can be observed at shallower depth than 300 m and in two zones at about 380–400 m and 650–685 m. The Q system classes most of the rock along the borehole as "very good rock" (Q > 40). "Good rock" (40 > Q > 10) is observed down to 300 m depth. Sections of poorer rock, sometimes characterised by Q between 1 and 10 can also be observed at the depths 385–410, 480–490, 610–620, 650–685 and a few short sections at a depth of about 850 m. A zone of intensive alteration, which did not coincide with very poor rock quality, was identified by both empirical systems between about 610 and 630 m.

The deformation modulus of the rock mass determined based on the correlations with the two empirical systems can be summarised along the borehole as follows: 45 GPa down to 300 m and between 610 and 680 m; 65 GPa between 300 and 610 m with the exception of 55 GPa between 380 and 430 m; 70 GPa between 680 m and 1,000 m.

The Poisson's ratio of the rock mass along the borehole would probably be on average about 0.2 and could increase with depth.

The uniaxial strength of the rock mass for the Hoek and Brown Criterion estimated based on the relations with RMR and Q presents the following ranges: 50–100 MPa for the upper 300 m; 100–150 MPa for depths larger than 300 m with the exception of the zones at 420–480 m where it becomes 70–120 MPa, and at 620–680 m, where it drops to 50–100 MPa.

The cohesion and friction angle of the rock mass are difficult to summarise because they depend on the rock stress confinement. For low confinement, the cohesion should be about 4–16 MPa and the friction angle around 61°. For a confinement between 10 and 30 MPa, the cohesion should probably increase to 19–30 MPa while the friction angle could decrease to about 45–51°. These results are presented graphically in Figure 8-1.

As mentioned before, all the mechanical parameters produced by the empirical rock quality estimation are indicative and should be verified against numerical models that reproduce the behaviour of the rock fracture network, or compared with back analysis of full-scale experiments or excavation, and measurements in-situ. Furthermore, one should keep in mind that all rock mechanical properties inferred in this study would apply to the rock mass interpreted as an equivalent continuum medium. This hypothesis is often not verified for large extensions of borehole KFM01A since the fracture frequency is very low. In this case, a discrete fractured model would probably better represent the rock mass behaviour.

As for numerical modelling, also for empirical rock mass characterisation, the scale at which the determination is performed plays a role on the magnitude, variability and uncertainty span of the rock mass quality and derived properties.

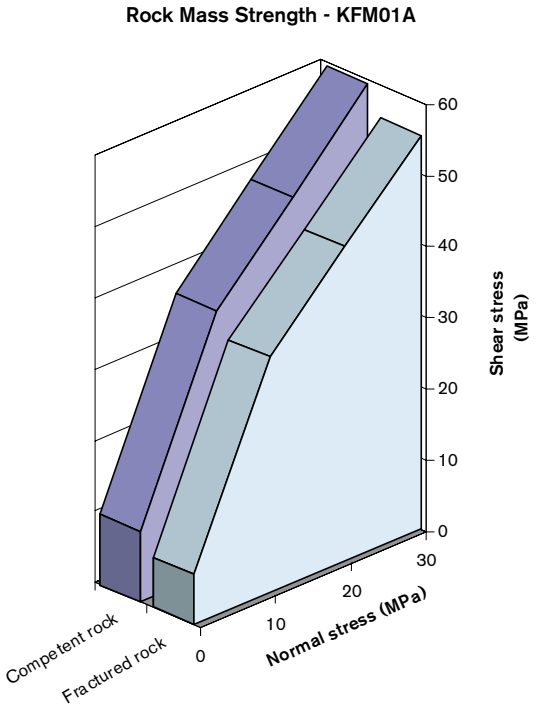

Figure 8-1. *Range of variation of the strength envelopes of the rock mass obtained from the empirical characterisation along borehole KFM01A. The two envelopes correspond to a uniaxial compressive strength spanning between 56 and 82 MPa. (A minor approximation is applied at the intersection by 10 MPa normal stress.)*

9 Remarks

The empirical systems require the knowledge of the mechanical properties of the intact rock and of the rock fractures. For borehole KFM01A, a testing campaign on intact rock cores is planned for determine the uniaxial compressive strength, the Young's modulus and the Poisson's ratio. At the time of the analysis contained in this report, no results from those tests were available (by May, 2004).

After the improvement of fracture aperture logging given by /Larsson and Sthråle, 2004/, it is auspicial that a clear distinction is made between open fractures with microscopic aperture (width = 0 mm and aperture = 0 mm) from mineralized and sealed fractures (width ≠ 0 mm and aperture = 0 mm). In fact, the first ones have to be ascribed to the group of "open" fractures, while the second ones to the group of "sealed" or "closed" fractures from a rock mechanics point of view. The two groups of fractures often exhibit a major difference in strength properties.

10 Data delivery to SICADA

The results of the rock mass characterisation are delivered to SKB's database SICADA. Before storage into the database, quality assessment routines are performed on the methods and delivered data. For what concerns the rock mechanics characterisation, SICADA contains already some activities that produced values according to the Q-system. These were, however, obtained in the past for the purpose of tunnel design and not for characterisation of the rock mass along boreholes. Furthermore, these activities are assigned to the activity group "Geology". For this reason, a new activity of characterisation of the rock mass by means of the RMR and Q systems for rock mechanics purposes has been created.

The results of this report are prepared to suit their applications and the database. The borehole is divided into homogenous sections (Rock Unit). For each Rock Unit, six values resulting from the characterisation are delivered to the database: the minimum RMR and Q, the average RMR, the most frequent Q (median), and the maximum RMR and Q, respectively. Also some other mechanical properties of the intact rock and of the rock mass are delivered to the database. The uniaxial compressive strength (UCS) of the intact rock is summarised for each Rock Unit based on the available primary data (cfg. Section 3). For the UCS, the minimum, average and maximum values are produced. These values are estimations based on all available laboratory results. Among the rock mechanics properties empirically determined, only the deformation modulus of the rock mass was judged to be relevant for storage in SICADA. Due to the nature of its determination, two sets of parameters could be delivered to SICADA, one obtained by means of RMR and one for Q, respectively, each of which consisting of minimum, average and maximum deformation modulus of the rock mass.

11 References

Abad J, Caleda B, Chacon E, Gutierrez V, Hidalgo E, 1984. Application of geomechanical classification to predict the convergence of coal mine galleries and to design their support, 5th Int. Congr. Rock Mech., Melbourne, Australia, pp 15–19.

Andersson J, Christiansson R, Hudson J A, 2002. Site Investigations Strategy for Rock Mechanics Site Descriptive Model, SKB TR-02-01, Svensk Kärnbränslehantering AB.

Barton N, 1995. The influence of joint properties in modelling jointed rock masses, Proc. Int. ISRM Congr. on Rock Mech, Tokyo, Japan, T. Fujii ed., A.A. Balkema: Rotterdam, p 1,023–1,032.

Barton N, 2002. Some new Q-value correlations to assist in site characterisation and tunnel design, I.J. Rock Mech. & Min. Eng., Vol. 39, p 185–216.

Barton N, 2003. KFM01A. Q-logging. SKB P-03-29, Svensk Kärnbränslehantering AB.

Bieniawski Z T, 1976. Rock mass classification in rock engineering, in Exploration for Rock Engineering (Bienawski Z T ed), A. A. Balkema Johannesburg, pp 97–106..

Bieniawski Z T, 1989. Engineering rock mass classifications. John Wiley & Sons.

Cameron-Clarke I S, Budavari S, 1981. Correlation of rock mass classification parameters obtained from borecore an in-situ observations, Int. J. Eng. Geo., Vol. 17, pp 19–53.

Carlsson A, Olsson T, 1982. Characterisation of deep-seated rock masses by means of borehole investigations, Research and Development Report, 5:1, The Swedish State Power Board.

Carlsson A, Christiansson R, 1987. Geology and tectonics at Forsmark, Sweden. SKB SFR-87-04, Svensk Kärnbränslehantering AB.

Carlsten S, Petersson J, Stephens M, Mattsson H, Gustafsson J, 2004. Forsmark site investigation – Geological single-hole interpretation of KFM01A, KFM01B and HFM01–03 (DS1). SKB P-04-116, Svensk Kärnbränslehantering AB.

Chryssanthakis P, 2003. Borehole: KFM01A. Results of Tilt Testing, Forsmark site investigation, SKB P-03-108, Svensk Kärnbränslehantering AB.

Delin P, 1983. Uttagna kärnbitar för tryckförsök och point-loadtester på KTH, KTH/Hagkonsult, (Personal Communication).

Hagkonsult AB, 1982a. Geologiska undersökningar och utvärderingar för lokalisering av SRF till Forsmark, Del 1, Arbetsrapport, SFR-81-13, Svensk Kärnbränslehantering AB.

Hagkonsult AB, 1982b. Geologiska undersökningar och utvärderingar för lokalisering av SRF till Forsmark, Del 2, Arbetsrapport, SFR-81-13, Svensk Kärnbränslehantering AB.

Hermanson J, Hansen L, Olofsson J, Sävås J, Vestgård J, 2003. Forsmark – Detailed fracture mapping at the KFM02 and KFM03 drill sites, SKB P-03-12, Svensk Kärnbränslehantering AB.

Hoek E, Brown E T, 1997. Practical estimates of rock mass strength. International Journal of Rock Mechanics and Mining Sciences, Vol. 34, No. 8, pp 1,165–1,186.

Hoek E, Carranza-Torres C, Corkum B, 2002. The Hoek-Brown Failure Criterion – 2002 Edition. 5th North American Rock Mechanics Symposium and 17th Tunneling Association of Canada Conference: NARMS-TAC, pp 267–271.

Larsson N-Å, Sthråle A, 2004. Nomenklatur vid Boremap-kartering, SKB PM 2004-02-04, Svensk Kärnbränslehantering AB.

Moreno Tallon E, 1980. Aplicacion de las clasificaciones geomecanicas a los tuneles de Parjares, 2do Curso de sostenimientos activos en galeria, Fundation Gomez-Pardo, Madrid, Spain.

Peebles P Z jr, 1993. Probability, random variables and random signal functions, McGraw-Hill Int. Eds.: Singapore, pp. 401.

Petersson J, Wängnerud A, 2003. Forsmark Site Investigation – Boremap mapping of telescopic drilled borehole KFM01A, SKB P-03-23, Svensk Kärnbränslehantering AB.

Rutledge J C, Preston R L, 1978. Experience with engineering classifications of rock, Proc. Int. Tunnelling Symp. Tokyo, Japan, pp A3.1–A3.7.

Röshoff R, Lanaro F, Jing L, 2002. Strategy for a Rock Mechanics Site Descriptive Model. Development and testing of the empirical approach, SKB R-02-01, Svensk Kärnbränslehantering AB.

Serafim J L, Pereira J P, 1983. Consideration of the geomechanics classification of Bieniawski, Proc. Int. Symp. Eng. Geol. & Underground Constr., p 1,133–1,144.

SKB, 2001a. Site investigations. Investigations methods and general execution programme. SKB TR-01-29, Svensk Kärnbränslehantering AB.

SKB, 2001b. Hantering av osäkerheter vid platsbeskrivande modeller, SKB TD-01-40, Svensk Kärnbränslehantering AB.

SKB, 2002. Forsmark – Site Descriptive Model Version 0. SKB R-02-32, Svensk Kärnbränslehantering AB.

SKB, 2004. Preliminary site description. Forsmark area – version 1.1, SKB R-04-15, Svensk Kärnbränslehantering AB.

Stille H, Fredriksson A, Widing E, Åhrling, G, 1985. Bergmekaniska beräkningar – FEM-analys av silo med anslutande tunnlar, Arbetsrapport, SFR 85-05, Svensk Kärnbränslehantering AB.

Tunbridge L, Chryssanthakis P, 2003. Borehole: KFM01A. Determination of P-wave velocity, transverse borehole core. Forsmark site investigation, SKB P-03-08, Svensk Kärnbränslehantering AB.

Appendix A

Intact rock properties

A.1 Uniaxial compressive tests in laboratory

A.1.1 All rock types

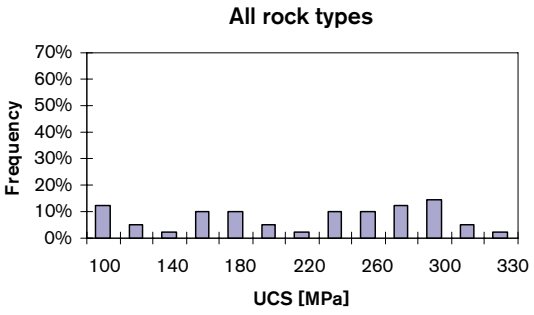

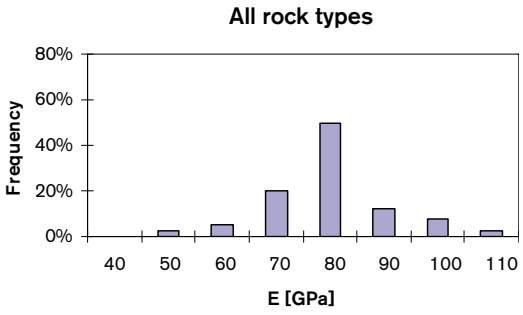

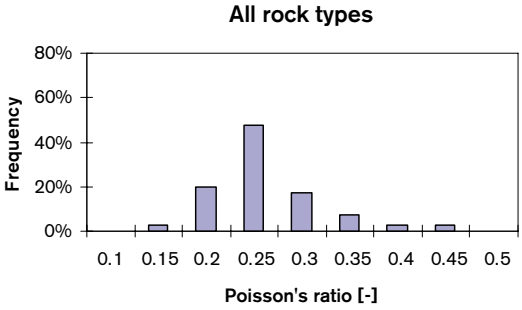

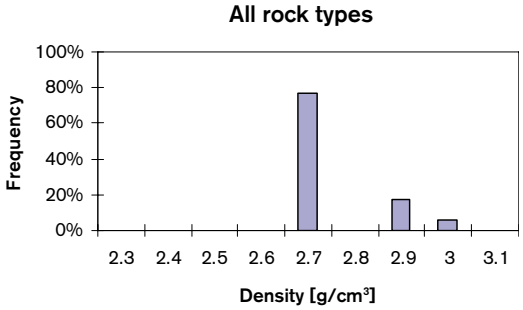

A.1.2 Gneiss

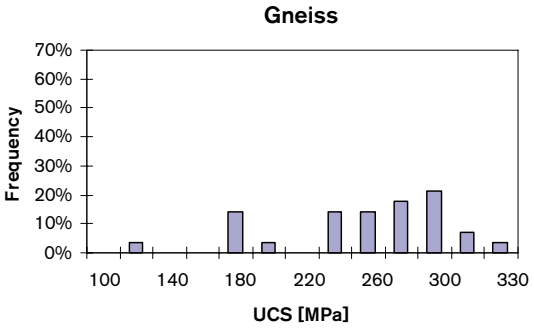

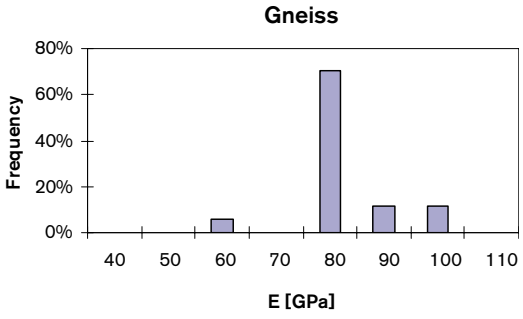

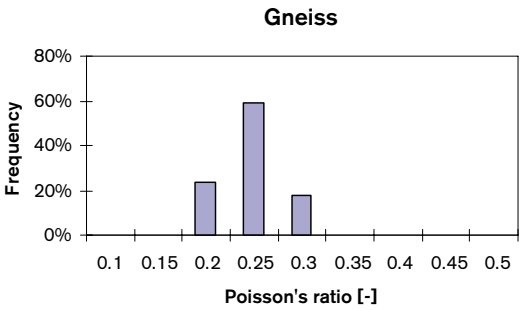

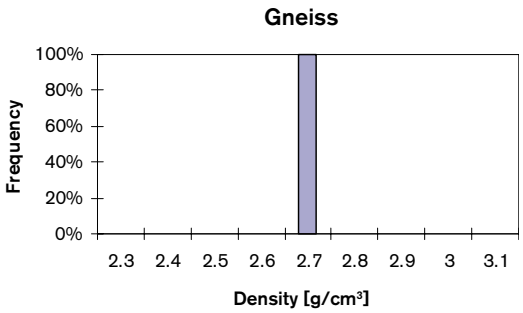

A.1.3 Metavolcanic rock

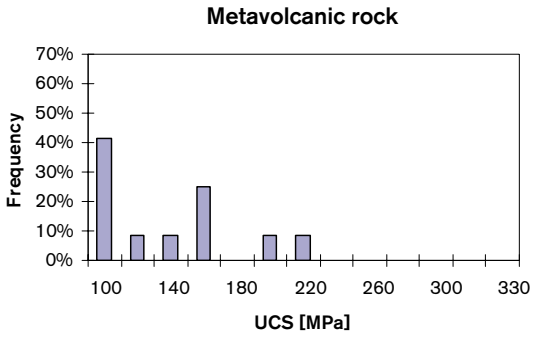

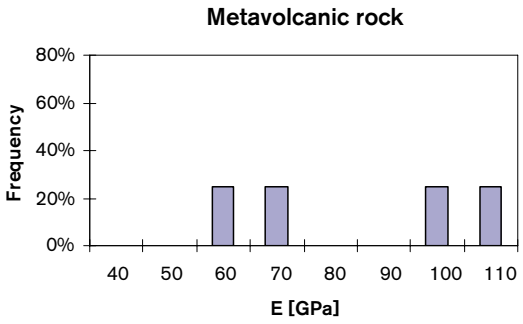

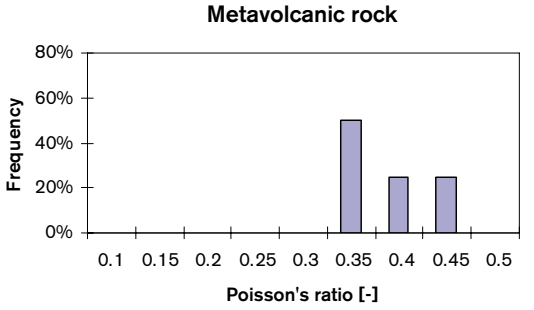

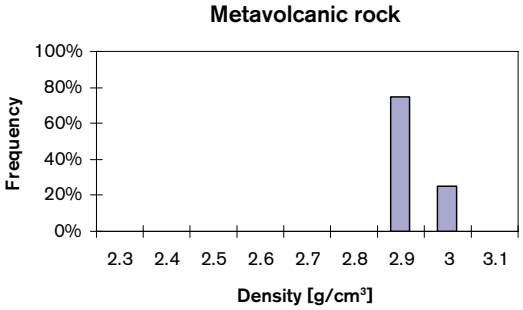

A.1.4 Gneissic granite

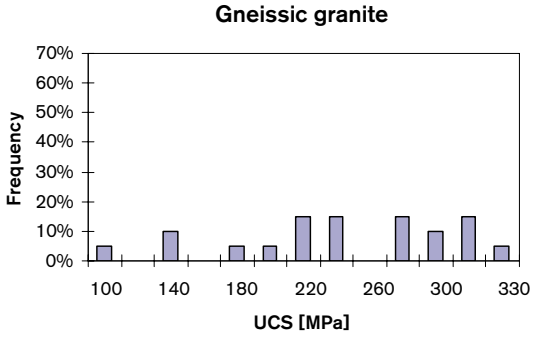

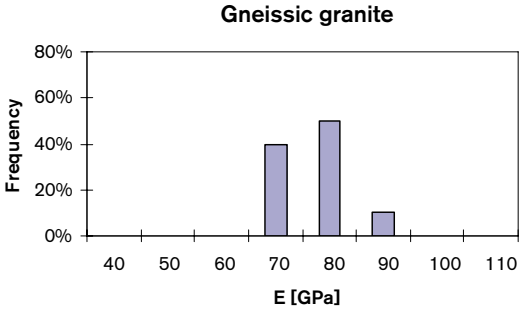

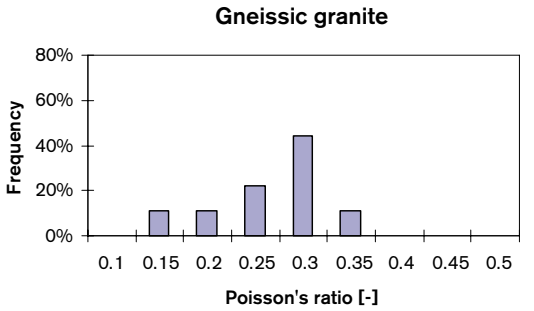

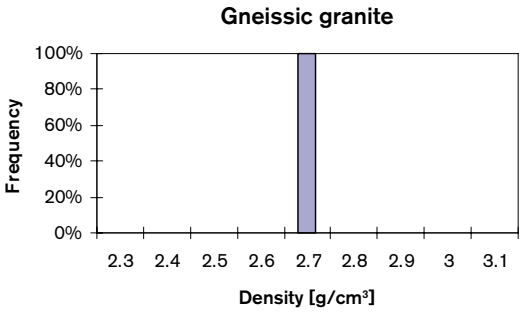

A.1.5 Pegmatite

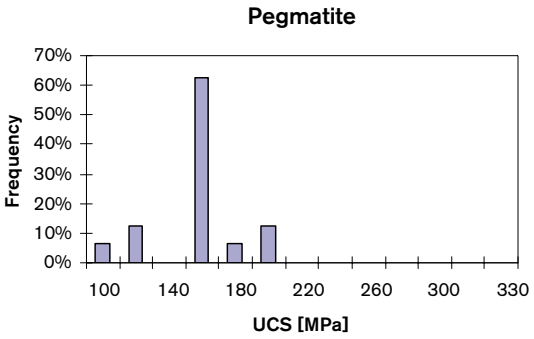

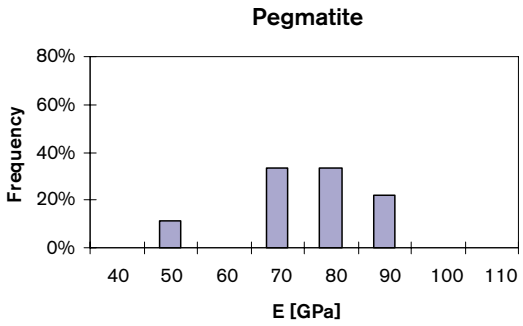

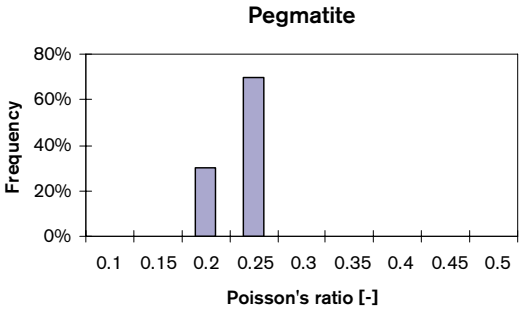

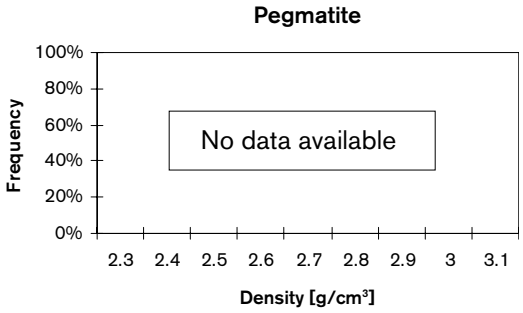

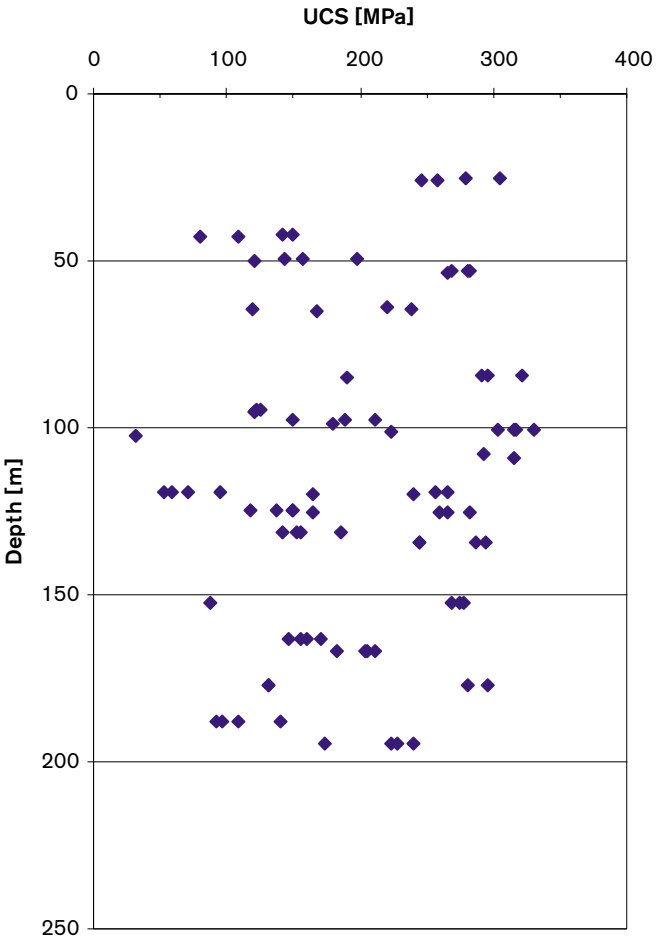

Variation of the uniaxial compressive strength of the intact rock with depth for the available samples from the SRF Repository in Forsmark.

A.2 Point load tests in-situ

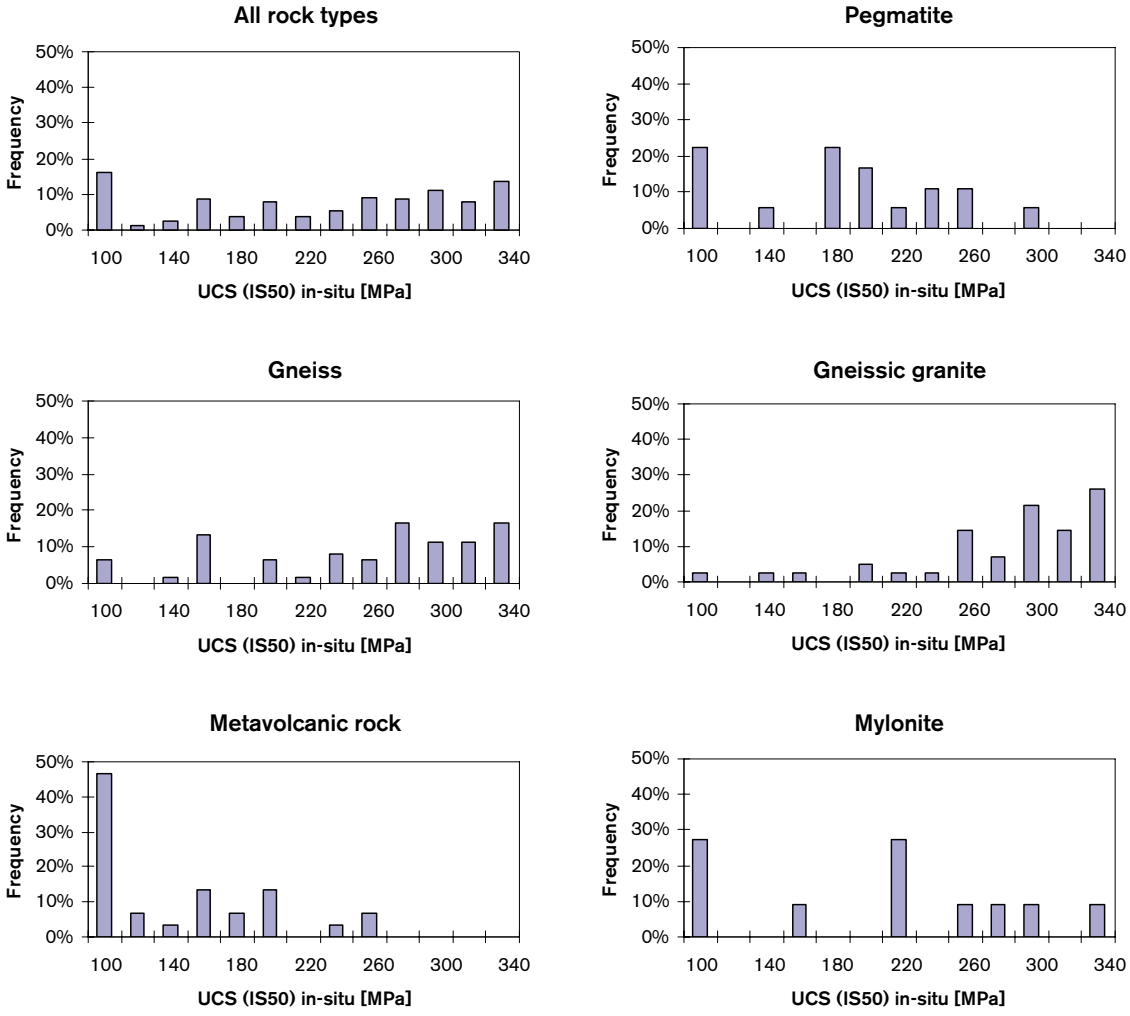

Point load test results available from the SRF Repository in Forsmark and performed in-situ. (IS50) = from Point Load Strength Index.

A.3 Point load tests in laboratory

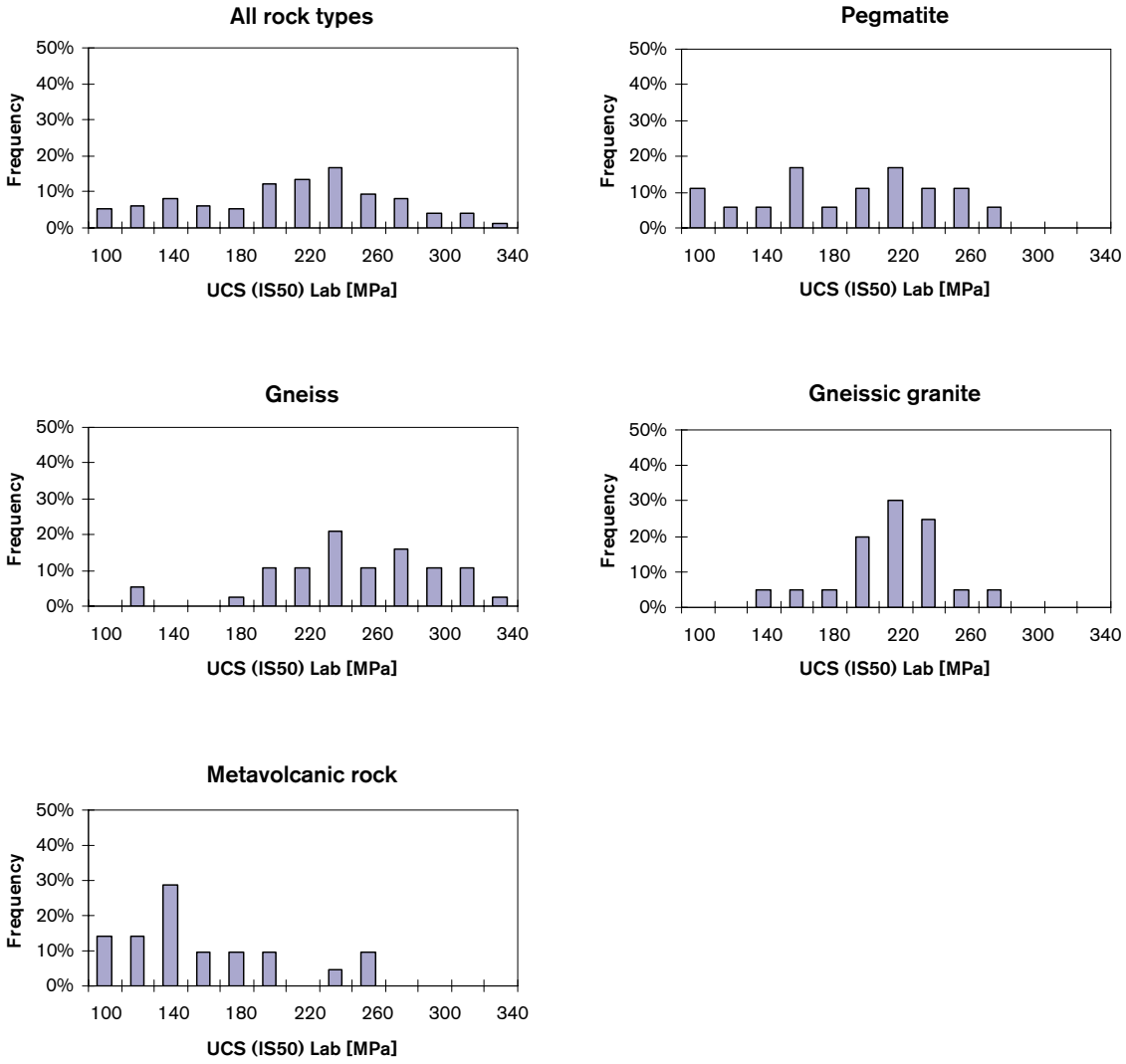

Point load test results available from the SRF Repository in Forsmark and performed in the laboratory. (IS50) = from Point Load Strength Index.

Appendix B

Rock fracture properties

B.1 Tilt test results /Chryssanthakis, 2003/

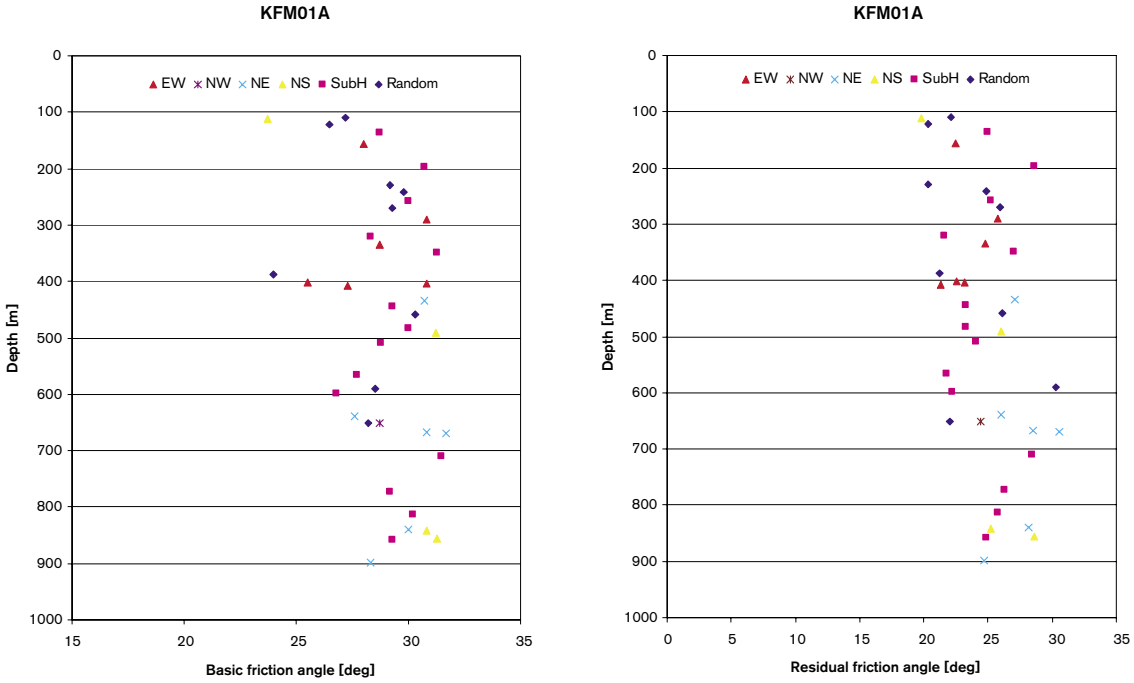

Variation of the basic and residual friction angle of the tested fractures from KFM01A.

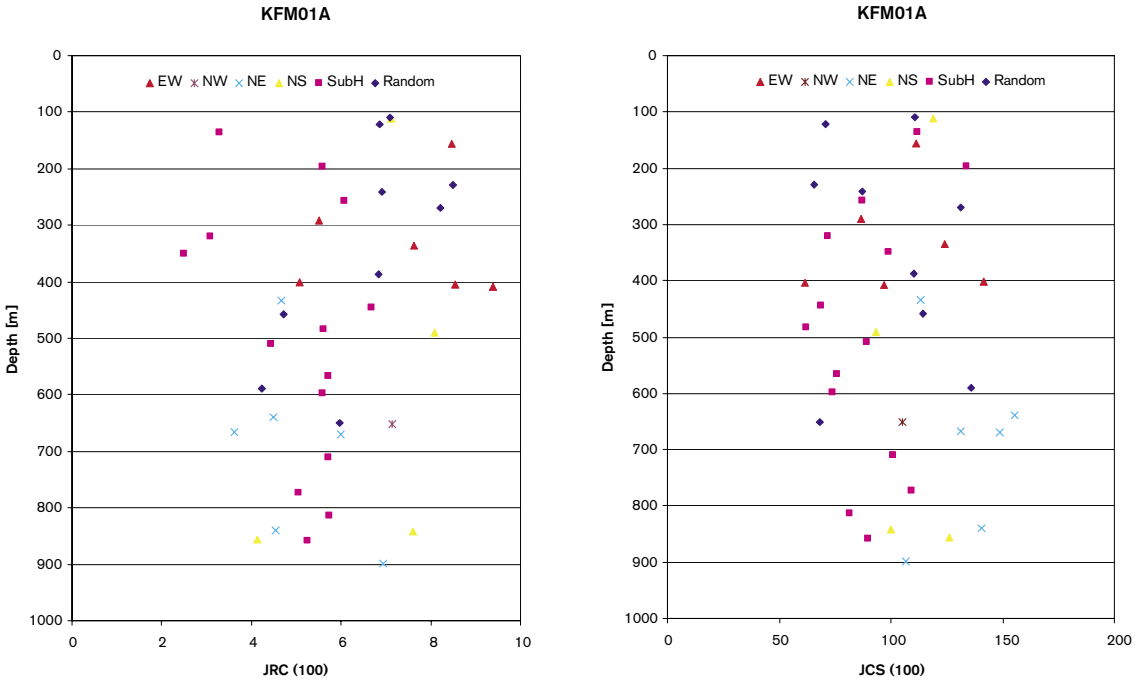

Variation of the Joint Roughness Coefficient (JRC) and Joint Compressive Strength (JCS) of the tested fractures from KFM01A.

B.2 Correlations

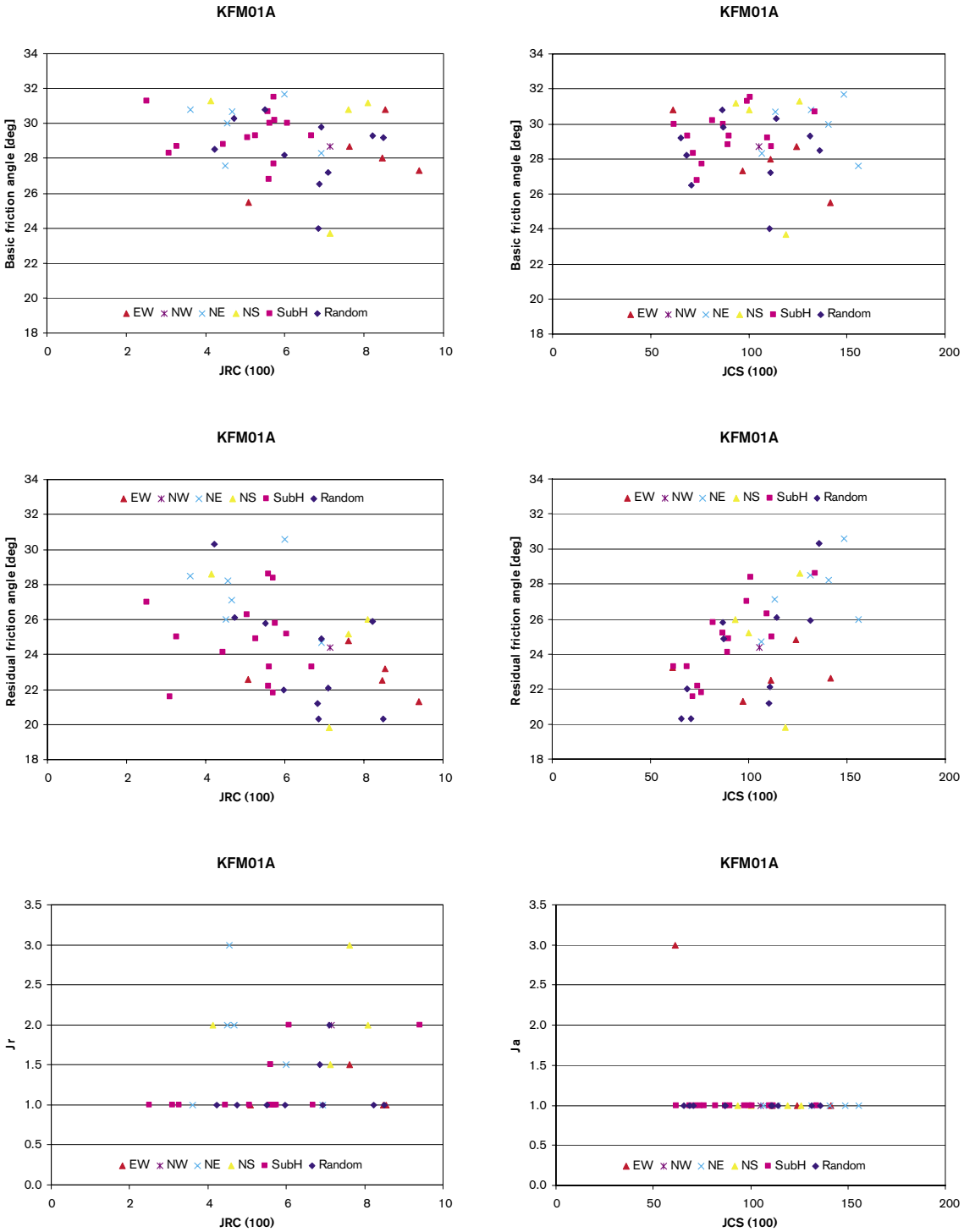

Correlations between the parameters obtained from the tilt tests for borehole KFM01A.

Appendix C

Characterisation of the rock mass

C.1 RMR

C.1.1 Statistics of the RMR-ratings (core sections of 5 m)

RMR-rating	Depth (m)	Minimum	Mean	Median	Maximum	Min possible	Max possible
UCS	100–1,000	9.5	14	14.3	15	9.5	15
RQD	100–155	19	19.4	19.3	20	16	20
	155–200	18	19.3	19.4	20	16	20
	200–265	18	19.7	19.9	20	17	20
	265–300	19	19.6	19.6	20	17	20
	300–385	19	19.8	20.0	20	17	20
	385–410	18	19.5	20.0	20	15	20
	410–650	20	20.0	20.0	20	18	20
	650–685	20	20.0	20.0	20	19	20
	685–1,000	20	20.0	20.0	20	20	20
Joint conditions	100–155	16	16.7	16.6	18	12	22
	155–200	15	15.4	15.4	16	11	22
	200–265	15	15.5	15.5	16	11	20
	265–300	14	15.1	15.1	17	3	16
	300–385	13	15.5	15.3	19	12	22
	385–410	15	15.2	15.2	16	12	20
	410–650	12	18.1	16.3	24	12	24
	650–685	14	16.0	15.0	22	9	22
	685–1,000	14	21.2	22.0	24	12	24
Joint spacing	100–155	8	11.7	10.2	20	5	20
	155–200	8	10.6	10.4	15	5	20
	200–265	7	14.9	14.5	20	5	20
	265–300	11	13.7	14.1	15	5	20
	300–385	11	17.3	19.4	20	5	20
	385–410	13	13.9	13.7	15	5	20
	410–650	10	17.9	20.0	20	5	20
	650–685	11	13.9	12.9	20	5	20
	685–1,000	8	19.8	20.0	20	5	20
Water	100–1,000	15	15.0	15.0	15	15	15
Orientation	100–1,000	0	0.0	0.0	0	0	0

C.1.2 Histograms of the RMR-ratings (core sections of 5 m)

Depth: 100–155 m

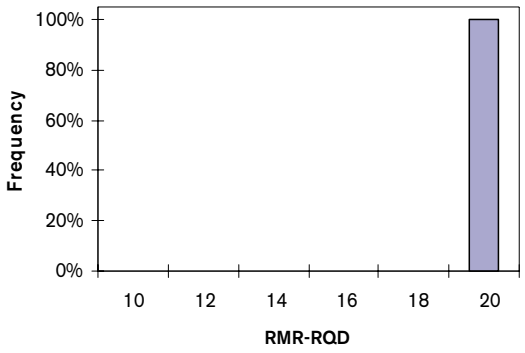

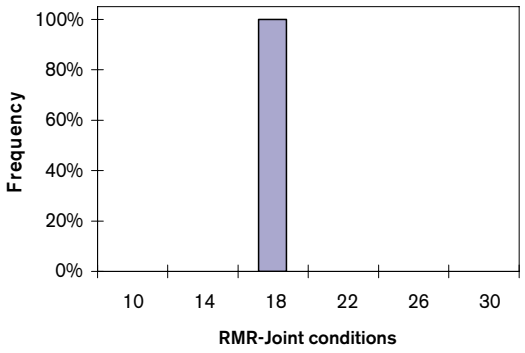

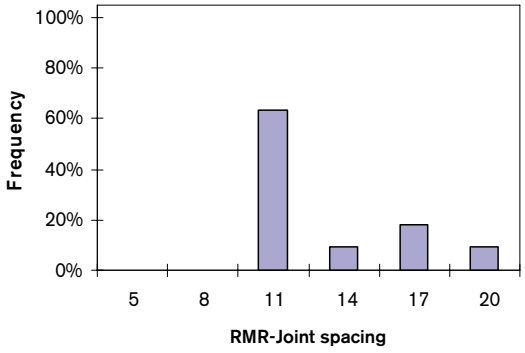

Depth: 155–200 m

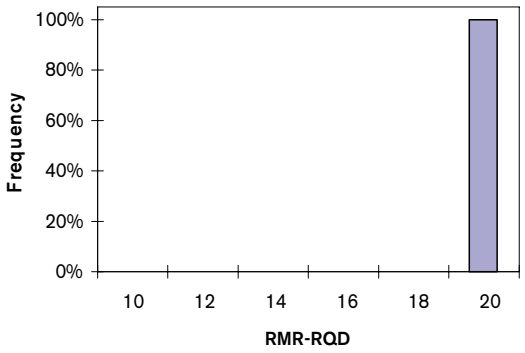

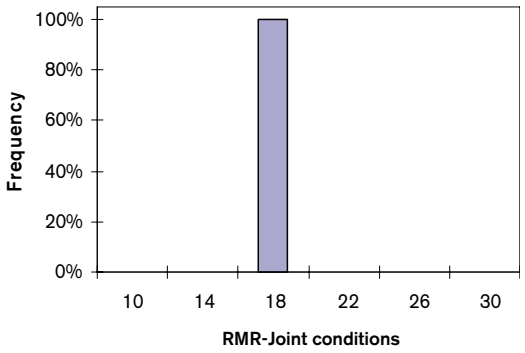

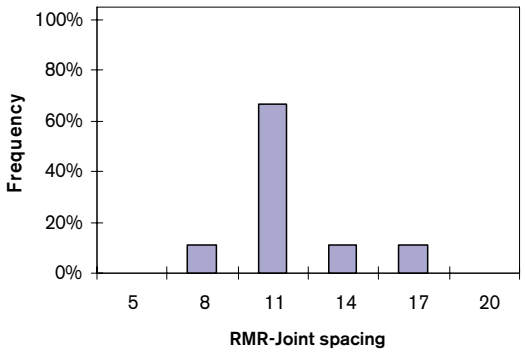

Depth: 200–265 m

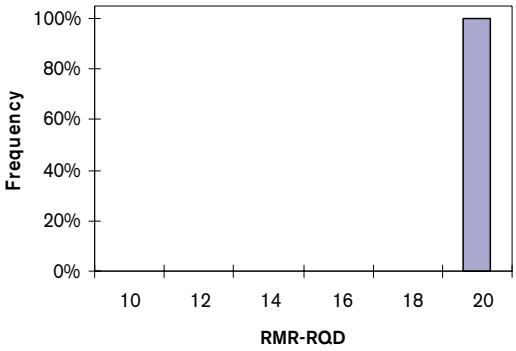

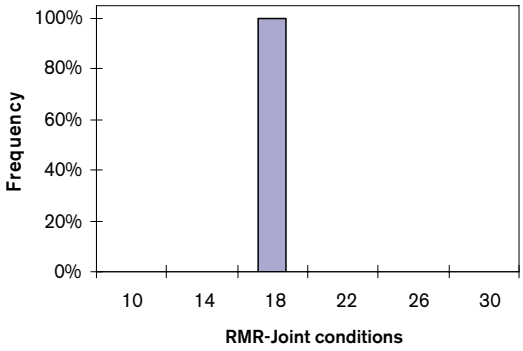

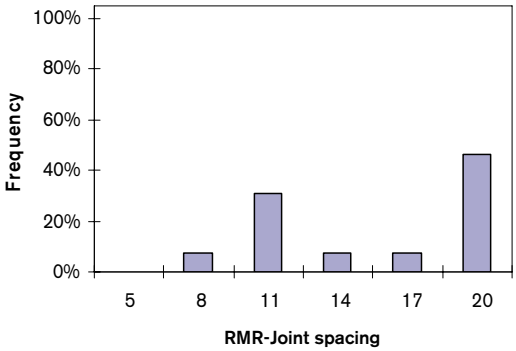

Depth: 265–300 m

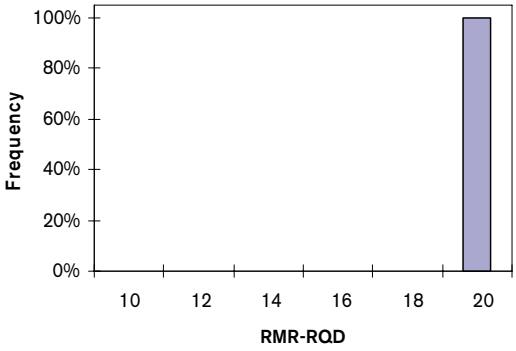

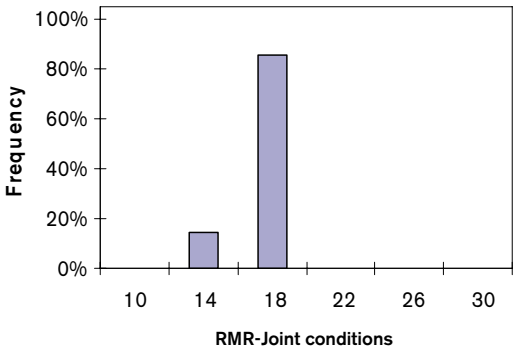

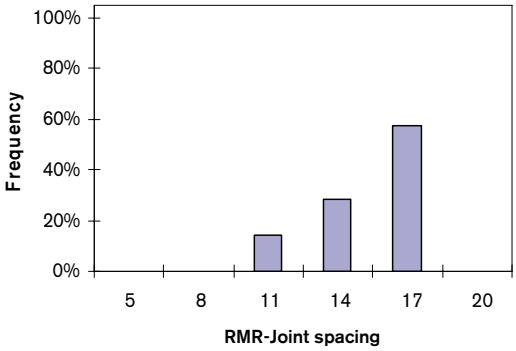

Depth: 300–385 m

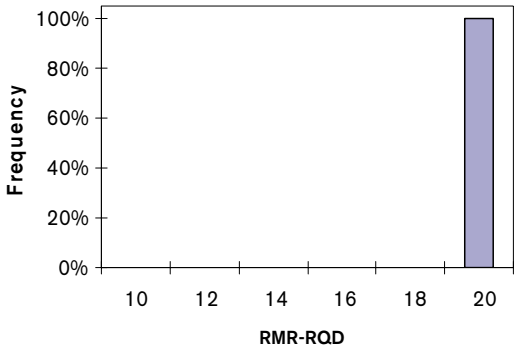

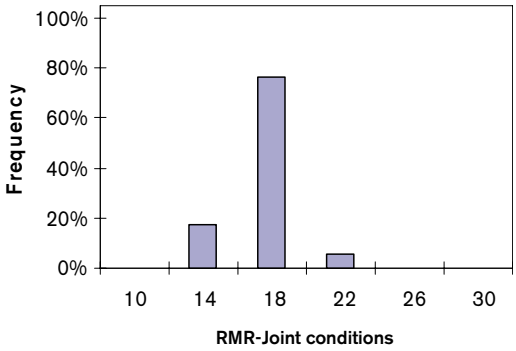

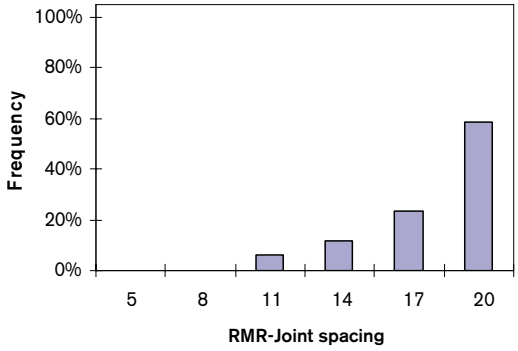

Depth: 385–410 m

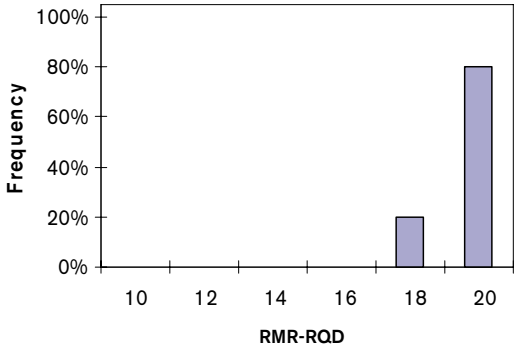

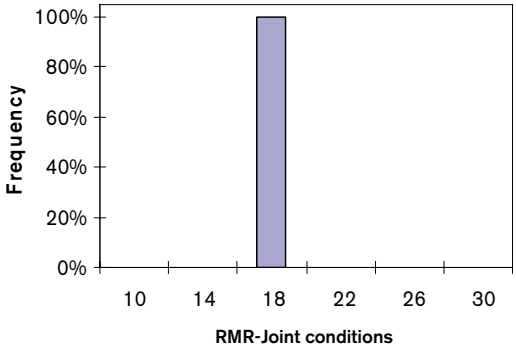

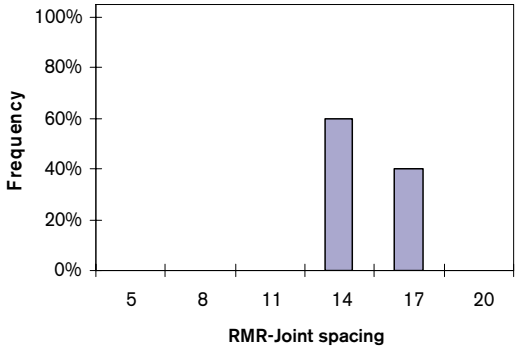

Depth: 410–650 m

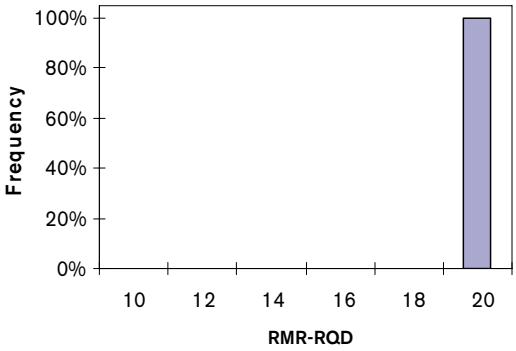

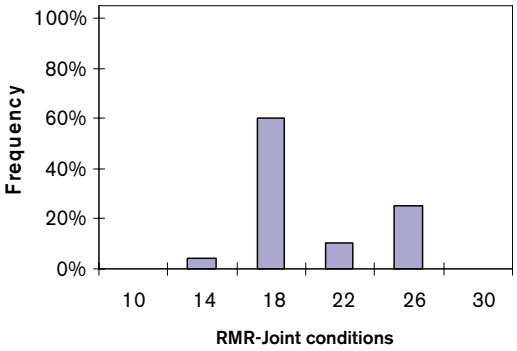

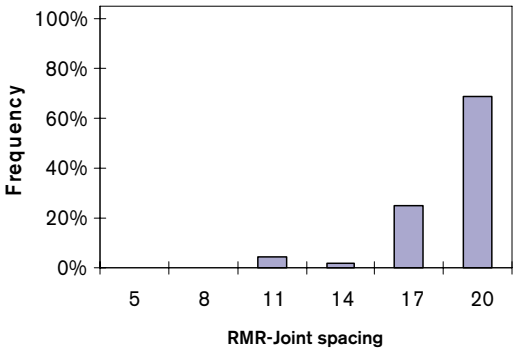

Depth: 650–685 m

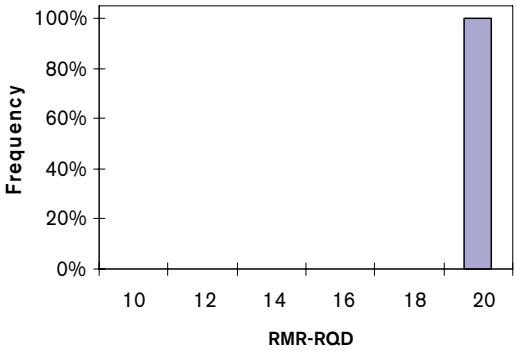

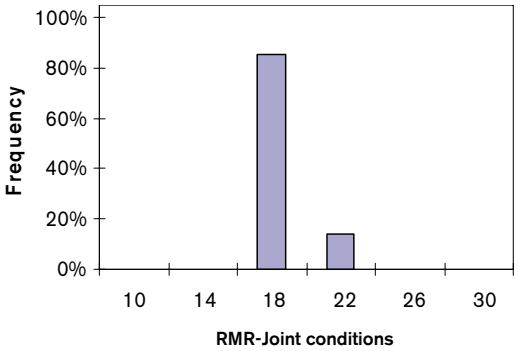

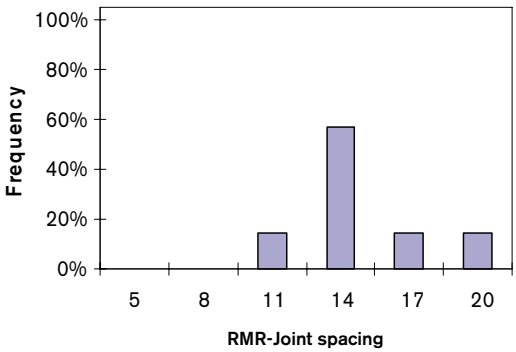

Depth: 685–1,000 m

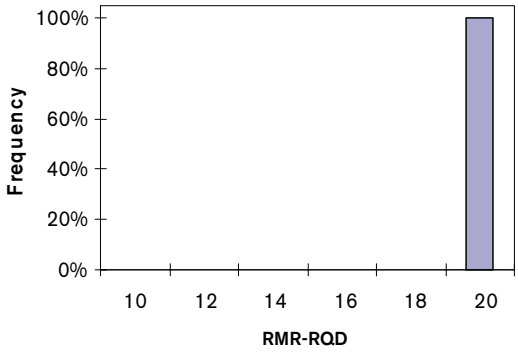

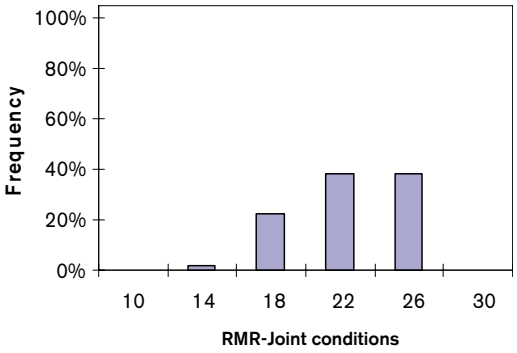

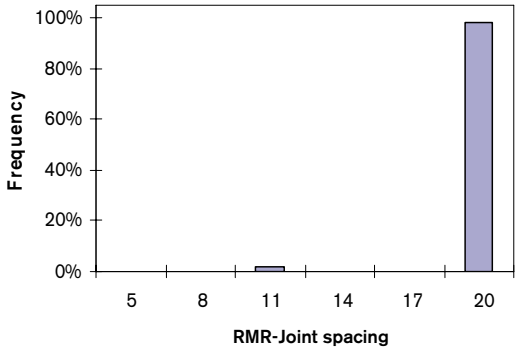

C.1.3 RMR values for the rock domains (core sections of 5 m)

Depth (m)	Minimum mean RMR	Average mean RMR	Frequent mean RMR	Maximum mean RMR	Standard deviation RMR	Min possible RMR	Max possible RMR
100–155	75.7	79.8	78.2	89.5	4.2	60.8	94
155–200	72.9	77.4	77.1	81.1	2.4	59.5	94
200–265	73.8	82	82	87.9	5.4	60.4	92
265–300	77	80.4	81.4	82.3	2.3	55	95
300–385	77.9	84.6	85	91	3.6	61.7	94
385–410	78.6	80.6	80.9	82.6	1.7	59.4	94
410–650	78.7	88	87	96	5.5	63.6	98
650–685	77.1	81.8	80.1	94	5.7	61.1	96
685–1,000	75.3	93	94	96	3.9	63.6	98

C.1.4 RMR values for the rock domains (core sections of 20 m)

Depth (m)	Minimum mean RMR	Average mean RMR	Frequent mean RMR	Maximum mean RMR	Standard deviation RMR	Min possible RMR	Max possible RMR
100–160	77.6	78.7	78.9	79.4	1.0	59.4	96
160–200	76.7	77.2	77.2	77.7	0.7	59.7	96
200–260	77.7	82.6	82.7	87.6	5.0	58.9	92.7
260–300	80.9	81	81	81	0.1	52.6	96
300–380	81.6	86.2	87.4	88.4	3.1	62.6	94
380–420	78.8	81.3	81.3	83.8	3.5	58.9	96
420–660	83.7	83.7	87.5	89.2	1.4	63.2	96
660–680	80.9	80.9	80.9	80.9	–	60.6	91
680–1,000	86.8	90.4	89	96	3.5	63.6	98

C.2 Q

C.2.1 Statistics of the Q-numbers (core sections of 5 m)

Q number	Depth (m)	Minimum	Mean	Median	Maximum	Min possible	Max possible
RQD	100–155	94	97.2	96.6	100	78	100
	155–200	91	96.6	97.0	100	81	100
	200–265	92	98.4	99.6	100	84	100
	265–300	94	97.9	98.0	100	85	100
	300–385	97	99.2	100.0	100	86	100
	385–410	89	97.3	100.0	100	77	100
	410–650	98	99.9	100.0	100	90	100
	650–685	98	99.8	100.0	100	93	100
	685–1,000	100	100.0	100.0	100	100	100
Jn	100–155	3	7.9	6.0	15	3	15
	155–200	4	8.9	6.0	15	4	15
	200–265	3	7.0	6.0	15	3	15
	265–300	2	5.9	6.0	12	2	2
	300–385	2	2.4	2.0	4	2	4
	385–410	3	9.6	12.0	15	3	15
	410–650	1	2.2	2.0	9	1	9
	650–685	1	5.7	4.0	12	1	12
	685–1,000	1	1.4	1.0	12	1	12
Jr	100–155	1	1.7	1.6	2	1	3
	155–200	1	1.3	1.2	2	1	3
	200–265	1	1.3	1.3	2	1	3
	265–300	1	1.3	1.4	1	1	2
	300–385	1	1.2	1.3	2	1	3
	385–410	1	1.3	1.3	2	1	3
	410–650	1	2.1	1.5	4	1	4
	650–685	1	1.7	1.3	4	1	4
	685–1,000	1	3.2	4.0	4	1	4
Ja	100–155	1	1.1	1.0	1	1	4
	155–200	1	1.1	1.0	1	1	4
	200–265	1	1.0	1.0	1	1	4
	265–300	1	1.0	1.0	1	1	3
	300–385	1	1.0	1.0	2	1	3
	385–410	1	1.1	1.0	1	1	3
	410–650	1	1.1	1.0	4	1	4
	650–685	1	1.1	1.0	1	1	4
	685–1,000	1	0.9	0.8	2	1	2
Jw	100–1,000	1	1.0	1.0	1	1	1
SRF	100–155	1.0	1.0	1.0	1.0	1.0	1.0
	155–200	1.0	1.0	1.0	1.0	1.0	1.0
	200–265	0.5	1.0	1.0	1.0	0.5	1.0
	265–300	0.5	0.5	0.5	0.5	0.5	0.5
	300–385	0.5	0.5	0.5	0.5	0.5	0.5
	385–410	0.5	0.5	0.5	0.5	0.5	0.5
	410–650	0.5	0.5	0.5	0.5	0.5	0.5
	650–685	0.5	0.5	0.5	0.5	0.5	0.5
	685–1,000	0.5	0.5	0.5	0.5	0.5	0.5

C.2.2 Histograms of the Q-numbers (5 m)

Depth: 100–155 m

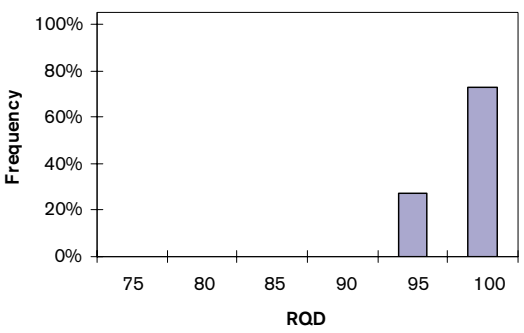

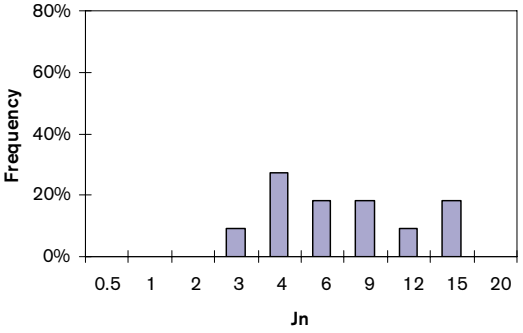

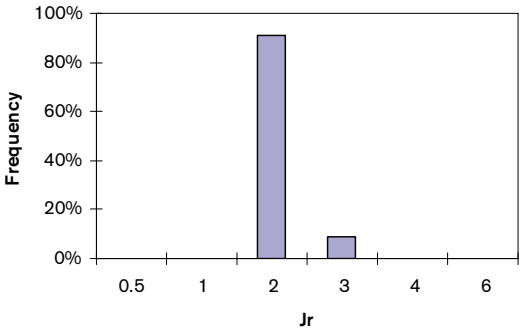

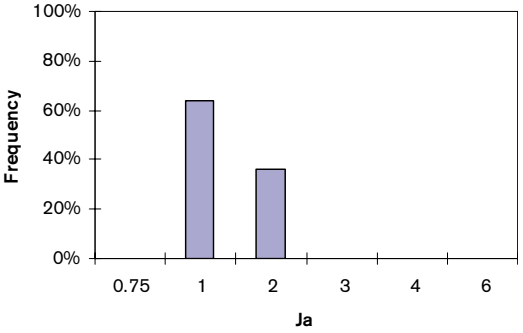

Depth: 155–200 m

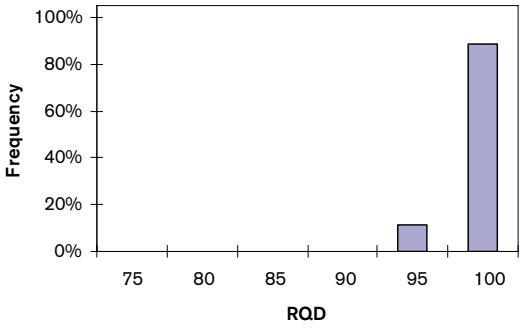

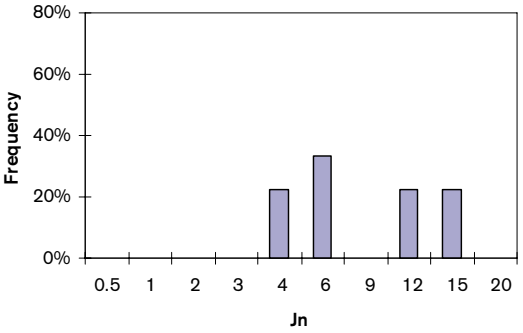

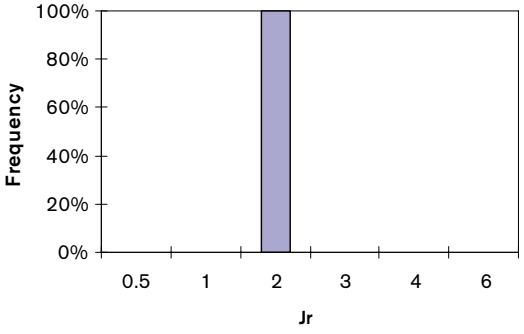

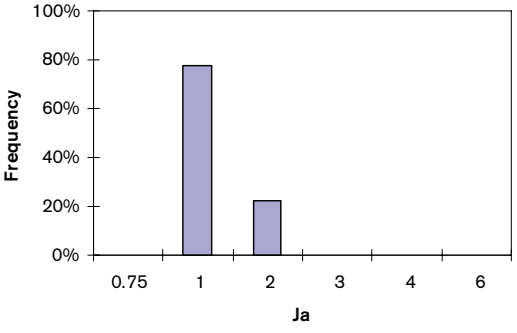

Depth: 200–265 m

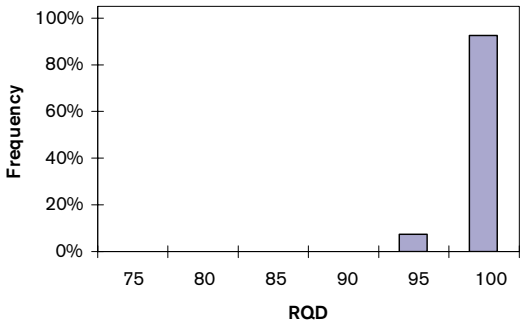

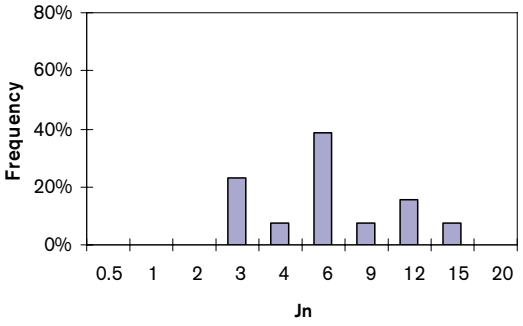

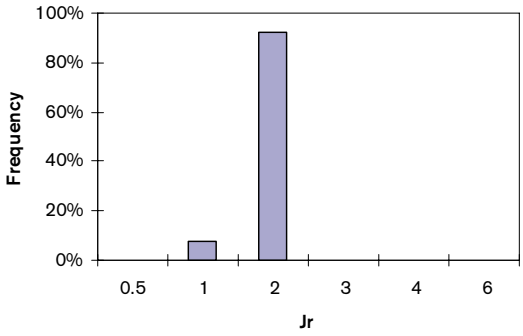

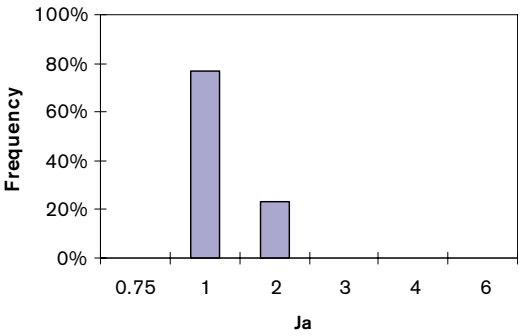

Depth: 265–300 m

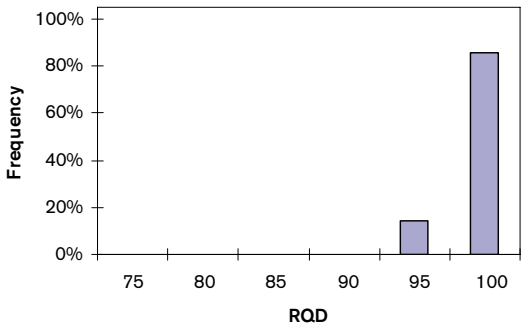

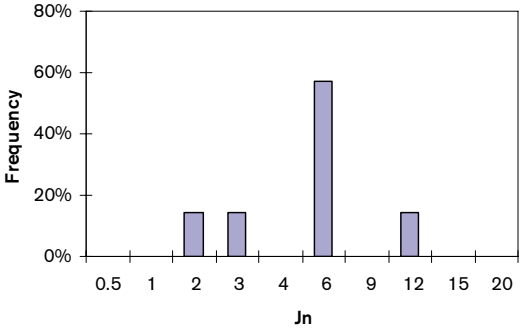

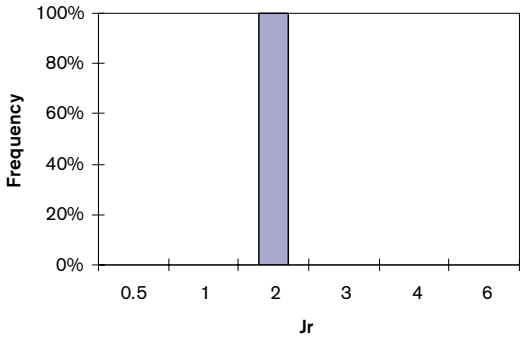

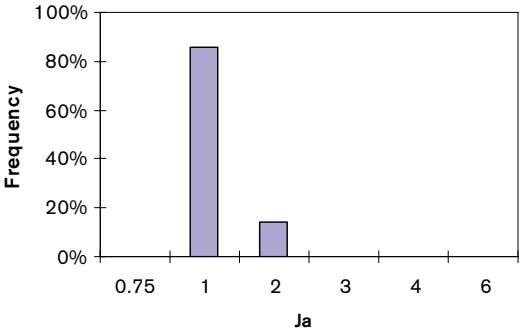

Depth: 300–385 m

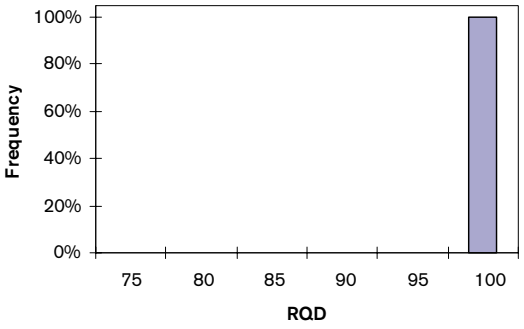

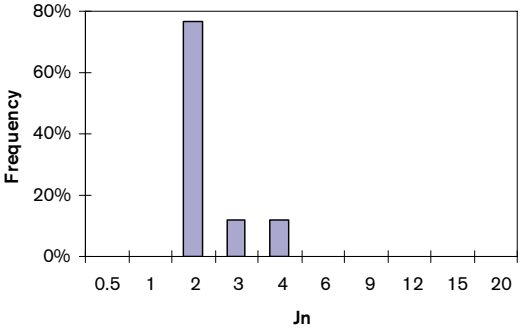

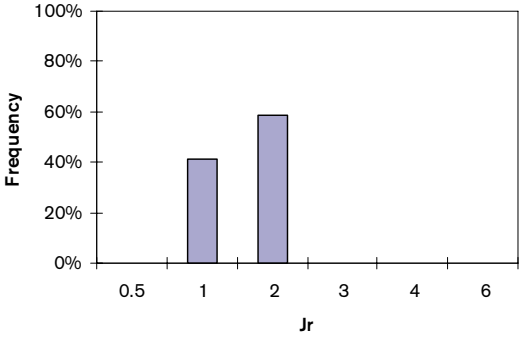

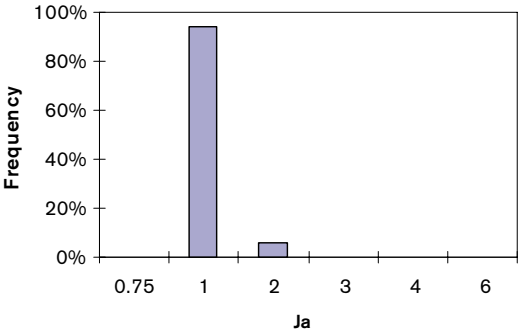

Depth: 385–410 m

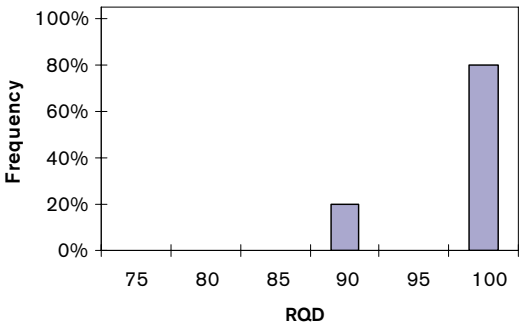

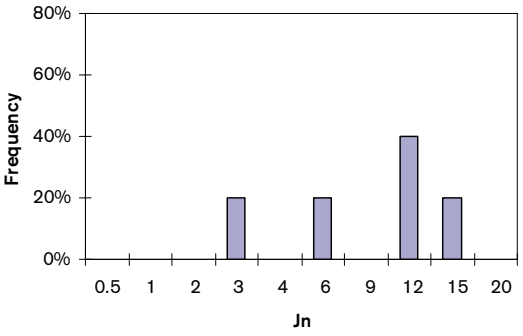

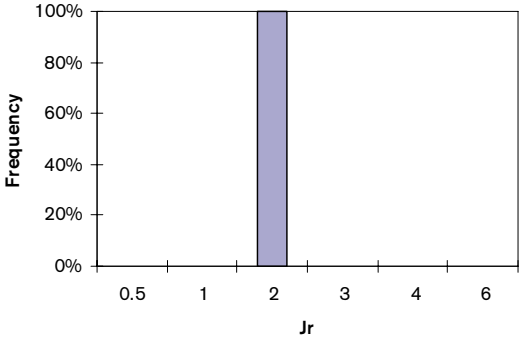

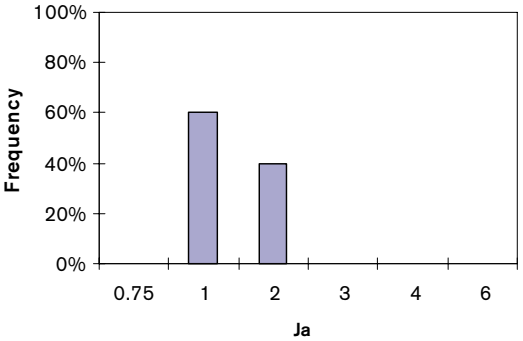

Depth: 410–650 m

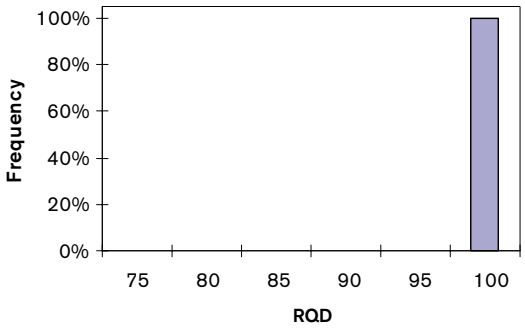

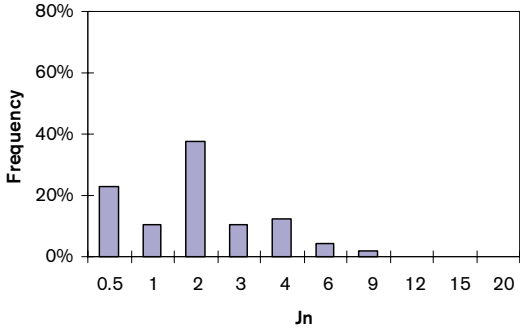

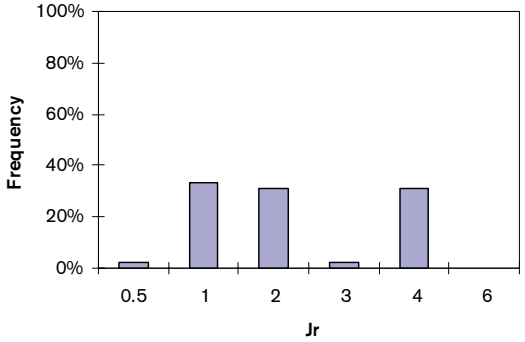

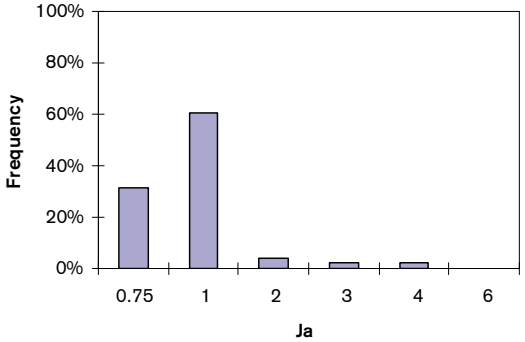

Depth: 650–685 m

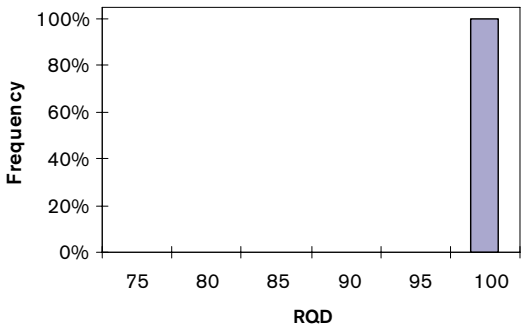

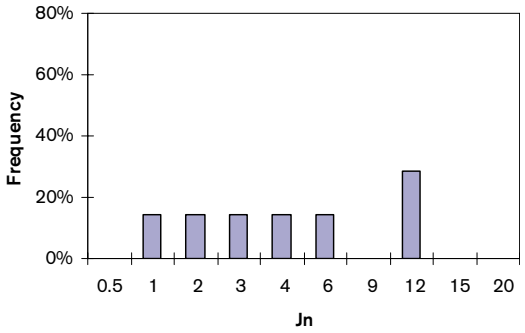

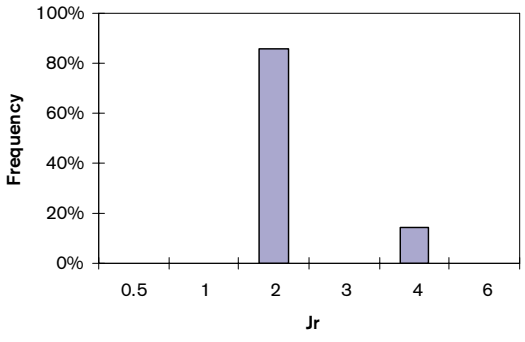

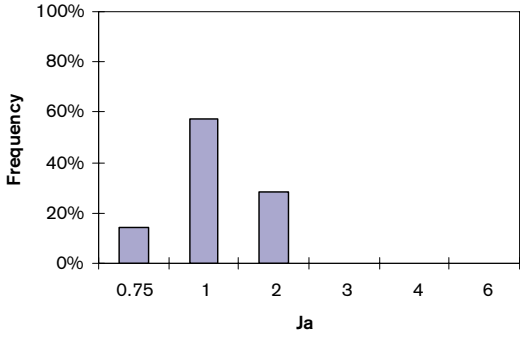

Depth: 685–1,000 m

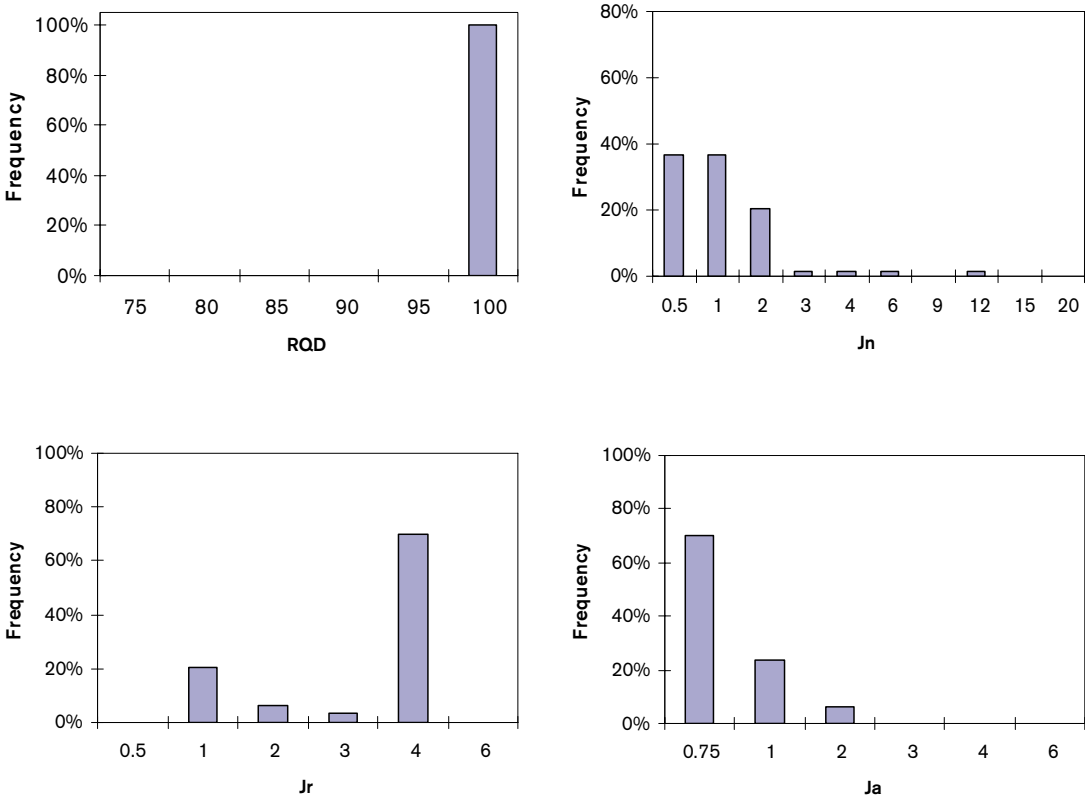

C.2.3 Q values for the rock domains (core sections of 5 m)

Depth (m)	Minimum mean Q	Average mean Q	Frequent mean Q	Maximum mean Q	Min possible Q	Max possible Q
100–155	10.1	25.1	21.8	50	1.6	100
155–200	7.6	16.6	14.1	32.5	2.8	75
200–265	9.2	29.9	20.2	80	2.8	133.3
265–300	22.9	57.2	44.4	139.7	9.4	300
300–385	60	107.1	100	150	33.3	200
385–410	15	32.3	25.8	66.7	5.6	133.3
410–650	20	643.7	100	2,133.3	8.3	2,133.3
650–685	15.2	199.3	62.5	1,066.7	4.2	1,066.7
685–1,000	33.3	1,176.8	1,066.7	2,133.3	16.7	2,133.3

C.2.4 Q values for the rock domains (core sections of 20 m)

Depth (m)	Minimum mean Q	Average mean Q	Frequent mean Q	Maximum mean Q	Min possible Q	Max possible Q
100–160	9.3	10.5	11.1	11.2	1	25
160–200	8	8.6	8.6	9.2	0.9	25
200–260	8.8	9.9	9.4	11.6	1.7	20
260–300	9.2	10	10	10.7	1.8	25
300–380	25	34.6	29.7	54.2	16.2	100
380–420	9	9.3	9.3	9.6	2.8	25
420–660	8.2	27.1	20.7	50	2.8	75
660–680	10.7	10.7	10.7	10.7	8.3	22.2
680–1,000	13.5	381.3	50	1,625.4	8.3	2,133.3

Appendix D

Rock mass properties

D.1 Deformation modulus

D.1.1 From RMR and Q

Summary of the deformation modulus E_m of the rock mass obtained from RMR (core sections of 5 m).

Rock unit	Minimum mean E_m (RMR)	Average mean E_m (RMR)	Frequent mean E_m (RMR)	Maximum mean E_m (RMR)	Standard deviation E_m (RMR)	Min possible E_m (RMR)	Max possible E_m (RMR)
100–160	44	55.2	50.7	75	11	18.6	90
160–200	37.4	48.7	47.6	59.8	6.6	17.3	90
200–260	39.3	61	63.1	75	14.4	18.2	90
260–300	47.4	57.9	61.1	64.3	7.5	13.3	90
300–380	49.9	68.9	75	75	8.1	19.6	90
380–420	52	58.4	59.2	65.2	5.5	17.2	90
420–660	52.3	71.1	75	75	6.5	21.9	90
660–680	47.3	58.7	56.4	75	9.5	18.9	90
680–1,000	42.9	74.5	75	75	4	21.9	90

Summary of the deformation modulus E_m of the rock mass obtained from Q (core sections of 5 m).

Rock unit	Minimum mean E_m (RMR)	Average mean E_m (RMR)	Frequent mean E_m (RMR)	Maximum mean E_m (RMR)	Standard deviation E_m (RMR)	Min possible E_m (RMR)	Max possible E_m (RMR)
100–160	27.3	35.9	35.2	46.4	6.5	11.8	66.9
160–200	24.8	31.3	30.4	40.2	5.6	14.1	60.8
200–260	26.4	37.1	34.3	54.3	9	14.1	73.7
260–300	35.8	46.7	44.6	65.4	9.9	21.1	90
300–380	49.3	59.4	58.5	66.9	5.5	32.2	84.3
380–420	31.1	38.8	37.2	51.1	7.9	17.7	73.7
420–660	34.2	61.6	58.5	75	12.1	20.3	90
660–680	31.2	49.7	50	75	15.3	16.1	90
680–1,000	40.5	69.7	75	75	10	25.5	90

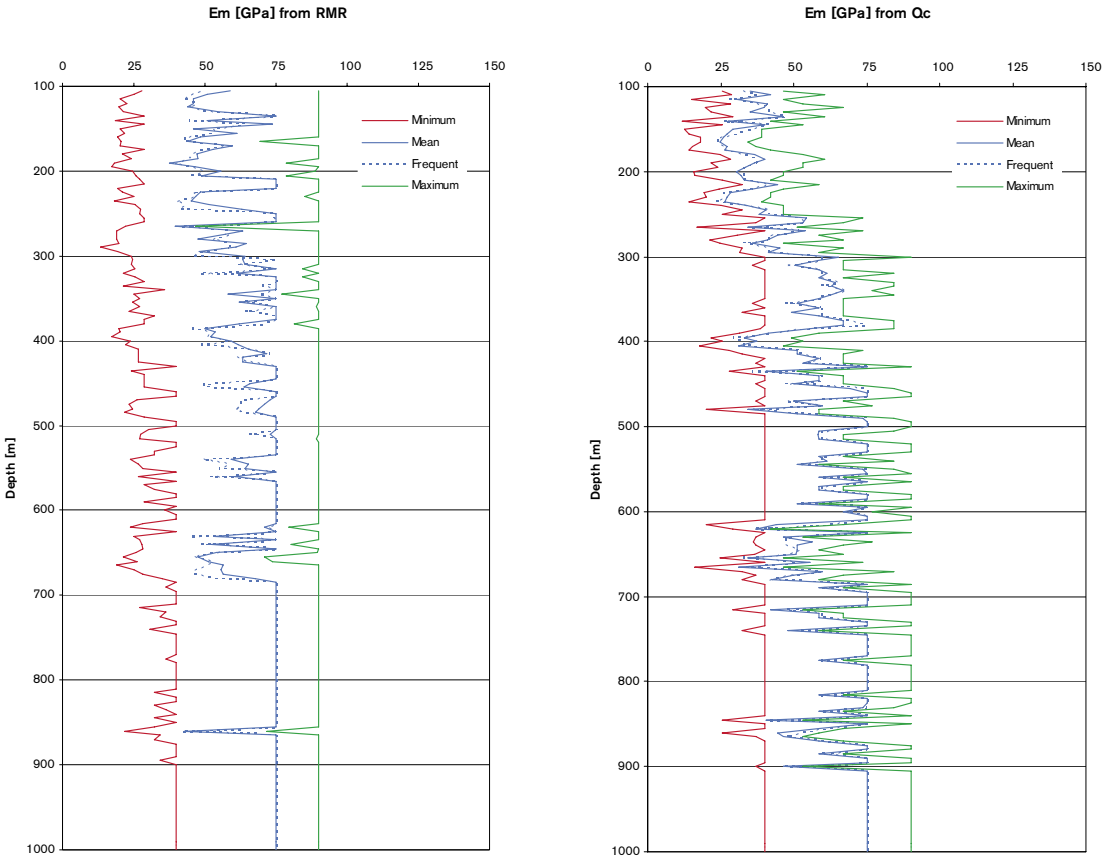

Variation of the deformation modulus of the rock mass obtained from RMR and from Q_c with depth. The values are given for each core section of 5 m.

D.1.2 Comparison

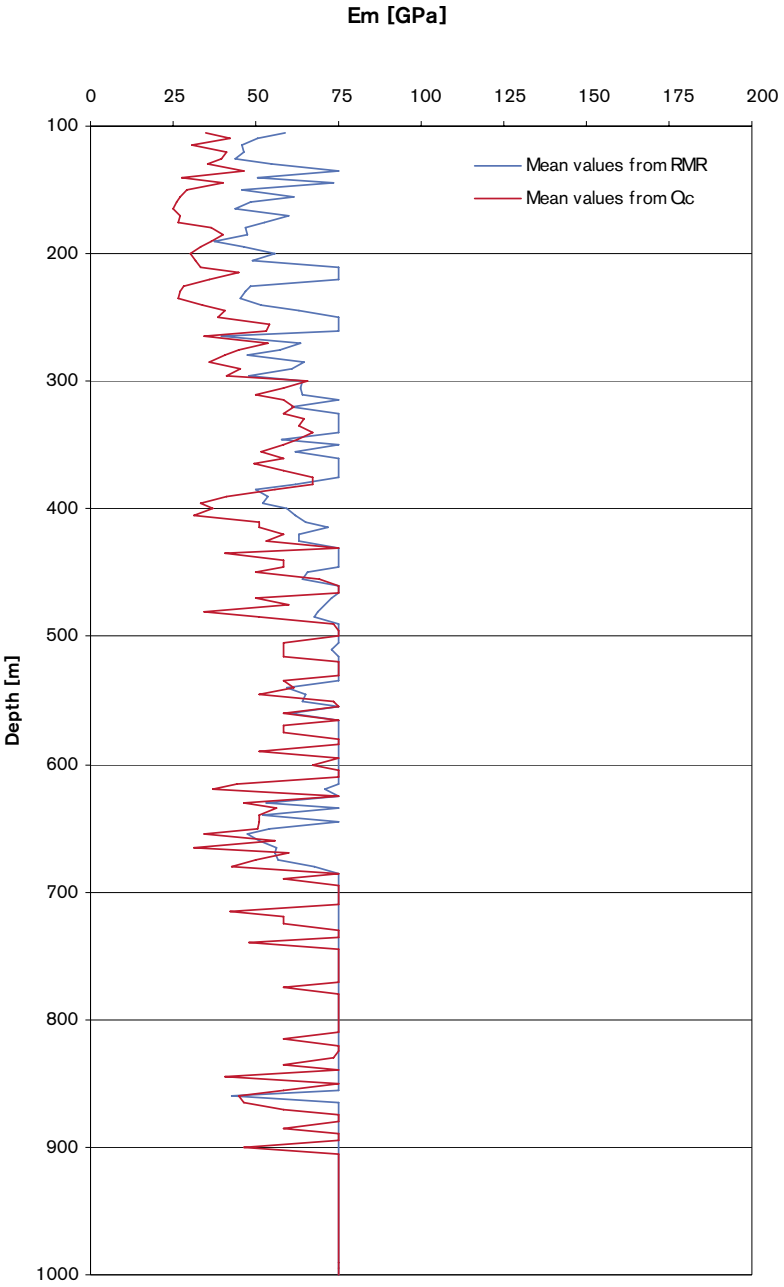

Comparison between the mean values of the deformation modulus E_m obtained from RMR and Qc for different depths. The values are given for each core section of 5 m.

D.2 Uniaxial compressive strength

D.2.1 From RMR and Q

Summary of the uniaxial compressive UCS_m strength of the rock mass according to the Hoek and Brown's failure criterion (core sections of 5 m, Hoek and Brown's a = 0.5).

Rock unit	Minimum mean UCS_m	Average mean UCS_m	Frequent mean UCS_m	Maximum mean UCS_m	Standard deviation UCS_m	Min possible UCS_m	Max possible UCS_m
100–160	39.3	50.6	45.1	84.5	13.5	8.6	162.8
160–200	33.6	43.4	42.4	52.9	5.7	8.0	162.8
200–260	35.3	58.2	55.7	77.1	16.9	8.4	145.6
260–300	42.3	51.3	54.0	56.8	6.4	6.2	172.1
300–380	44.5	65.7	65.8	91.9	13.0	9.0	163.1
380–420	46.3	51.7	52.4	57.6	4.7	7.9	162.8
420–660	46.5	81.5	73.6	121.3	25.4	10.0	203.3
660–680	42.5	58.0	50.1	108.5	22.9	8.7	182.0
680–1,000	38.4	104.8	108.5	121.3	19.1	10.0	203.3

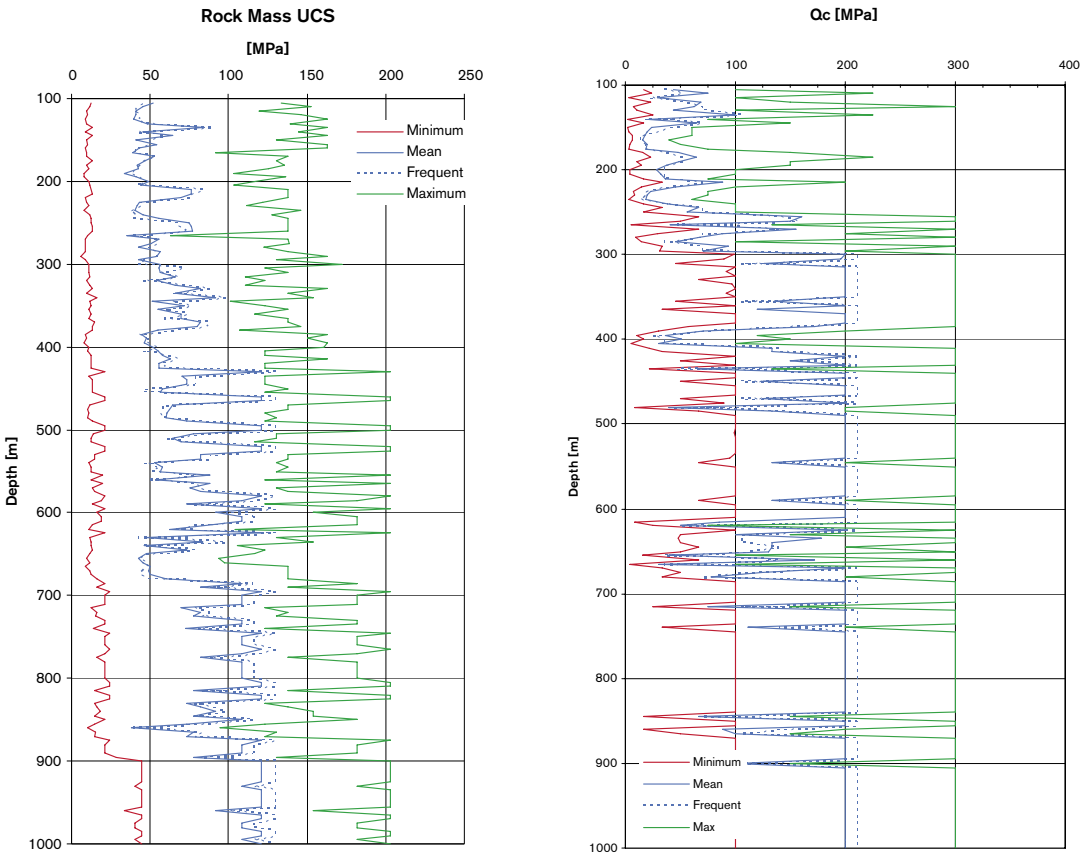

Variation of the uniaxial compressive strength UCSm of the rock mass (Hoek and Brown's a = 0.5), and of Qc with depth. The values are given for each core section of 5 m.

D.2.2 Comparison

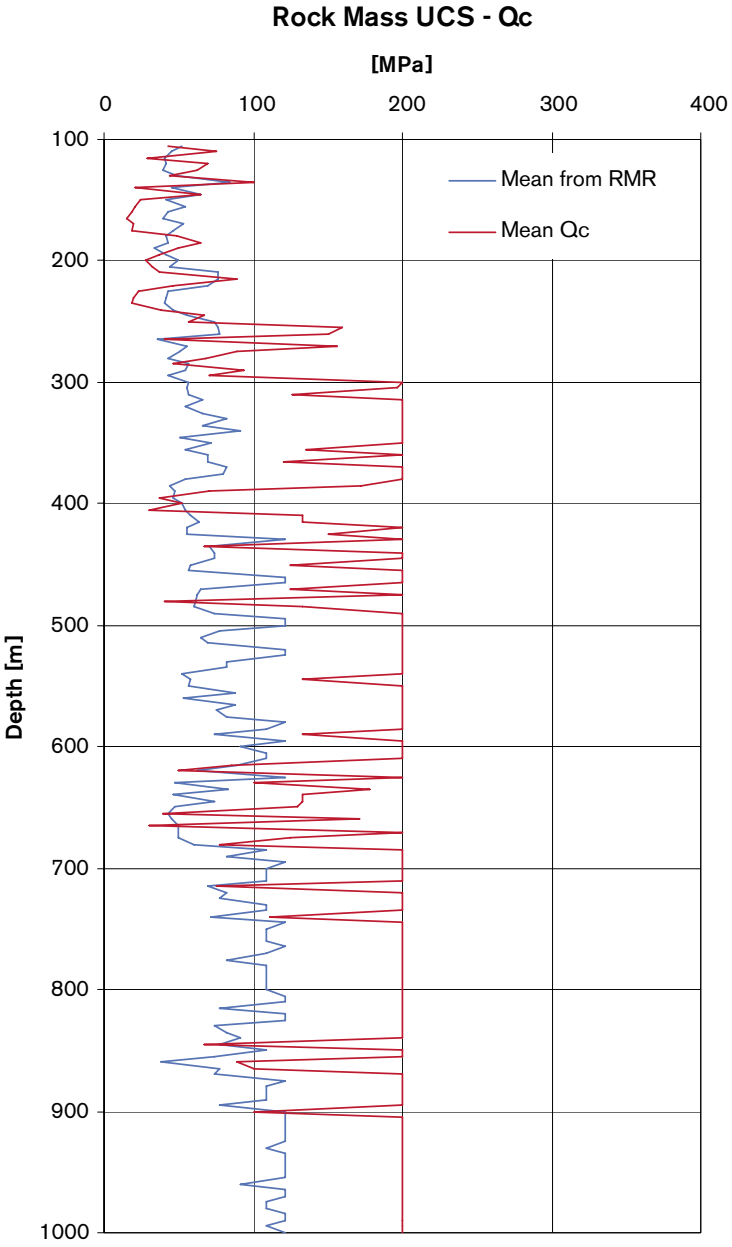

Comparison of the rock mass compressive strength from RMR and Qc for borehole KFM01A (Hoek and Brown's a = 0.5). The values are given for each core section of 5 m.

D.3 Cohesion and friction of the rock mass

D.3.1 From RMR

Summary of the friction angle φ' of the rock mass derived from RMR (10–30 MPa) (core sections of 5 m, Hoek and Brown's a = 0.5).

Rock unit	Minimum mean φ' (°)	Average mean φ' (°)	Frequent mean φ' (°)	Maximum mean φ' (°)	Standard deviation φ' (°)	Min possible φ' (°)	Max possible φ' (°)
105–155	46.3	47.3	46.9	49.7	1.1	34.5	54.7
160–200	45.5	46.7	46.6	47.7	0.6	34.1	54.7
205–265	45.7	47.9	47.9	49.3	1.4	34.4	54.3
270–300	46.6	47.5	47.8	48.0	0.6	32.8	54.8
305–385	46.9	48.5	48.7	50.0	0.9	34.8	54.7
390–410	47.0	47.5	47.6	48.1	0.4	34.1	54.7
415–650	47.1	49.3	49.1	51.0	1.2	35.4	55.3
655–685	46.6	47.8	47.4	50.7	1.3	34.6	55.0
685–1,000	46.1	50.4	50.7	51.0	0.9	35.4	55.3

Summary of the cohesion c' of the rock mass derived from RMR (10–30 MPa) (core sections of 5 m, Hoek and Brown's a = 0.5).

Rock unit	Minimum mean c' (MPa)	Average mean c' (MPa)	Frequent mean c' (MPa)	Maximum mean c' (MPa)	Standard deviation c' (MPa)	Min possible c' (MPa)	Max possible c' (MPa)
105–155	19.7	21.3	20.6	25.6	1.8	12.1	35.6
160–200	18.9	20.3	20.2	21.6	0.8	11.9	35.6
205–265	19.2	22.2	22.0	24.7	2.2	12.1	33.6
270–300	20.2	21.4	21.7	22.1	0.9	11.3	36.7
305–385	20.5	23.2	23.3	26.6	1.7	12.3	35.7
390–410	20.7	21.4	21.5	22.2	0.6	11.9	35.6
415–650	20.7	25.3	24.3	30.3	3.2	12.6	40.4
655–685	20.2	22.2	21.2	28.7	2.9	12.2	37.9
685–1,000	19.6	28.2	28.7	30.3	2.4	12.6	40.4

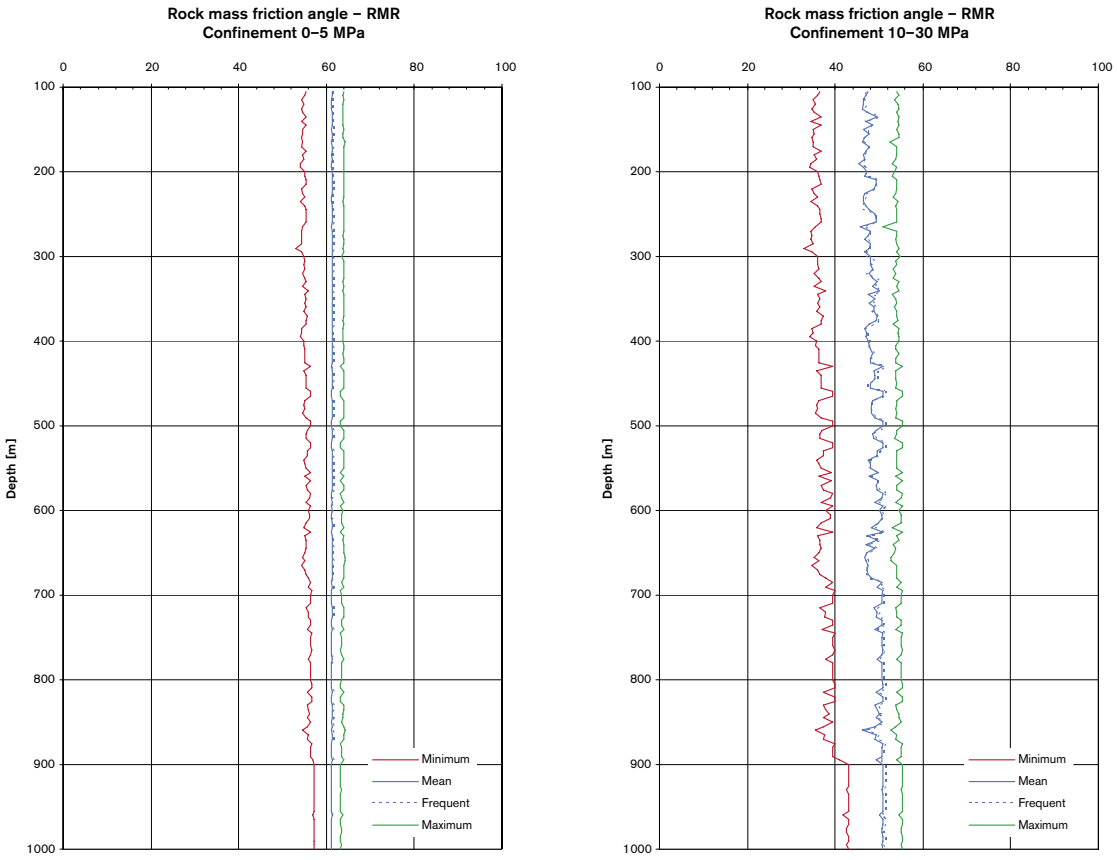

Variation of the rock mass friction angle from RMR for borehole KFM01A under stress confinement of 0–5 MPa and 10–30 MPa (Hoek and Brown's a = 0.5). The values are given for each core section of 5 m.

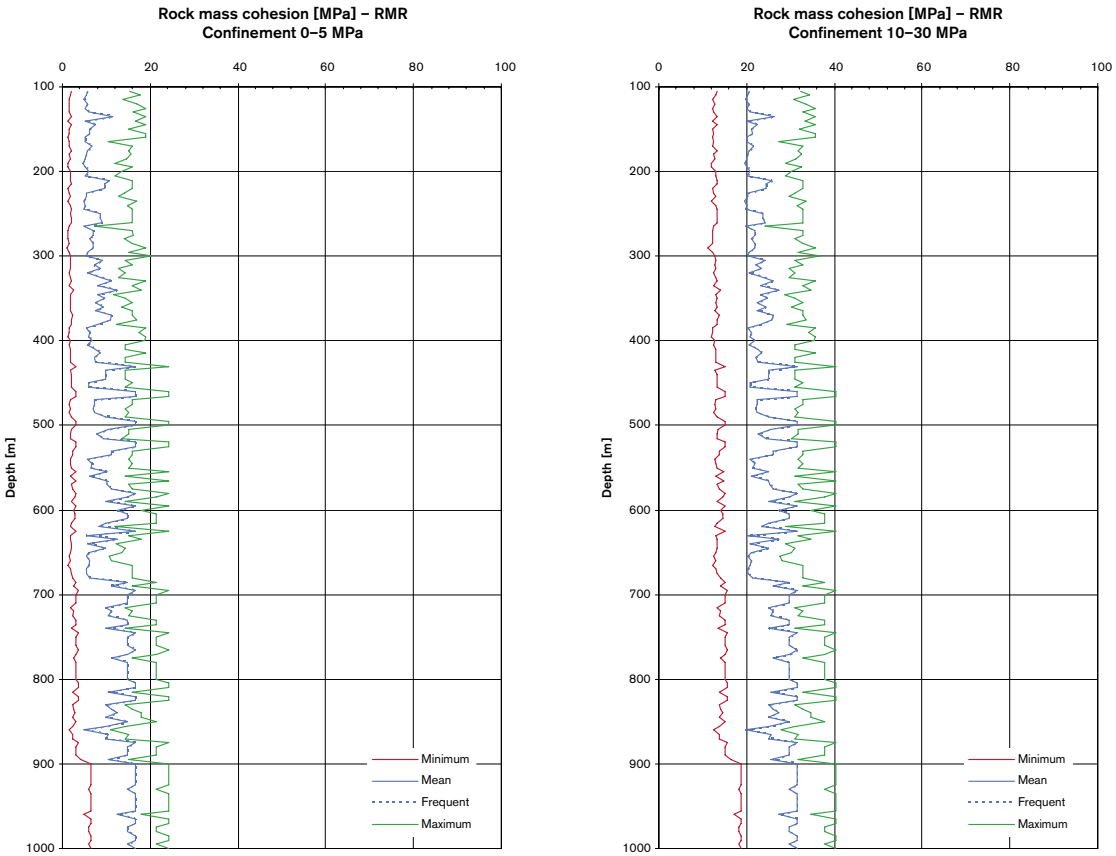

Variation of the rock mass cohesion from RMR for borehole KFM01A under stress confinement of 0–5 MPa and 10–30 MPa (Hoek and Brown's a = 0.5). The values are given for each core section of 5 m.

D.3.2 From Q

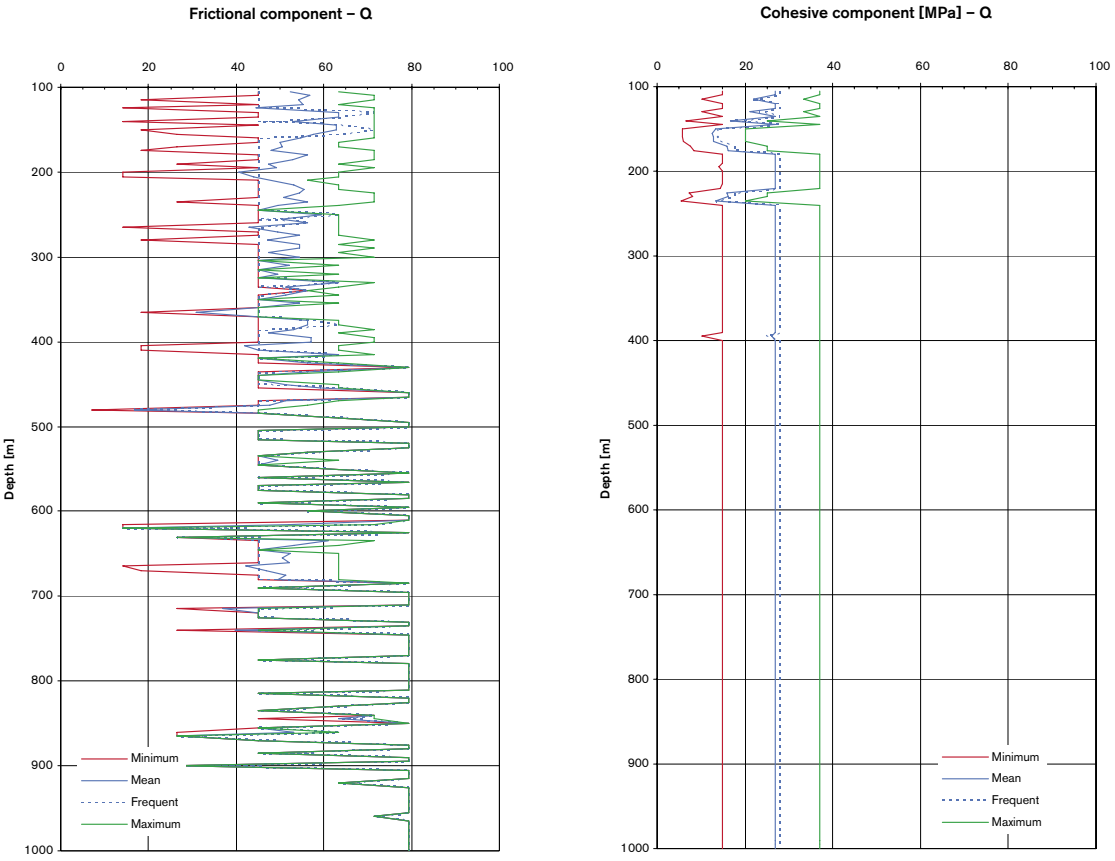

Variation of the frictional FC and the cohesive component CC from Q for borehole KFM01A. The values are given for each core section of 5 m.

D.3.3 Comparison

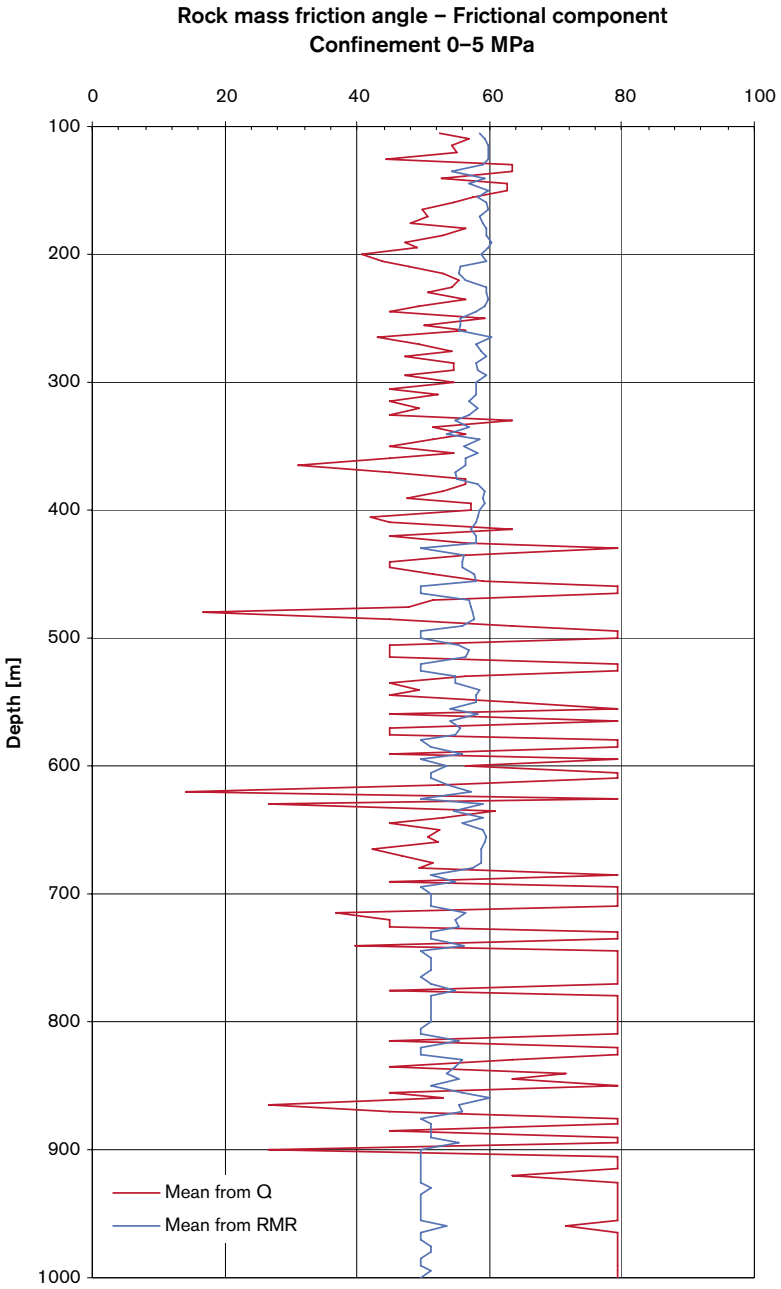

Comparison of the rock mass friction angle from RMR and Q for borehole KFM01A under stress confinement of 0–5 MPa (Hoek and Brown's a = 0.5). The values are given for each core section of 5 m.

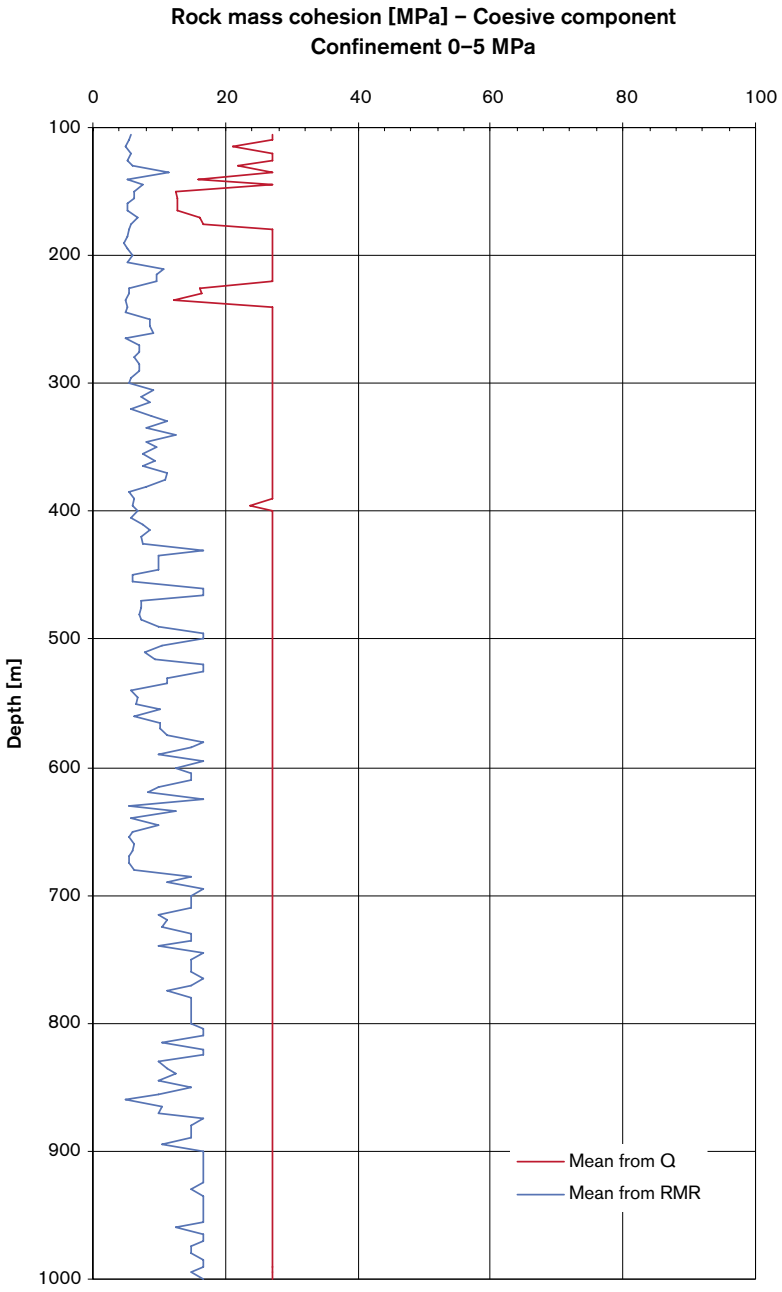

Comparison of the rock mass cohesion from RMR and Q for borehole KFM01A under stress confinement 0–5 MPa (Hoek and Brown's a = 0.5). The values are given for each core section of 5 m.